Supporting information

Iron(IV) Complexes with Tetraazaadamantane-based Ligands: Synthesis, Structure, Application in Dioxygen Activation and Labeling of Biomolecules

Ivan S. Golovanov,[a] Anton V. Leonov,[a,b] Vladislav K. Lesnikov,[a] Evgeny V. Pospelov,[a,b] Kirill V. Frolov,[c] Alexander A. Korlyukov,[d] Yulia V. Nelyubina,[d] Valentin V. Novikov,[d] Alexey Yu. Sukhorukov [a,e,f *]

[a] N. D. Zelinsky Institute of Organic Chemistry, Russian Academy of Sciences, Leninsky prospect, 47, Moscow, Russia, 119991

[b] M. V. Lomonosov Moscow State University, Leninskiye Gory,1, Moscow, Russia, 119991

[c] Shubnikov Institute of Crystallography of FSRC "Crystallography and Photonics", Russian Academy of Sciences, Leninsky prospect, 59, Moscow, Russia, 119991

[d] A. N. Nesmeyanov Institute of Organoelement Compounds, Russian Academy of Sciences, Vavilov str. 28, Moscow, Russia, 119991

[e] Plekhanov Russian University of Economics, Stremyanny per. 36, Moscow, Russia, 117997

[f] D. Mendeleev University of Chemical Technology of Russia, Miusskaya sq. 9, Moscow, Russia 125047

Corresponding Author*: Alexey Yu. Sukhorukov. Email: sukhorukov@ioc.ac.ru

Table of contents

1. General methods and Instrumentation....................S2
2. Synthetic procedures for preparation of compounds **1-4**....................S4
3. Mössbauer, NMR, UV-Vis, IR spectra of **1-4**....................S10
4. Aerobic oxidation reactions catalyzed by Fe-TAAD complexes....................S29
5. X-ray and powder XRD data for **1**....................S47
6. Study of stability of complex **1** in MeOH....................S49
7. NMR spectroscopy and Evans method for complex **1**....................S50
8. Electrochemical properties of complex **1**....................S52
9. Mössbauer spectra of **1** in various conditions and DFT calculations of δ and ΔE_Q....................S54
10. DFT calculations....................S60
10.1. Calculation of relative energies of cations derived from complex **1**....................S60
10.2. Procedure for DFT calculation of Mossbauer parameters of **1**....................S69
11. References....................S73

1. General Methods and Instrumentation

All reactions were carried out in oven-dried (150°C) glassware. CH_2Cl_2 and Et_3N were distilled over CaH_2; THF was distilled over $LiAlH_4$, other solvents were distilled without drying agents. **TAAD**,[1] **TAAD·HCl**,[2] (3*β*)-21-Bromo-20-oxopregna-5,16-dien-3-yl acetate (**2a**),[3] quaternary salt **4a**,[4] 2-bromoacetyl chloride[5] and polymer **PS-CH$_2$-TAAD**[6] were prepared according to previously described protocols. 1,4,7-Triazacyclononane trihydrochloride (**TACN·3HCl)**, 1,8-bis(dimethylamino)naphthalene (proton sponge), glycylglycylglycine, *p*-thiocresol, *n*-heptanethiol, glutathione and all inorganic reagents were commercial grade and used as received.

NMR spectra were recorded at room temperature with residual solvent peaks as internal standards.[7] Multiplicities are indicated by s (singlet), d (doublet), dd (doublet of doublets), t (triplet), m (multiplet), and br (broad). ^1H NMR spectra of complex **1** were recorded from CD_3OD solutions with a Bruker Avance 400 spectrometer. Data acquisition and processing were performed with Topspin 2.1 and Mestrenova 12.0.0 software, respectively. The magnetic susceptibility of the paramagnetic iron complex **1** in a CD_3OD solution was evaluated by the Evans method[8] at 305 K using a Wilmad NMR tube with a coaxial insert. The inner (reference) tube was filled with CD_3OD with approximately 1% of Me_4Si, the outer tube contained a CD_3OD solution of the paramagnetic complex **1** with a known concentration and the same amount of Me_4Si. The molar magnetic susceptibility was calculated from the difference between the chemical shift of Me_4Si in pure CD_3OD and its shift in the CD_3OD solution of the paramagnetic complex by the standard Evans method procedure.[9] The molar diamagnetic contribution to the paramagnetic susceptibility was estimated using Pascal's constants.[10]

Melting points were determined on a Kofler heating stage and were not corrected. HRMS experiments were performed on a mass-spectrometer with electrospray ionization and a time-of-flight (TOF) detector. Peaks in FT-IR spectra data are reported in cm^{-1} with the following relative intensities: s (strong), m (medium), w (weak), br (broad), sh (shoulder). UV-Vis spectra were recorded on a SF2000 spectrophotometer for the solutions of the investigated compounds. Peaks in UV-Vis spectra data are reported in nm. GC-MS was performed on a Chromatec 5000 with an Agilent DB-1MS column 122−0132.

Cyclic voltammetry experiments were performed for dimethylformamide solutions with 0.1 M tetrabutylammonium hexafluorophosphate as a supporting electrolyte using a Metrohm Autolab PGSTAT128N potentiostat with a conventional one-compartment three-electrode cell (5 mL of solution). Platinum disk electrode (MF-2013, BASi), which was used as a working electrode, was thoroughly polished with 0.05 μm alumina slurry, sonicated for two minutes in deionized water and rinsed before every measurement. A platinum wire counter electrode and a standard Ag/AgCl/NaCl(aq) reference electrode (RE-5B, BASi) were used. To account for a drift of the reference electrode, the ferrocene was added after the measurements as an internal standard, and all the potentials are reported relative to the Fc/Fc^+ redox couple. The solutions were thoroughly deaerated by passing argon through them before the CV experiments and above these solutions during the measurements.

^{57}Fe Mossbauer absorption spectra of powdered samples were recorded using a conventional constant-acceleration Mössbauer spectrometer MC-1104Eм equipped with the closed-cycle helium cryostat RTI CryoFree-104.[11] Spectra were recorded without external magnetic field at atmospheric pressure and within temperature range from 10 K to 295 K in transmission geometry with a ^{57}Co(Rh) source (MCo7.114).[12] For a recording of Mossbauer absorption spectrum 50 mg of powdered sample was put into thin aluminum container (tablet) with approx. square 0.3 cm^2. The plane of the tablet was placed perpendicular to the direction of γ-rays propagation. Isomer shifts are given relative to an α-Fe foil (30 μm MRA.2.6).[13] Simulations of the experimental data were performed with the Univem MS program.

X-ray diffraction experiments were carried out at 120 K with a Bruker APEX2 DUO CCD diffractometer, using graphite monochromated Mo-Kα radiation (λ = 0.71073 Å). CCDC 2110176 contains the supplementary crystallographic information for complex **1**.

The powder X-ray diffraction patterns of the sample were measured in reflection mode. The measurements were performed with a Bruker D8 Advance diffractometer equipped with motorized slits and a LynxEye 1D position-sensitive detector. The measurement range was 4–60° in 2θ angle. All calculation was carried out with TOPAS 4.2 software.[14]

DFT calculations were performed with the Gaussian 16 Rev C.01[15] or ORCA 4.2.1[16] quantum chemistry programs.

2. Synthetic procedures for preparation of compounds 1–4

Synthesis of iron(IV)-TAAD complex 1

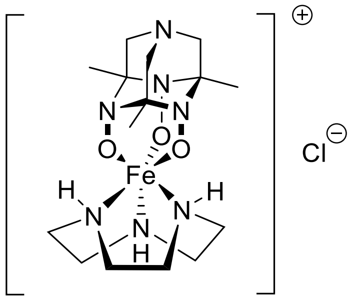

To a mixture of **TAAD·HCl** (107 mg, 0.4 mmol), **TACN·3HCl** (96 mg, 0.4 mmol), anhydrous $FeCl_3$ (64 mg, 0.4 mmol) and proton sponge (856 mg, 4.0 mmol) was added methanol (10 mL). The reaction mixture was stirred for 1 hour at room temperature under air and then kept for additional 24 hours with a closed cap. The precipitate was centrifuged off and a clear solution containing complex **1** was concentrated in a vacuum. The residue was dried at 0.1 Torr for 30 min and a mixture of Et_2O (40 mL) and CH_2Cl_2 (40 mL) was added to the crude product. The mixture was left to stay in a refrigerator at 4°C for 4 days. Then the precipitate was separated from the mother liquor and dried at 0.1 Torr for 30 min. The resulting solid material was placed in a centrifuge cup and centrifuged with CH_2Cl_2-Et_2O 5:1 mixture (6 × 12 mL). The residual solid was dissolved in 6 mL of methanol (dark maroon solution) and centrifuged. A clear solution was separated from a small amount of undissolved material and concentrated in a vacuum. This operation was repeated with 4 mL of methanol. The solid material was dried in a vacuum at 0.1 Torr to give 102 mg (yield 48%) of complex **1** as a black solid. Mp. above 260°C. FT-IR (KBr): 3440 (br), 3277 (s), 3126 (s), 2972 (s), 2932 (s), 2876 (s), 1728 (w), 1629 (s), 1456 (s), 1437 (s), 1373 (s), 1265 (m), 1214 (m), 1175 (m), 1162 (m), 1103 (s), 1070 (w), 1033 (s), 965 (s), 873 (w), 826 (s), 800 (m), 775 (w), 750 (m), 697 (s), 633 (s), 606 (m), 586 (w), 540 (s), 504 (s), 473 (w), 420 (s). UV−vis spectrum: (MeOH, $c = 5.9 \times 10^{-3}$ M) peaks λ nm: 345, 496, 577. Mössbauer spectrum, 295K: δ, (mm/s) = 0.2745; $|\Delta E_Q|$, (mm/s) = 3.2089. ESI-HRMS m/z: $[M\text{-}Cl]^+$ Calcd for $[C_{15}H_{30}FeN_7O_3]^+$ 412.1754; Found 412.1753. Anal. Calcd for $C_{15}H_{30}ClFeN_7O_3 \cdot 2CH_3OH \cdot H_2O$: C, 38.54; H, 7.61; N, 18.51. Found: C, 38.79; H, 7.26; N, 18.85.

Preparation of crystals for X-ray analysis: complex **1** (50 mg) was dissolved in 1 mL of methanol and the solution was filtered through a syringe filter. Slow vapor diffusion of diethyl ether into the methanol solution produced black crystals of **1**·CH_3OH suitable for X-Ray diffraction analysis.

Synthesis of complex 3a

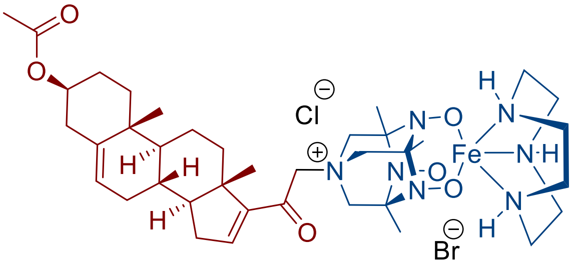

Synthesis of complex 3a from quaternary salt 4a (strategy 2). To a mixture of quaternary salt **4a** (62 mg, 0.09 mmol), **TACN·3HCl** (22 mg, 0.09 mmol), anhydrous $FeCl_3$ (14 mg, 0.09 mmol) and proton sponge (193 mg, 0.9 mmol) was added methanol (2.5 mL). The reaction mixture was stirred for 1 hour at room temperature under air and then kept for additional 24 hours with a closed cap. The precipitate was centrifuged off and clear solution containing complex **3a** was concentrated in a vacuum. The residue was dried at 0.1 Torr for 30 min and a mixture of Et_2O (10 mL) and CH_2Cl_2 (10 mL) was added to the crude product. The mixture was left to stay in a refrigerator at 4°C for 10 days. Then the precipitate was separated from mother liquor and dried at 0.1 Torr for 30 min. The residue was placed in a centrifuge cup and centrifuged with CH_2Cl_2-Et_2O 5:1 mixture (3 × 6 mL). The residual solid was dissolved in 1.5 mL of methanol (dark maroon solution) and centrifuged. A clear solution was separated from small amount of undissolved material and concentrated in a vacuum. Solid material was dried in a vacuum at 0.1 Torr to give 38 mg (yield 46%) of complex **3a** as a black solid. Mp. above 260°C. FT-IR (KBr): 3436 (br), 2933 (br), 1728 (s), 1667 (s), 1633 (s), 1582 (m), 1455 (s), 1376 (s), 1245 (s), 1199 (w), 1178 (w), 1101 (m), 1035 (s), 1014 (m), 964 (s), 908 (w), 877 (w), 834 (w), 805 (s), 776 (m), 711 (m), 649 (m), 610 (m), 591 (m), 543 (w), 510 (m), 484 (m), 422 (m). UV–vis spectrum: (MeOH, $c = 3.0 \times 10^{-3}$ M) peaks λ nm: 240, 297, 344, 491. Mössbauer spectrum, 295K: δ, (mm/s) = 0.2007; $|\Delta E_Q|$, (mm/s) = 3.0904 ESI-HRMS m/z: $[M\text{-}Cl\text{-}Br]^{2+}$ Calcd for $[C_{38}H_{61}FeN_7O_6]^{2+}$ 383.7011; Found 383.7009. $[M\text{-}Cl\text{-}Br\text{-}H]^{+}$ Calcd for $[C_{38}H_{60}FeN_7O_6]^{+}$ 766.3950; Found 766.3924. Anal. Calcd for $C_{38}H_{61}BrClFeN_7O_6 \cdot 2CH_3OH \cdot 2H_2O$: C, 48.86; H, 7.48; N, 9.97. Found: C, 47.99; H, 7.42; N, 10.53.

Synthesis of complex 3a from 1 and 2a (strategy 1). To a mixture of complex **1** (45 mg, 0.1 mmol) and bromide **2a** (44 mg, 0.1 mmol) was added methanol (3 mL). The reaction mixture was stirred for 7 days at room temperature. The precipitate was centrifuged off and clear solution containing complex **3a** was concentrated in a vacuum. The residue was dried in a vacuum at 0.1 Torr to give 60 mg of crude complex **3a** (see Mössbauer spectrum for details). Black solid. Mössbauer spectrum, 295K: δ, (mm/s) = 0.2306; $|\Delta E_Q|$, (mm/s) = 3.1154. ESI-HRMS m/z: $[M\text{-}Cl\text{-}Br]^{2+}$ Calcd for $[C_{38}H_{61}FeN_7O_6]^{2+}$ 383.7011; Found 383.7004.

Synthesis of (2-bromoacetyl)glycylglycylglycine (2b).

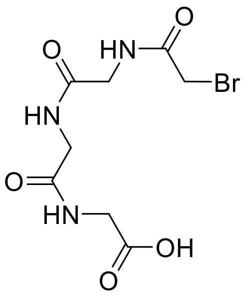

To a suspension of glycylglycylglycine (55 mg, 0.29 mmol) in water (0.5 mL) and acetone (0.5 mL) was added K_2CO_3 (81 mg, 0.59 mmol). Then reaction mixture was cooled to 0°C and 2-bromoacetyl chloride (300 μL, 0.36 mmol) was added dropwise. The resulting mixture was stirred at 0°C for 2 hours. Then acetone was removed under reduced pressure and residue was acidified to pH = 2 with 36% wt. aqueous HCl solution (approx. 5 drops). The mixture was left to stay in a refrigerator at 4°C for 8 hours. Then precipitate was separated from mother liquor washed with acetone (2 × 500 μL) and dried in a vacuum at 0.1 Torr to give 76 mg (yield 84%) of **2b** as a white solid. Mp. 215-220°C. ^{1}H NMR (300 MHz, DMSO-d_6, δ, ppm): 3.74 (m, 6 H), 4.13 (s, 2 H), N*H* and O*H* protons are not observed. FT-IR (KBr): 3276 (s, br), 3087 (s,br), 1718 (s), 1645 (s) 1560 (s), 1422 (s), 1406 (s), 1379 (m), 1337 (w), 1286 (s), 1242 (s, br), 1145 (m), 1089 (w), 1032 (s), 904 (s,br), 791 (m), 700 (s, br), 591 (m), 553 (s), 483 (m). ESI-HRMS m/z: $[M+Na]^+$ Calcd for $[C_8H_{12}BrN_3O_8Na]^+$ 331.9849; Found 331.9853.

Synthesis of 1-({[({[(carboxymethyl)carbamoyl]methyl}carbamoyl)methyl]carbamoyl}methyl)-4,6,10-trihydroxy-3,5,7-trimethyl-1,4,6,10-tetraazatricyclo[3.3.1.1^{3,7}]decan-1-ium bromide

(***quaternary salt 4b***).

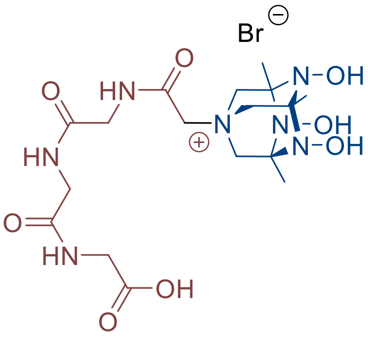

To a suspension of **2b** (60 mg, 0.19 mmol) in water (1 mL) and methanol (1 mL) was added **TAAD** (45 mg, 0.19 mmol). The reaction mixture was stirred for 120 hours at room temperature. Then KI (32 mg, 0.19 mmol) was added and the reaction mixture was stirred for additional 24 hours at room temperature and afterwards was concentrated under reduced pressure. The residue was dried in a vacuum until constant weight to give 114 mg of mixture **4b** and KI as yellow oil, which was used without further purification in the next stage. ^{1}H NMR (300 MHz, DMSO-d_6, δ, ppm): 1.25 (s, 9 H), 3.60-3.64 (br, 6 H), 3.76 and 3.84 (2 m, 4 H and 2H), 4.17 (s, 2 H), N*H* and O*H* protons are not observed. ESI-HRMS m/z: [M-Br]$^+$ Calcd for $[C_{17}H_{30}N_7O_8]^+$ 460.2150; Found 460.2141.

Synthesis of complex 3b.

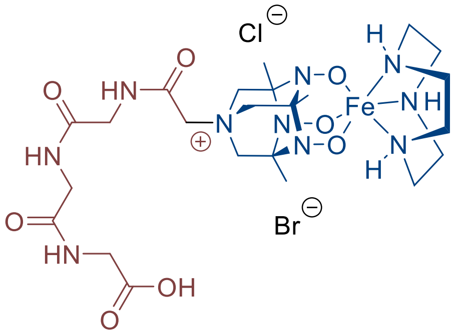

Synthesis of complex 3b from quaternary salt 4b (strategy 2). To a mixture of **4b** and KI from the previous step (112 mg of mixture containing 80 mg of **4b** 0.15 mmol), **TACN·3HCl** (37 mg, 0.15 mmol), anhydrous $FeCl_3$ (24 mg, 0.15 mmol) and proton sponge (265 mg, 1.24 mmol) were added 2 mL of methanol and 2 mL of water. The reaction mixture was stirred for 1 hour at room temperature under air and then kept for additional 24 hours with a closed cap. The precipitate was centrifuged off and a clear solution containing complex **3b** was concentrated in a vacuum. The residue was dried at 0.1 Torr for 30 min and a mixture of Et_2O (20 mL) and CH_2Cl_2 (20 mL) was added to the crude product. The mixture was left to stay in a refrigerator at 4°C for 4 days. Then the precipitate was separated from the mother liquor and dried at 0.1 Torr for 30 min. The residue was placed in a centrifuge cup and centrifuged with CH_2Cl_2 (3 × 10 mL). The residual solid was dissolved in 3 mL of methanol (dark maroon solution) and centrifuged. The clear solution was separated from a small amount of undissolved material and concentrated in a vacuum. The solid material was dried in a vacuum at 0.1 Torr to give 64 mg of crude complex **3b** (see Mössbauer spectrum for details). Black solid. Mp. above 260°C. FT-IR (KBr): 3470 (br), 3272 (br), 2930 (m), 1727 (s), 1663 (s, br), 1568 (s), 1549 (s), 1454 (s), 1376 (s), 1337 (w), 1269 (s), 1238 (s), 1181 (w), 1102 (s), 1032 (s), 965 (s), 872 (m), 822 (m), 806 (s), 774 (s), 743 (m), 706 (s), 650 (m), 633 (m), 609 (m), 585 (m,br), 540 (s), 512 (s), 482 (s), 421 (s). Mössbauer spectrum, 293K: δ, (mm/s) = 0.1983; $|\Delta E_Q|$, (mm/s) = 3.1145. ESI-HRMS m/z: $[M\text{-}Cl\text{-}Br]^{2+}$ Calcd for $[C_{23}H_{42}FeN_{10}O_8]^{2+}$ 321.1263; Found 321.1274. $[M\text{-}Cl\text{-}Br\text{-}H]^+$ Calcd for $[C_{23}H_{41}FeN_{10}O_8]^+$ 641.2453; Found 641.2449.

Synthesis of complex 3b from 1 and 2b (strategy 1). To a mixture of complex **1** (45 mg, 0.1 mmol) and **2b** (31 mg, 0.1 mmol) was added water (3 mL). The reaction mixture was stirred for 7 days at room temperature and the clear solution containing complex **3b** was concentrated in a vacuum. The residue was dried in a vacuum at 0.1 Torr to give 75 mg of crude complex **3b** (see Mössbauer spectrum for details). Black solid. Mössbauer spectrum, 293K: δ, (mm/s) = 0.2228; $|\Delta E_Q|$, (mm/s) = 3.1045. ESI-HRMS m/z: $[M\text{-}Cl\text{-}Br\text{-}H]^+$ Calcd for $[C_{23}H_{41}FeN_{10}O_8]^+$ 641.2453; Found 641.2430.

Synthesis of polymer supported complex 3c.

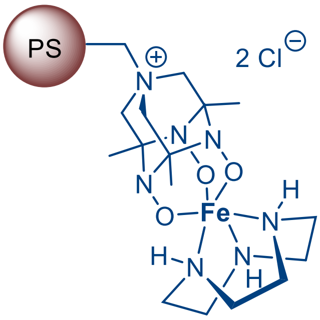

To a mixture of polymer **PS-CH$_2$-TAAD** (153 mg, 72% loading of **TAAD**, ca. 0.1 mmol), **TACN·3HCl** (24 mg, 0.1 mmol), anhydrous FeCl$_3$ (16 mg, 0.1 mmol) and proton sponge (214 mg, 1.0 mmol) were added 2 mL of methanol and 1 mL of THF. The reaction mixture was stirred for 4 hours at room temperature under air and then kept for 17 hours with a closed cap. Thereafter the mixture was stirred for additional 8 hours at room temperature under air. Then the polymeric material was filtered off using a sorbent-free PrepSep column and washed with 10 mL of THF. The residual solid was dried in a vacuum at 0.1 Torr to give 185 mg of polymer **3c** as a black solid. FT-IR (KBr): 3433 (br), 3082 (s), 3061 (m), 3025 (m), 2923 (s), 2854 (s), 1944 (m), 1871 (m), 1803 (m), 1729 (m), 1630 (s), 1601 (s), 1548 (w), 1492 (s), 1451 (s), 1374 (s), 1322 (m), 1268 (m), 1234 (m), 1176 (m), 1156 (m), 1110 (m), 1062 (s), 1028 (s), 986 (s), 973 (s), 944 (s), 906 (m), 870 (w), 832 (m), 795 (s), 755 (s), 698 (s), 650 (m), 615 (m), 537 (s, br), 482 (m), 421 (m). Mössbauer spectrum, 293K: δ, (mm/s) = 0.2040; $|\Delta E_Q|$, (mm/s) = 3.0992. Anal. Found C, 73.77; H, 7.16; Fe, 2.5; N, 4.90 (23% loading of **complex 1** calculated based on elemental analysis and Mössbauer spectral data).

3. Mössbauer, NMR, UV-Vis, IR spectra of 1-4

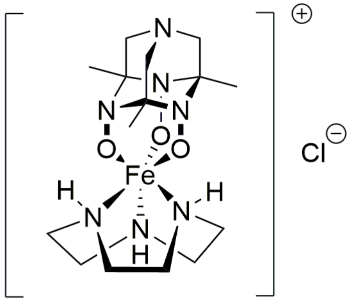

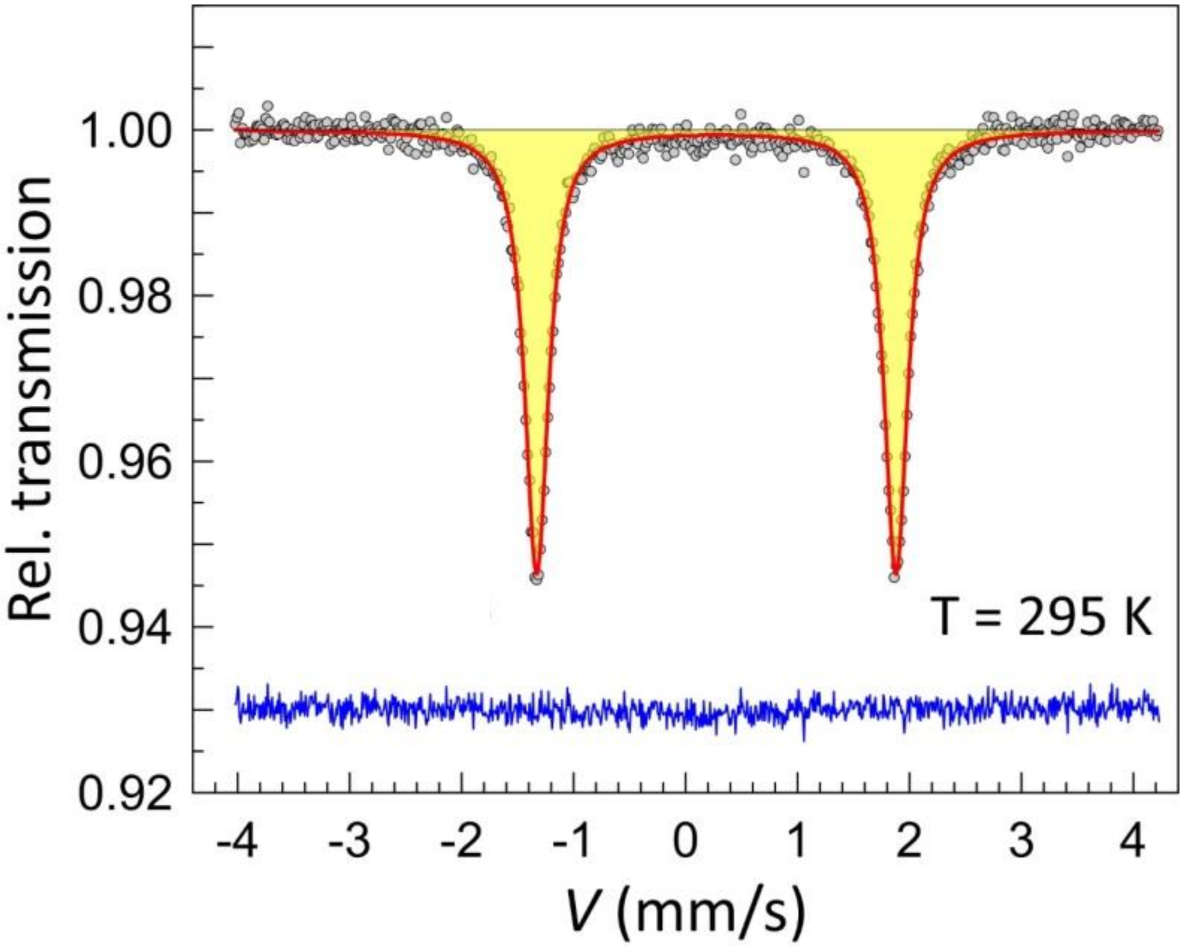

Mössbauer spectrum of 1

Component	δ, (mm/s)	$\lvert\Delta E_Q\rvert$, (mm/s)	S rel, %	Γ, (mm/s)
Doublet 1	0.2745	3.2089	100.00	0.2573

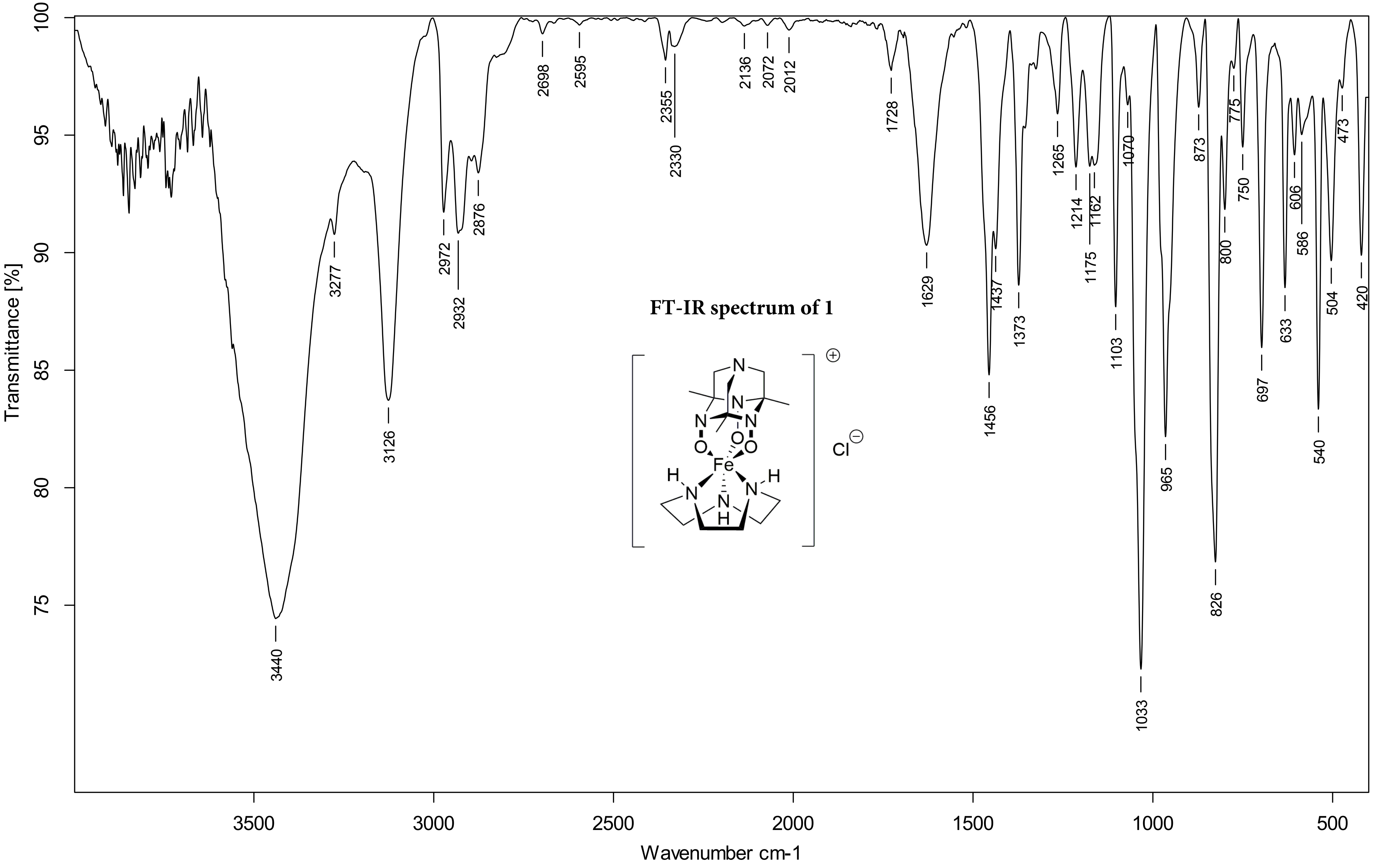
FT-IR spectrum of 1
Transmittance [%]
100
95
90
85
80
75
Wavenumber cm-1
3500
3000
2500
2000
1500
1000
500
3440
3277
3126
2972
2932
2876
2698
2595
2355
2330
2136
2072
2012
1728
1629
1456
1437
1373
1265
1214
1175
1162
1103
1070
1033
965
873
826
800
775
750
697
633
606
586
540
504
473
420
N
N
N
N
O
O
O
Fe
H
N
H
N
N
H
H
⊕
Cl⊖

UV–vis spectrum of 1

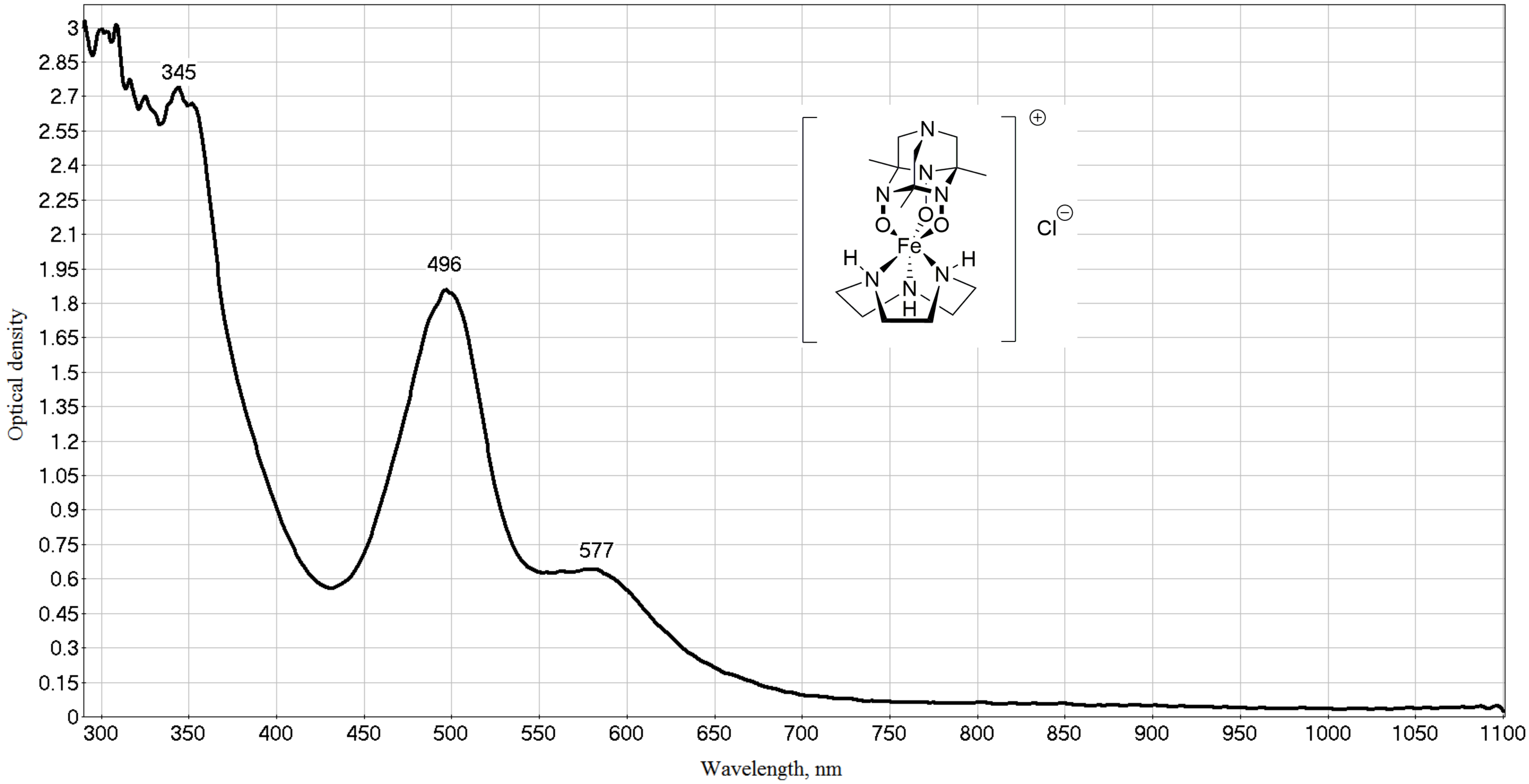

Mössbauer spectrum of 3a (*strategy 2*)

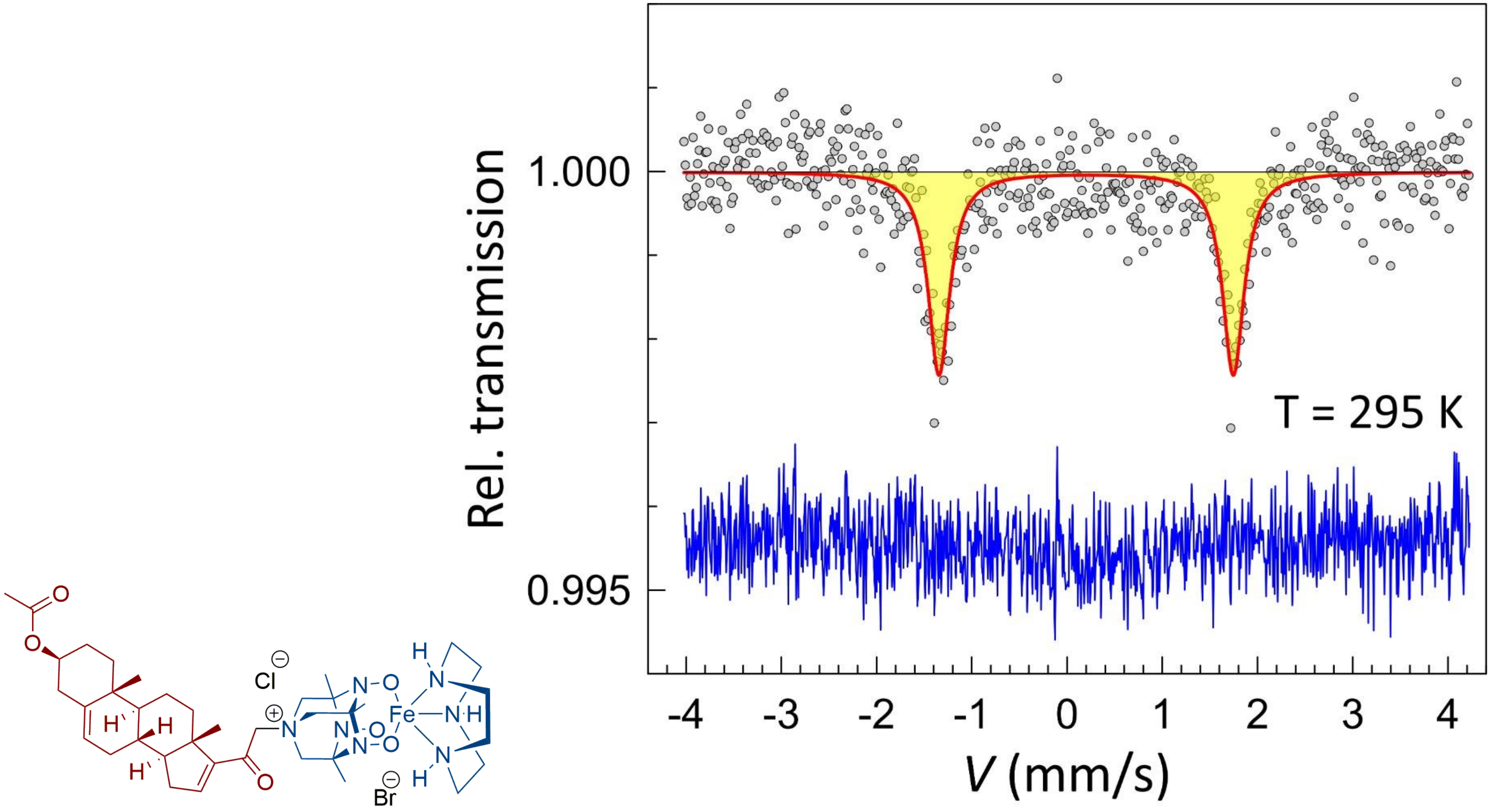

Component	δ, (mm/s)	$\lvert\Delta E_Q\rvert$, (mm/s)	S rel, %	Γ, (mm/s)
Doublet 1	0.2007	3.0904	100.00	0.2753

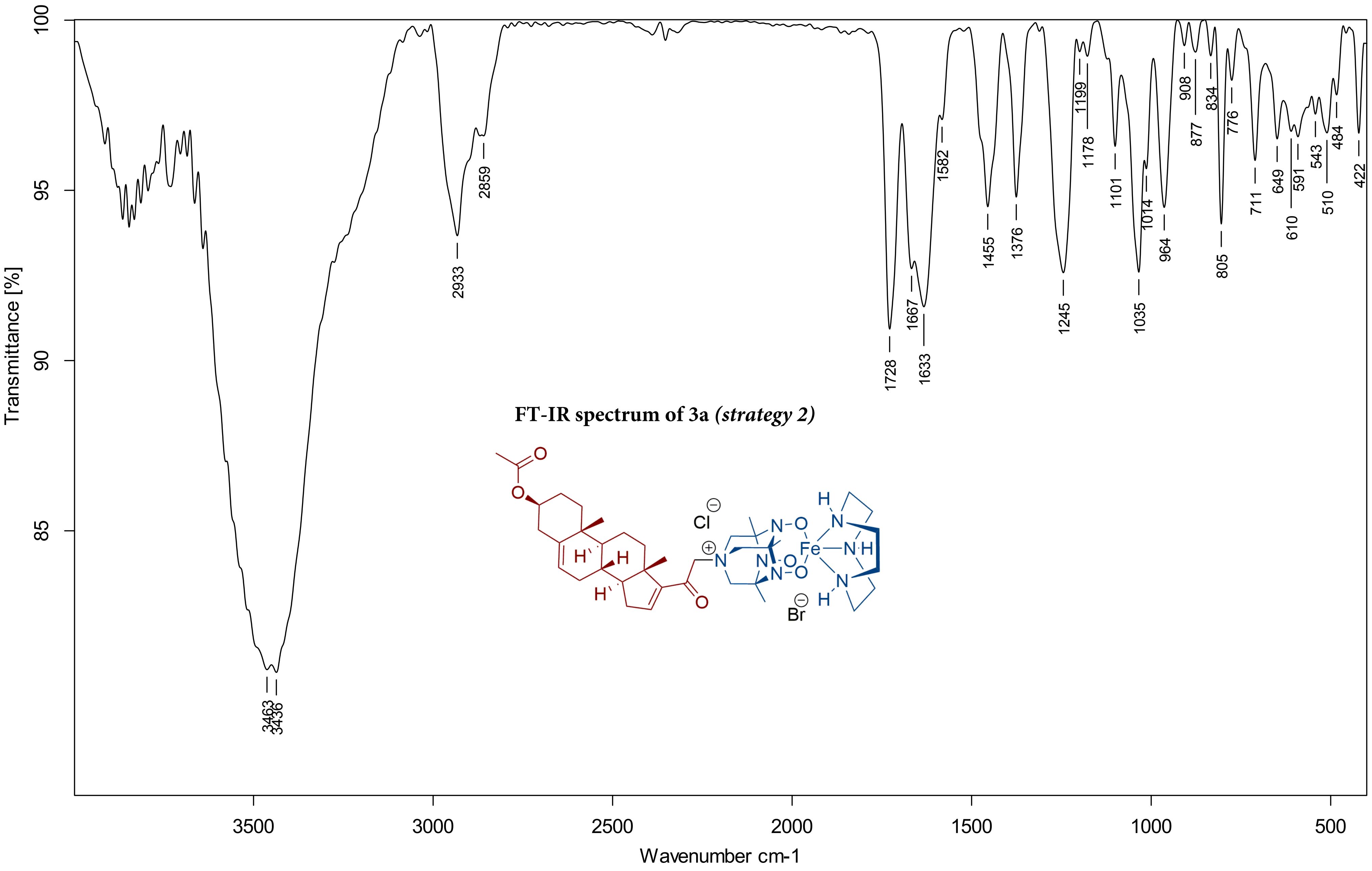

FT-IR spectrum of 3a *(strategy 2)*

UV–vis spectrum of 3a *(strategy 2)*

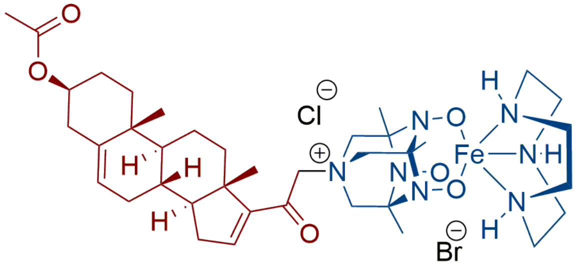

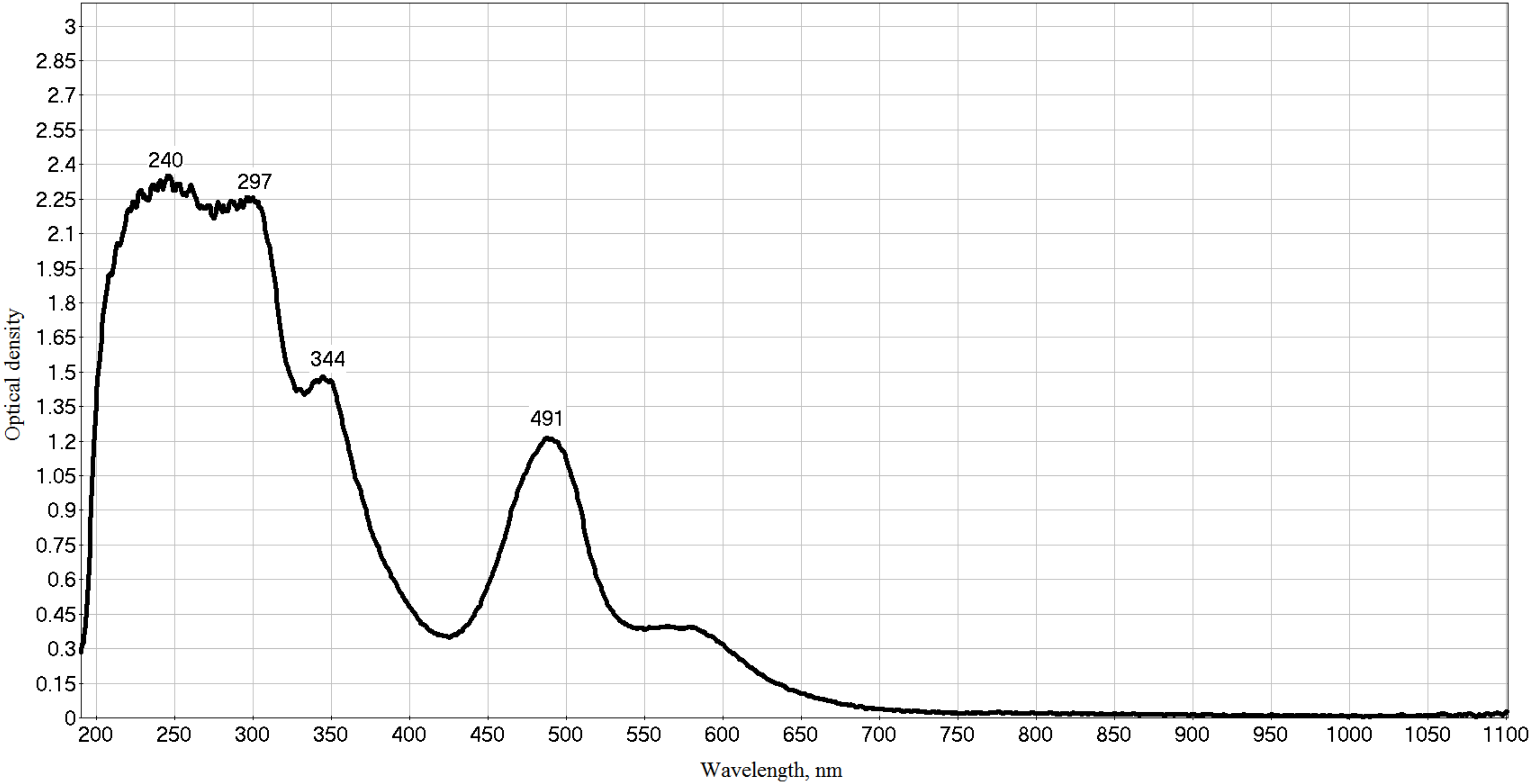

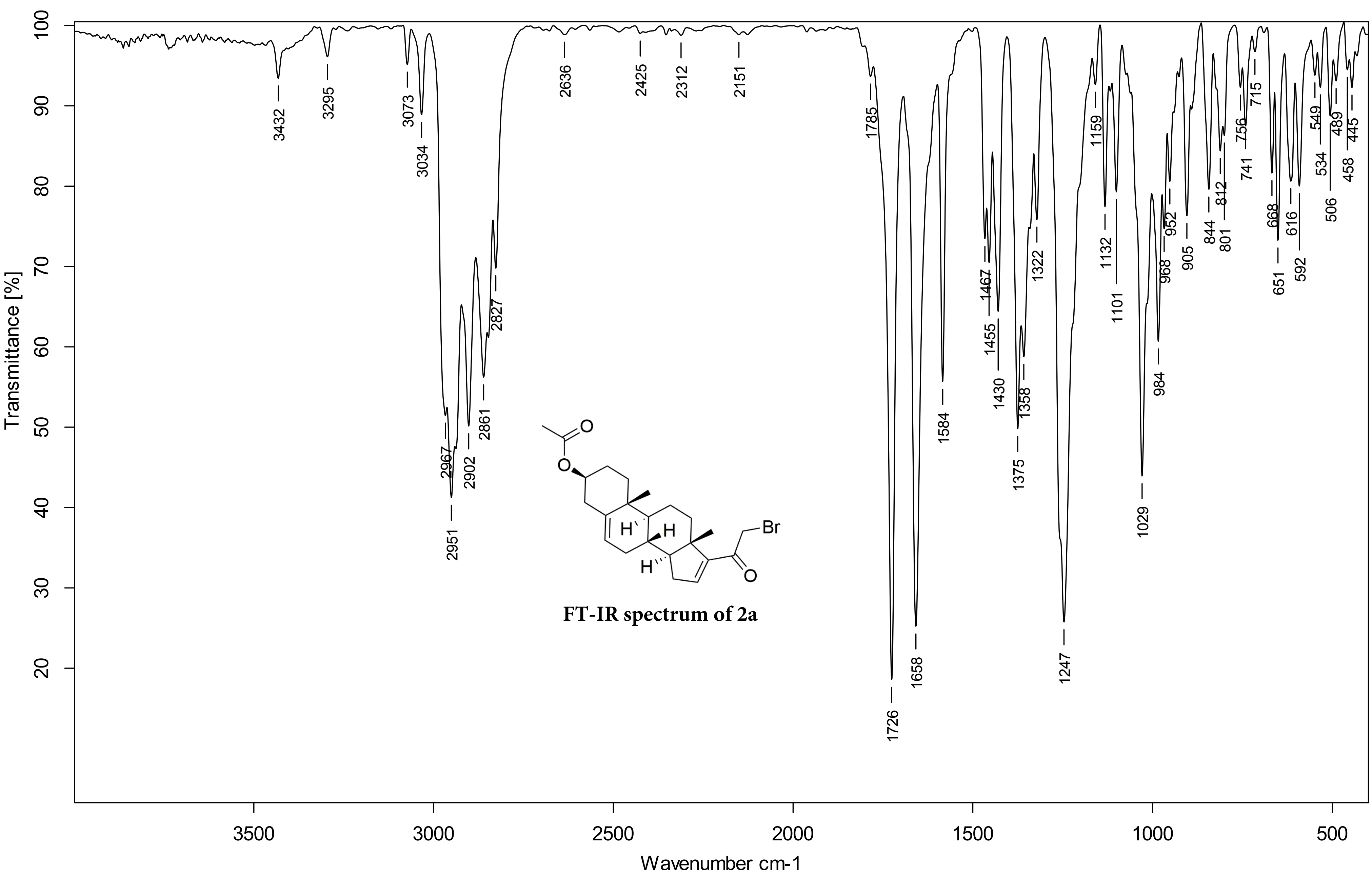

FT-IR spectrum of 2a

Table S1. Comparison of IR frequencies **1**, **2a** an **3a**.

Compound	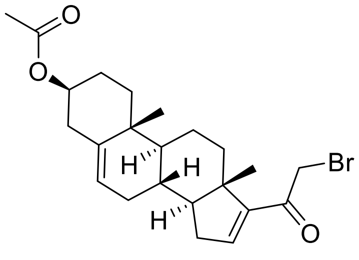 **(2a)**	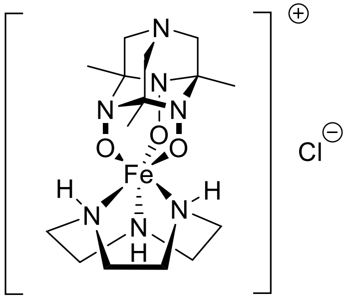 **(1)**	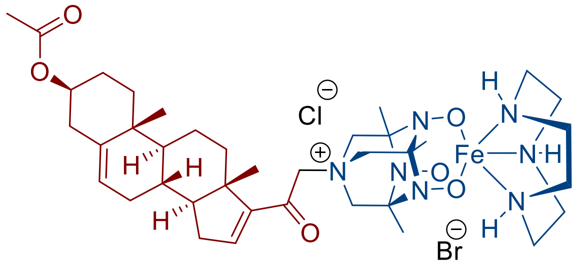 **(3a)**
IR frequency	**1726 (s)**	-	**1728 (s)**
	1584 (s)	-	**1582 (m)**
	1247 (s)	-	**1245 (s)**
	-	**1456 (s)**	**1455 (s)**
	-	**826 (s)**	**805 (s)**
	-	**697 (s)**	**711 (m)**

Mössbauer spectrum of 3a synthesized from 1 and 2a (*strategy 1*)

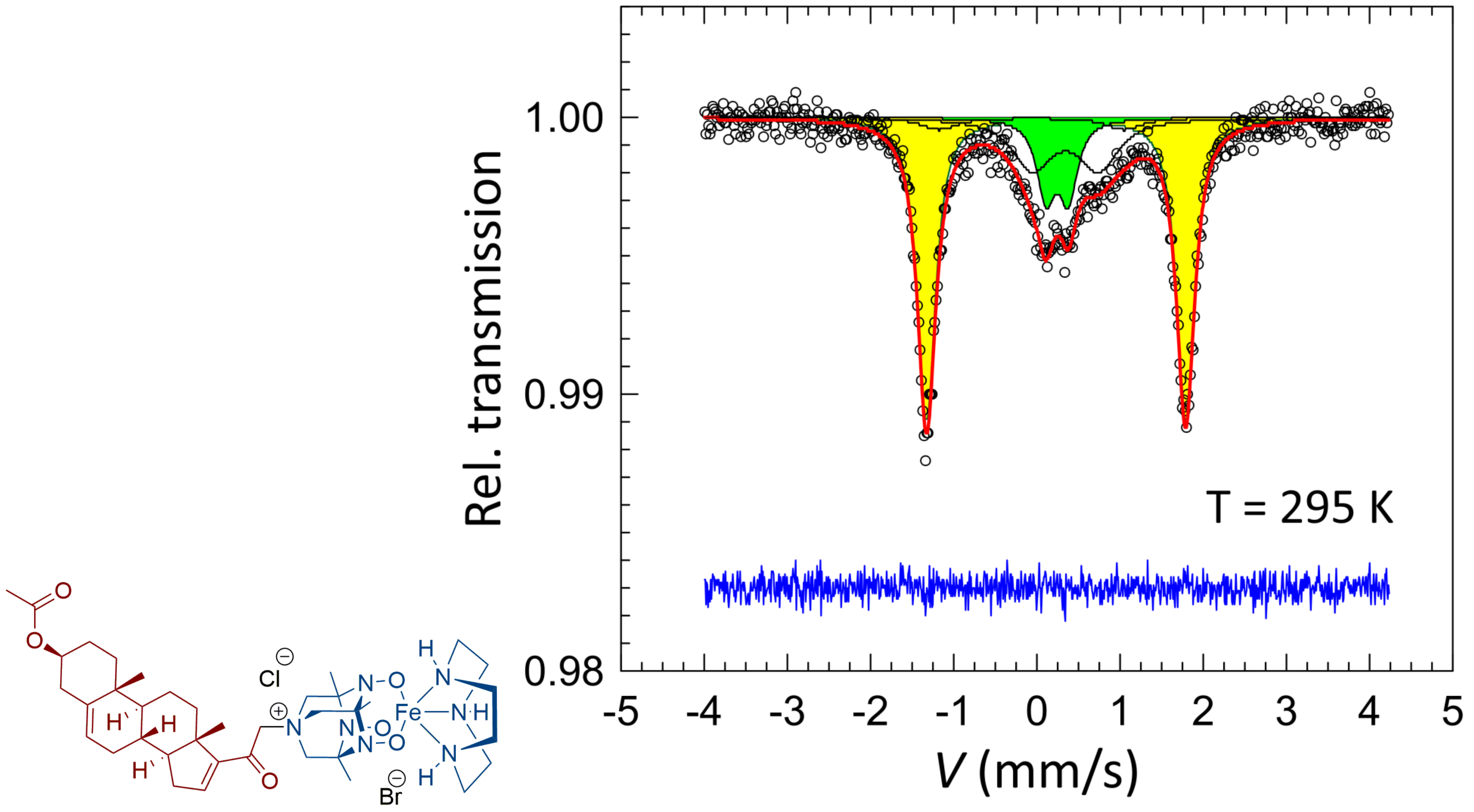

Component	δ, (mm/s)	$\lvert\Delta E_Q\rvert$, (mm/s)	S rel, %	Γ, (mm/s)
Doublet 1	0.2306	3.1154	58.75	0.2609
Doublet 2	0.2439	0.2670	15.21	0.2678
Doublet 3	0.3435	0.7969	21.25	0.5819
Doublet 4	-0.0636	2.2252	4.79	0.5308

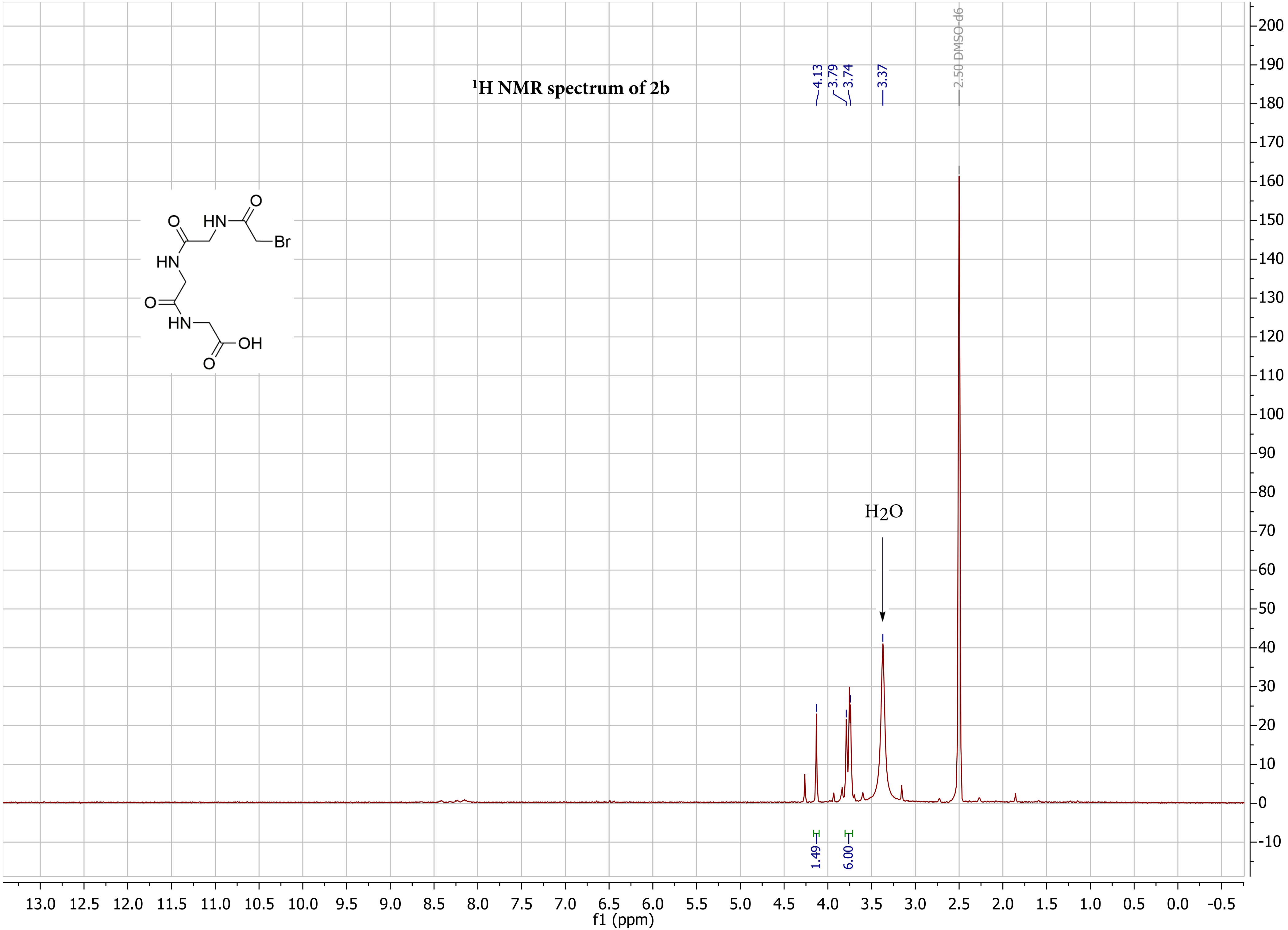

^{1}H NMR spectrum of 2b

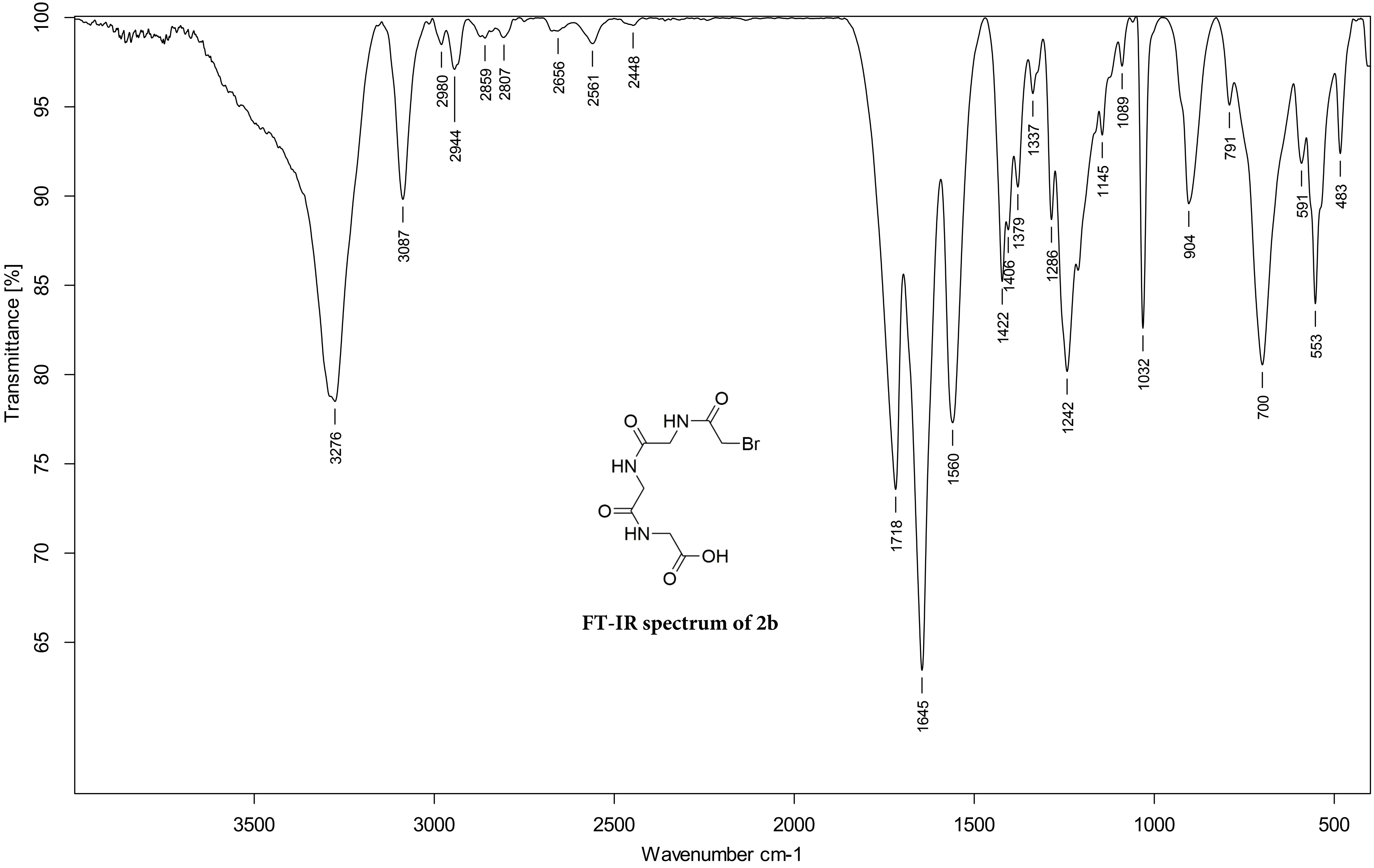

FT-IR spectrum of 2b

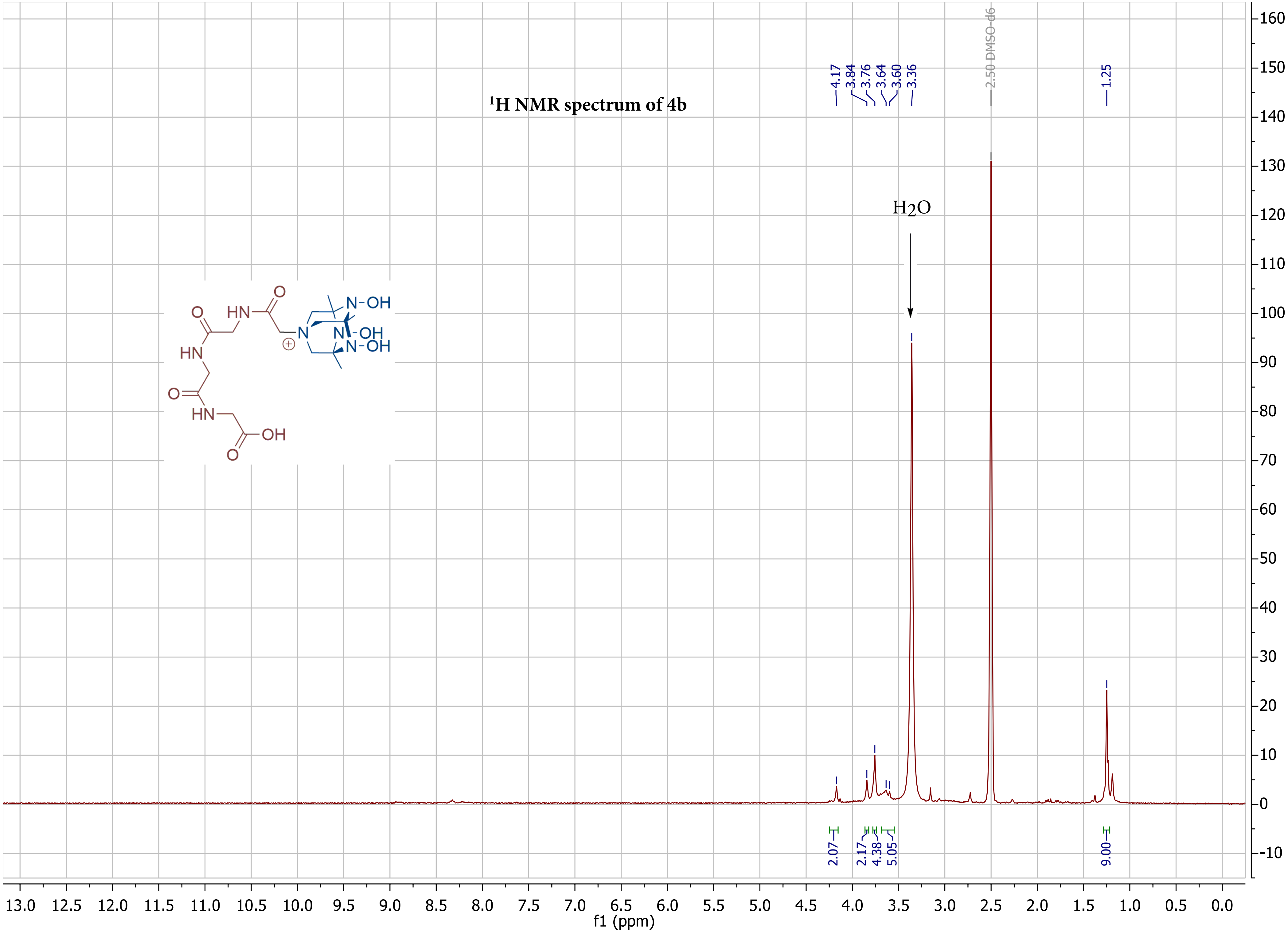

^{1}H NMR spectrum of 4b

^1H NMR spectrum of 4b

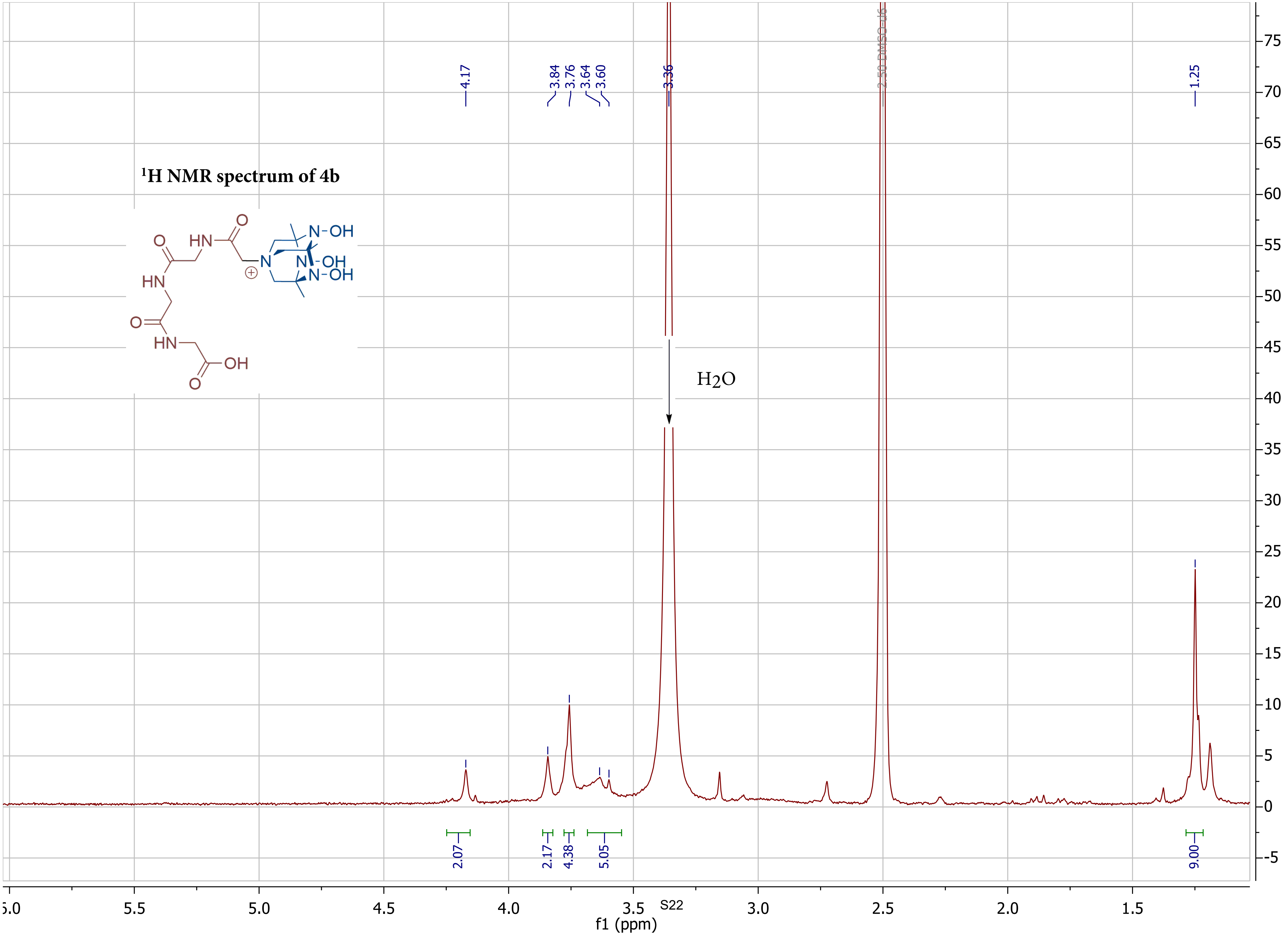

Mössbauer spectrum of 3b (*strategy 2*)

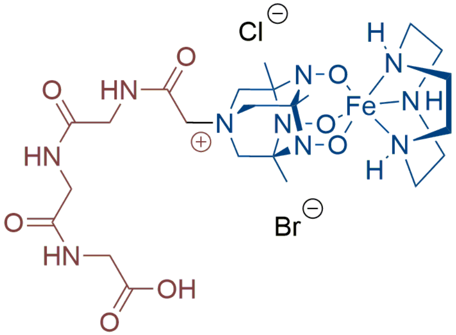

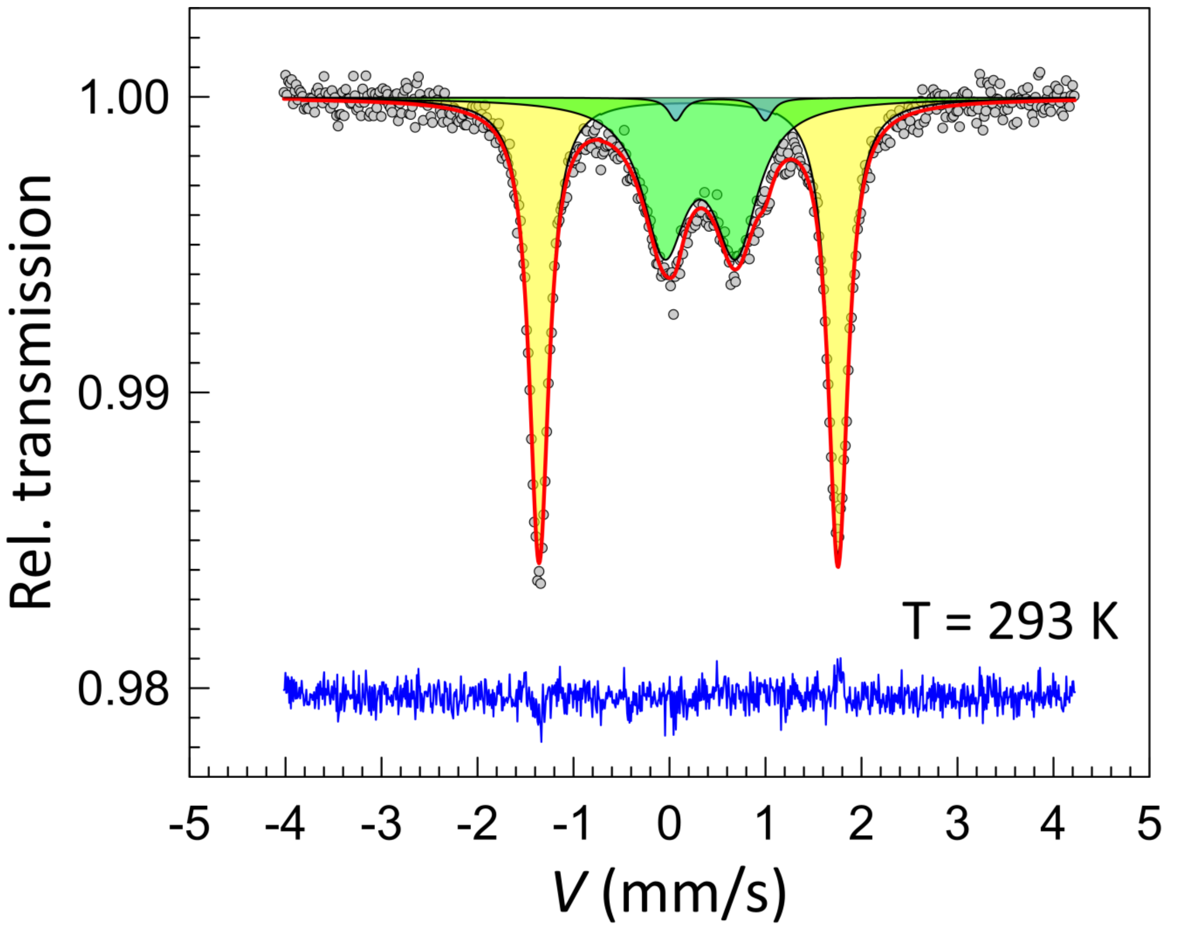

Component	δ, (mm/s)	$\lvert\Delta E_Q\rvert$, (mm/s)	S rel, %	Γ, (mm/s)
Doublet 1	0.1983	3.1145	57.63	0.2470
Doublet 2	0.3190	0.7441	40.22	0.5500
Doublet 3	0.5318	0.9319	2.16	0.1867

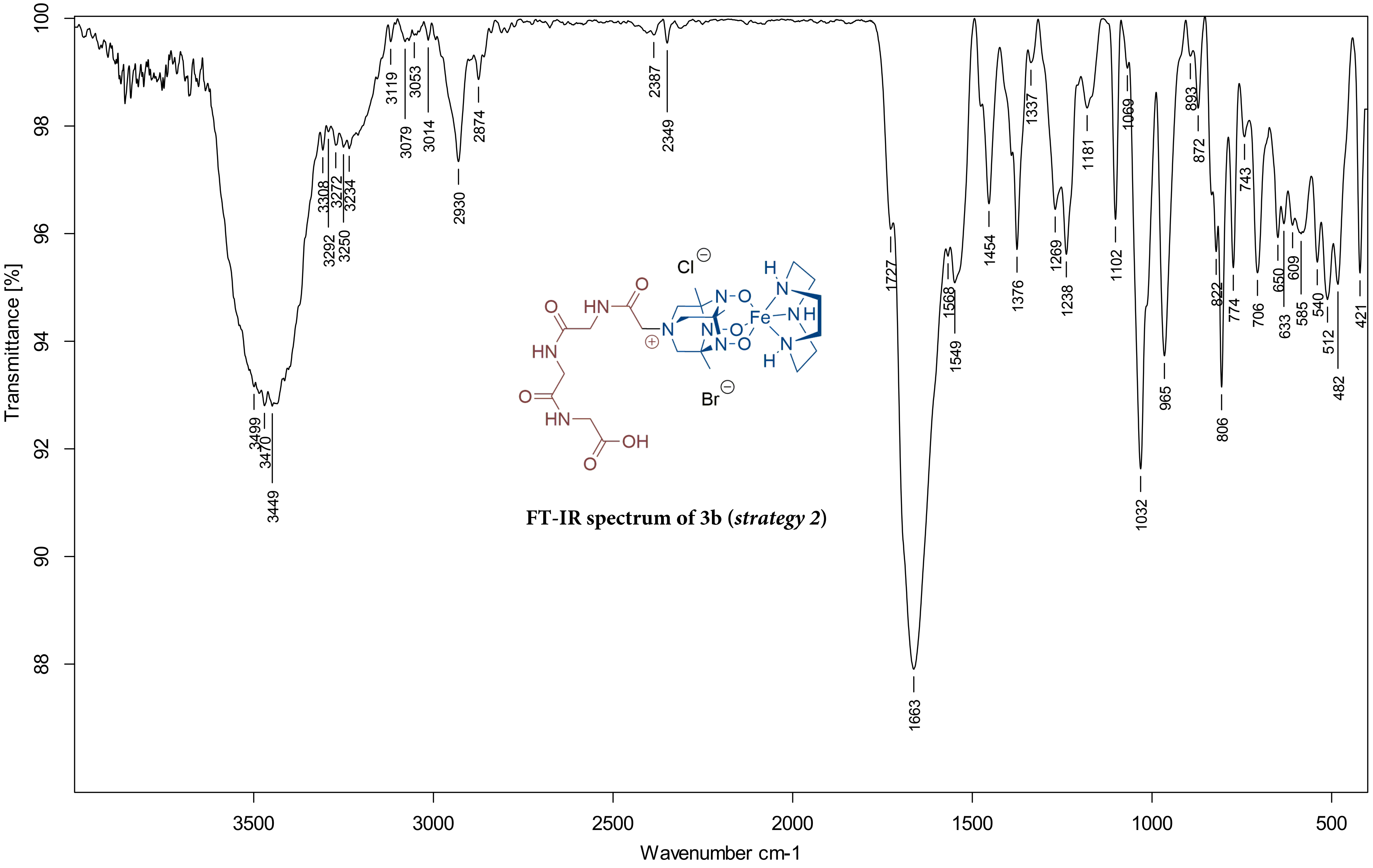

FT-IR spectrum of 3b (*strategy 2*)

Table S2. Comparison of IR frequencies **1**, **2b** and **3b**.

Compound	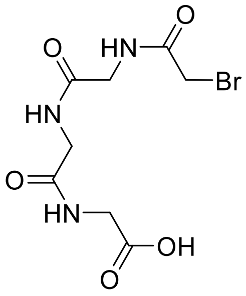 **(2b)**	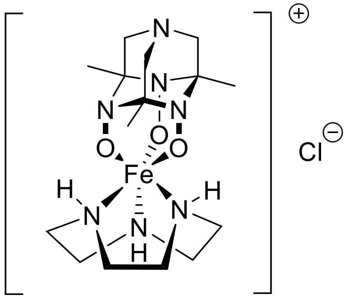 **(1)**	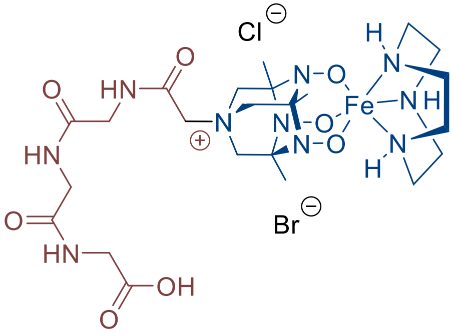 **(3b)**
IR frequency	**1718 (s)**	**-**	**1727 (s)**
	1645 (s)	**-**	**1663 (s, br)**
	1560 (s)	**-**	**1549 (s)**
	-	**965 (s)**	**965 (s)**
	-	**826 (s)**	**806 (s)**

Mössbauer spectrum of 3b synthesized from 1 and 2b (*strategy 1*)

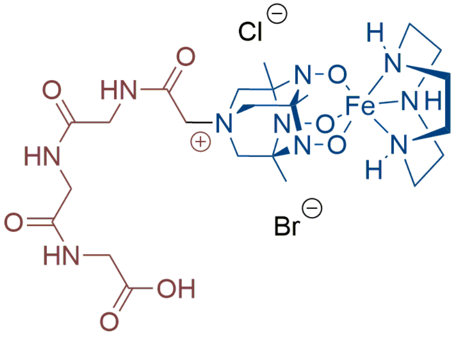

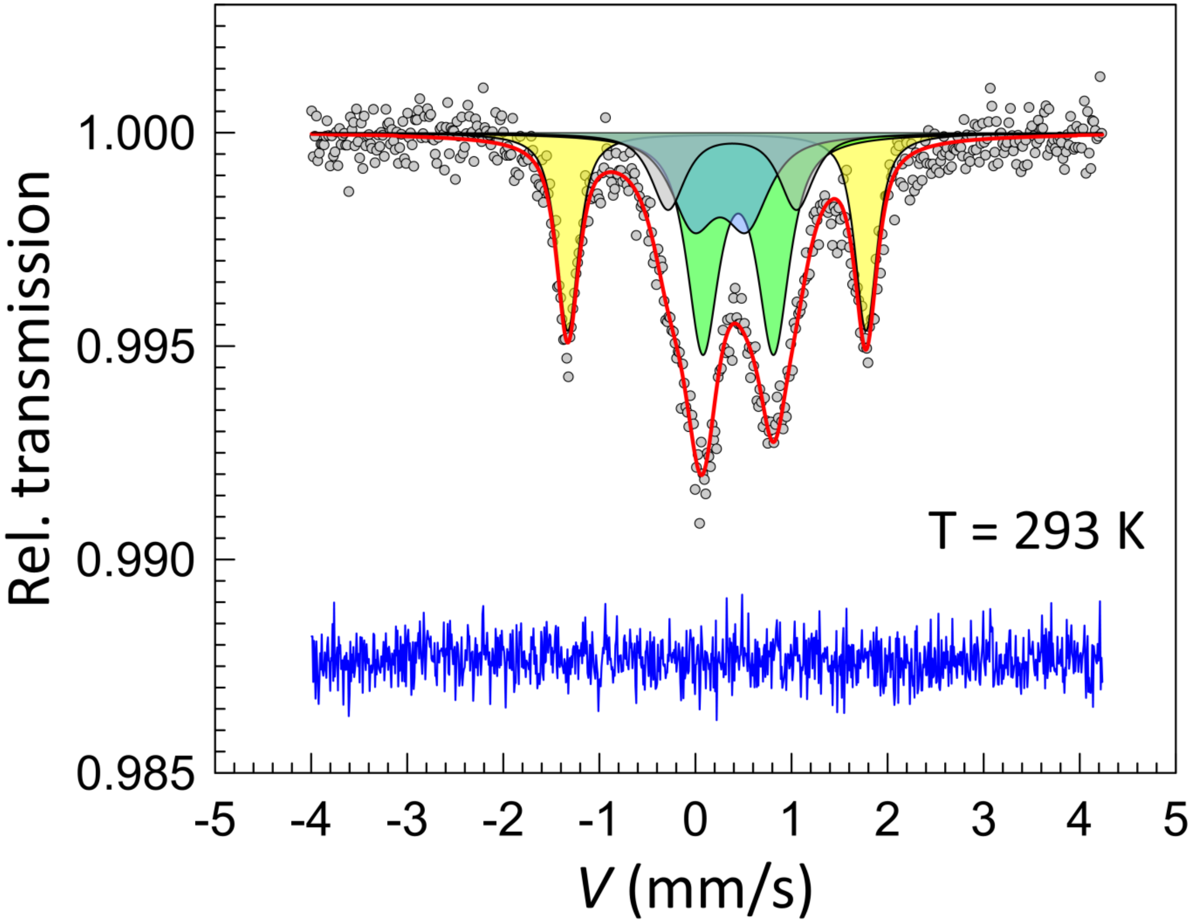

Component	δ, (mm/s)	$|\Delta E_Q|$, (mm/s)	S rel, %	Γ, (mm/s)
Doublet 1	0.2228	3.1045	25.42	0.2761
Doublet 2	0.4455	0.7382	38.27	0.3900
Doublet 3	0.2560	0.5546	21.64	0.5507
Doublet 4	0.3834	1.3369	14.68	0.4180

Mössbauer spectrum of 3c

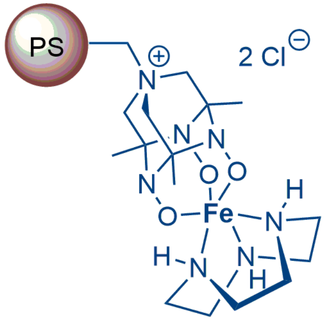

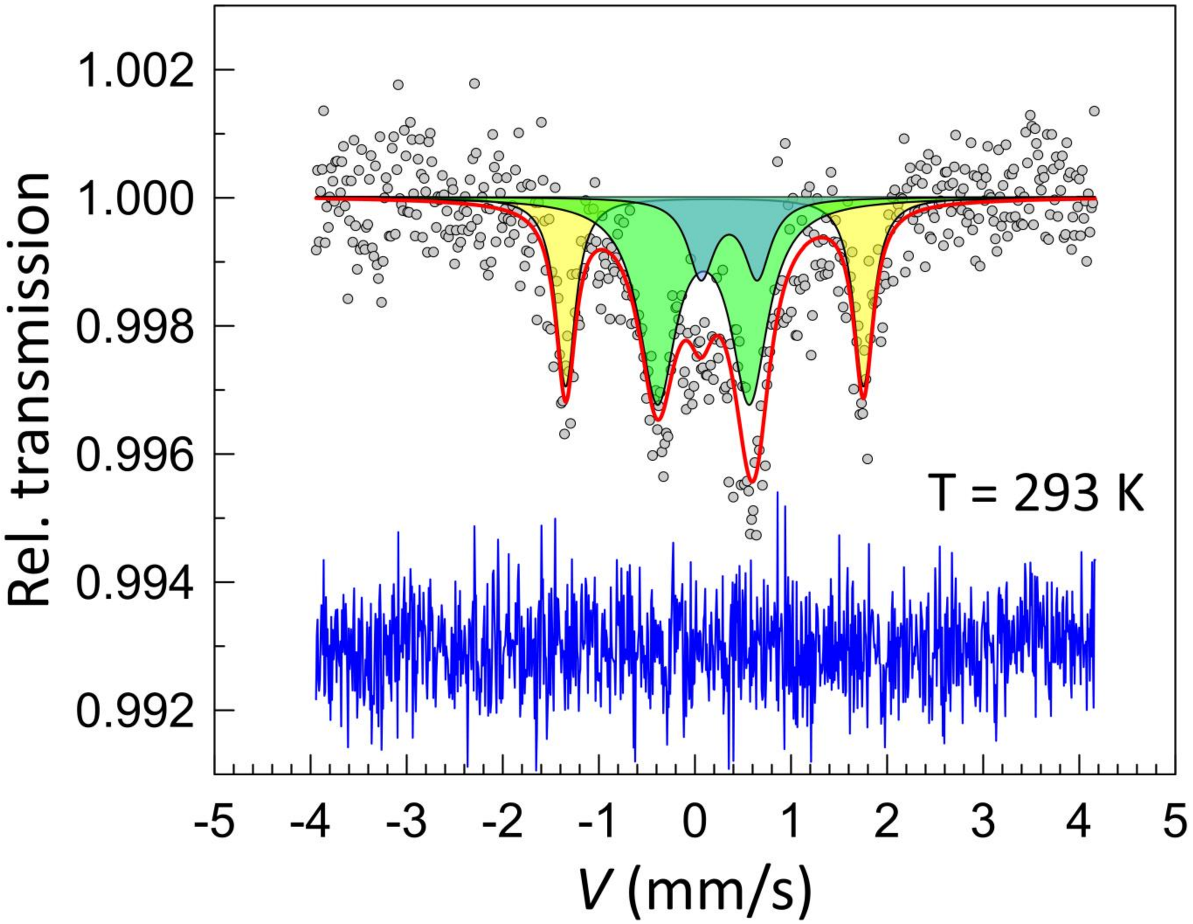

Component	δ, (mm/s)	$\lvert\Delta E_Q\rvert$, (mm/s)	S rel, %	Γ, (mm/s)
Doublet 1	0.2040	3.0992	28.71	0.2477
Doublet 2	0.0885	0.9580	55.47	0.4629
Doublet 3	0.3564	0.5864	15.83	0.3319

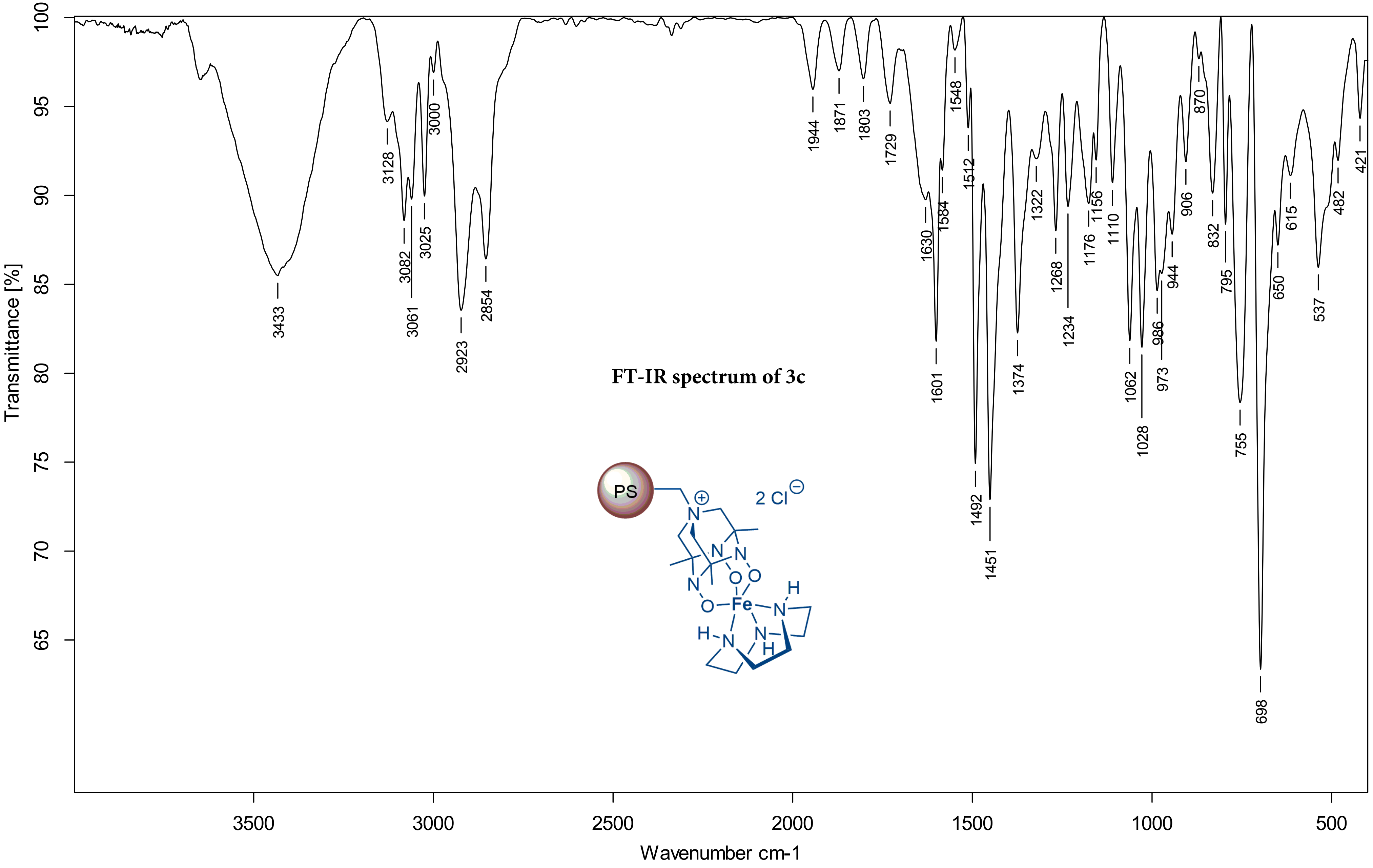
FT-IR spectrum of 3c

4. Aerobic oxidation reactions catalyzed by Fe-TAAD complexes

Oxidation of p-thiocresol (blank experiment without catalyst). A solution of *p*-thiocresol (25 mg, 0.19 mmol) in methanol (1 mL) was stirred in a closed vessel equipped with a magnetic stirrer and an air-filled balloon for 24 hours. The resulting solution was concentrated under reduced pressure. Hexane (2 mL) and water (1 mL) were added to the residue and the mixture was intensively shaken.

Analysis by ^{1}H NMR with internal standard (trichloroethylene) showed that the product is a mixture of unreacted *p*-thiocresol (yield: 64 %) and p-tolyl disulfide (yield: 33 %). GC-MS, retention time: 4.82 min; m/z = 124 ($[M]^{+\bullet}$, p-thiocresol); 10.00 min; m/z = 246 ($[M]^{+\bullet}$, *p*-tolyl disulfide). *p*-Thiocresol: ^{1}H NMR (300 MHz, $CDCl_3$, δ, ppm): 2.32 (s, 3 H), 3.40 (s, 1 H), 7.05 (m, 2 H), 7.19 (m, 2 H).

Aerobic oxidation of p-thiocresol catalyzed by complex 1 in the presence of base. *p*-Thiocresol (25 mg, 0.20 mmol, 100 equiv.) and Et_3N (19 mg, 0.19 mmol, 100 equiv.) were added to a 1 mM solution of complex **1** in methanol (2 mL, 0.002 mmol, 1 equiv.). The mixture was stirred in a closed vessel equipped with a magnetic stirrer and an air-filled balloon for 24 hours. The resulting solution was concentrated under reduced pressure. Hexane (2 mL) and water (1 mL) were added to the residue and the mixture was intensively shaken. The organic phase was collected and the aqueous layer was washed with hexane (2 × 2 mL). The combined organic phase was dried over sodium sulfate, concentrated under reduced pressure and dried until constant weight to give 21 mg (84 %) of *p*-tolyl disulfide as a white solid.

***p*-Tolyl disulfide.** White solid. Mp. 46 °C (Lit.[17] 43–46 °C). GC-MS, retention time 10.01 min; m/z = 246 ($[M]^{+\bullet}$). ^{1}H NMR (300 MHz, $CDCl_3$, δ, ppm): 2.36 (s, 6 H), 7.14 (m, 4 H), 7.43 (m, 4 H). ^{1}H NMR spectrum is in agreement with literature data.[17]

Aerobic oxidation of p-thiocresol catalyzed by polymer supported complex 3c. To a solution of *p*-thiocresol (24 mg, 0.20 mmol) in methanol (1 mL) was added polymer-supported complex **3c** (10 mg, 2 mol% Fe). The mixture was stirred in a closed vessel equipped with a magnetic stirrer and an air-filled balloon for 24 hours. The resulting mixture was concentrated under reduced pressure. Hexane (2 mL) and water (1 mL) were added to the residue and the mixture was intensively shaken. The organic phase was collected and the aqueous layer was washed with hexane (2 × 2 mL). The combined organic phase was dried over sodium sulfate, concentrated under reduced pressure and dried until constant weight to give 23 mg (98%) of *p*-tolyl disulfide as a white solid. GC-MS and ^{1}H NMR data are in agreement with the sample prepared by the reaction catalyzed with complex **1** (see previous procedure).

GC-MS and ^{1}H NMR analyses of aerobic oxidation reactions of *p*-thiocresol

p-Thiocresol (authentic sample)

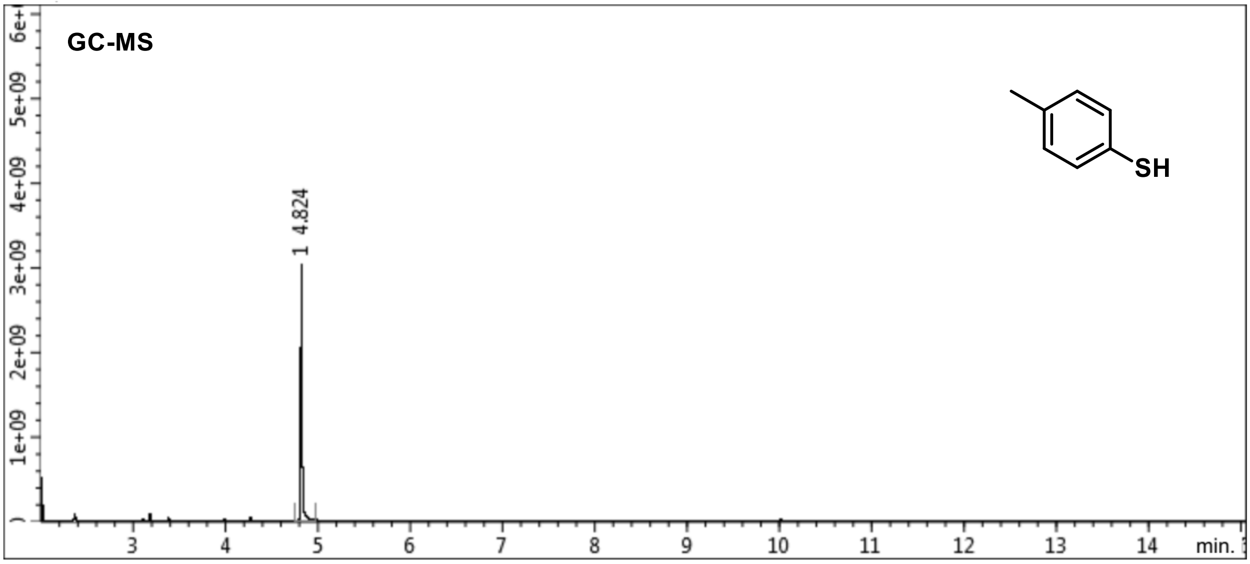

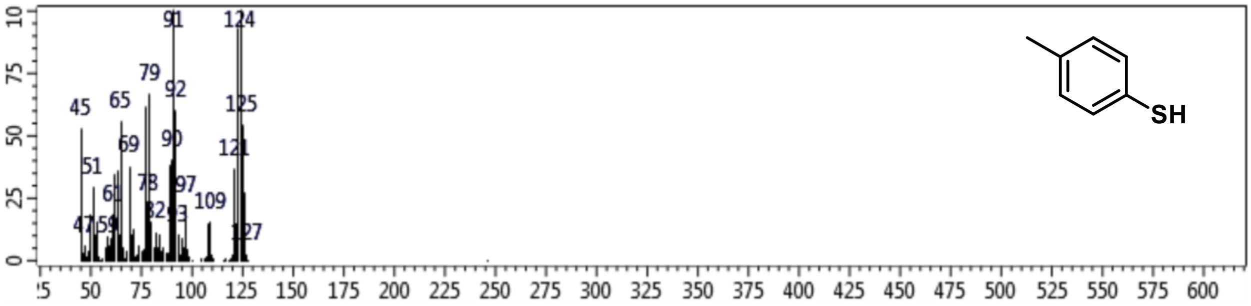

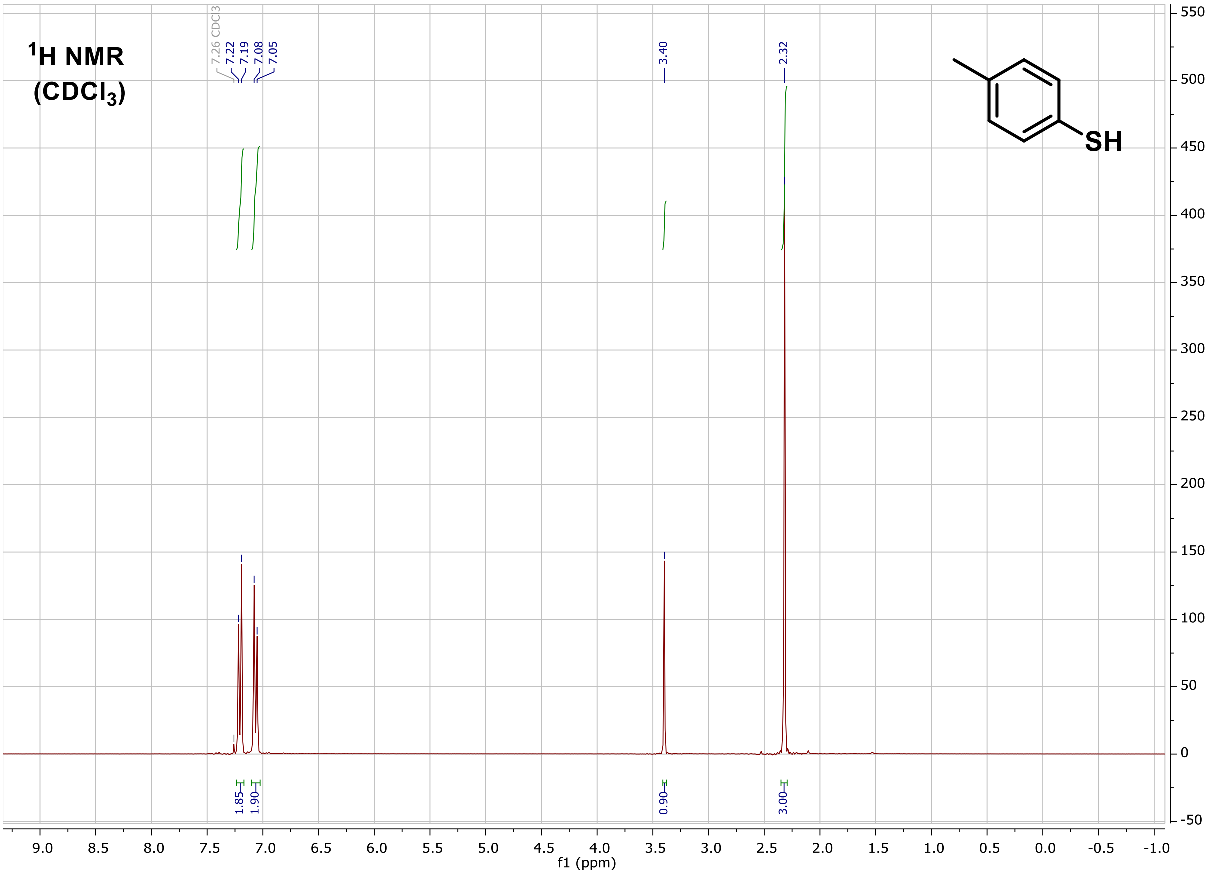

Oxidation of *p*-thiocresol (blank experiment without catalyst)

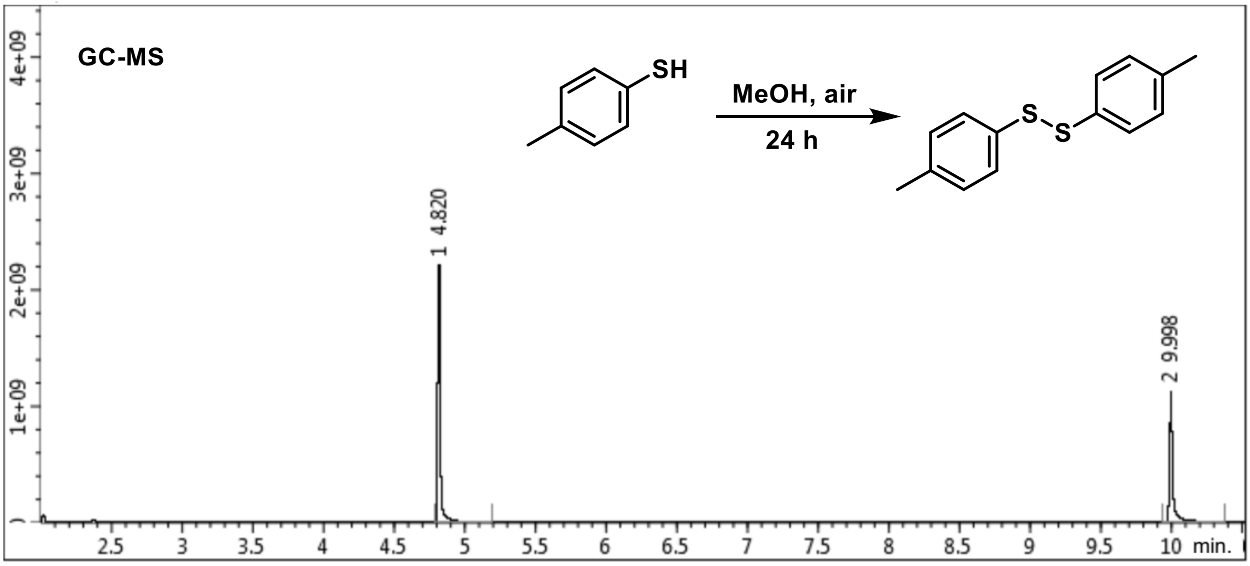

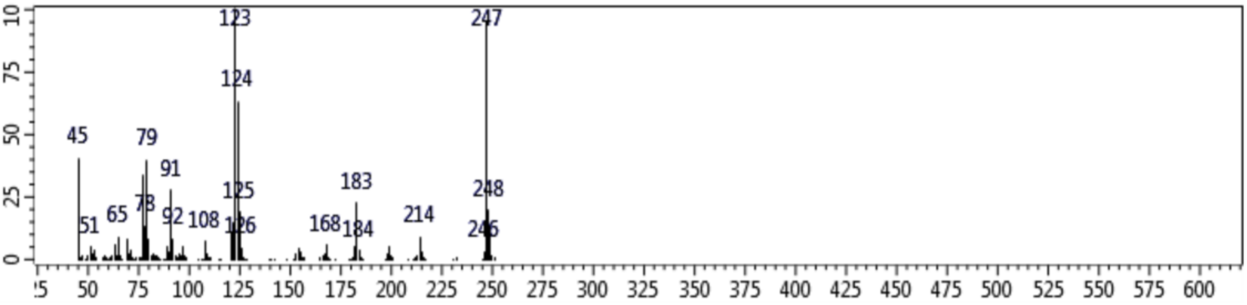

Aerobic oxidation of *p*-thiocresol catalyzed by complex 1 in the presence of base

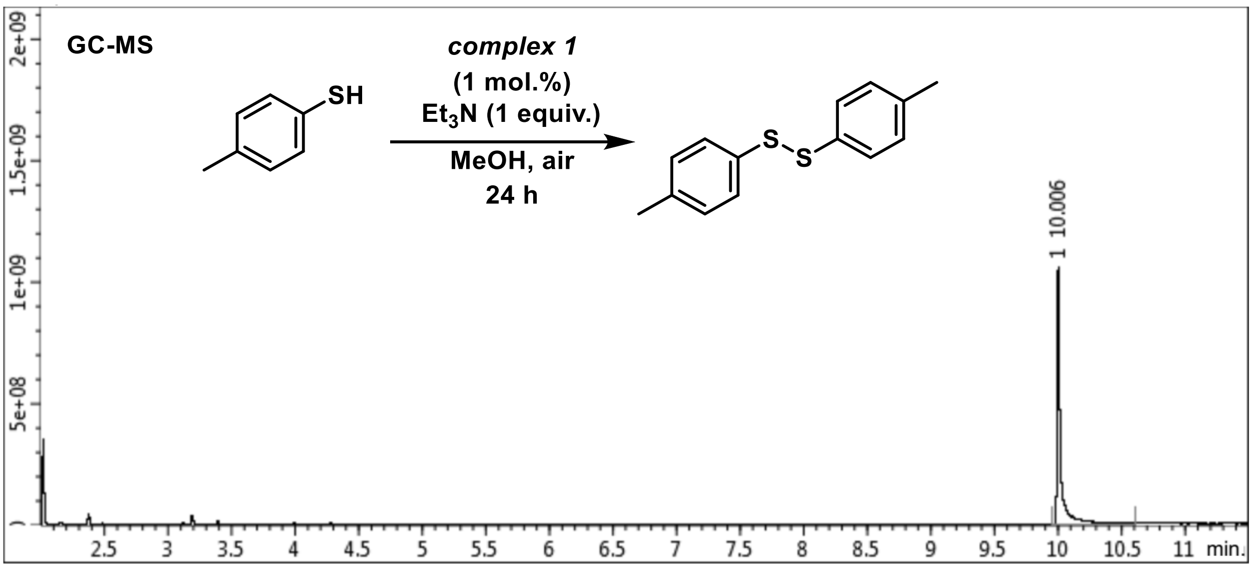

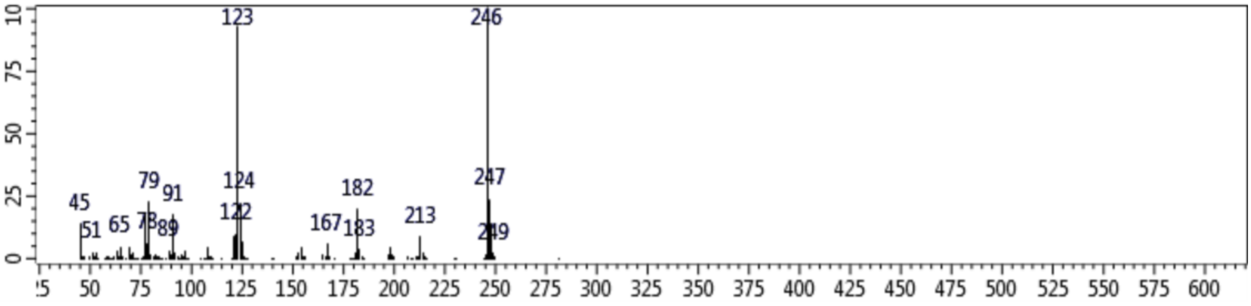

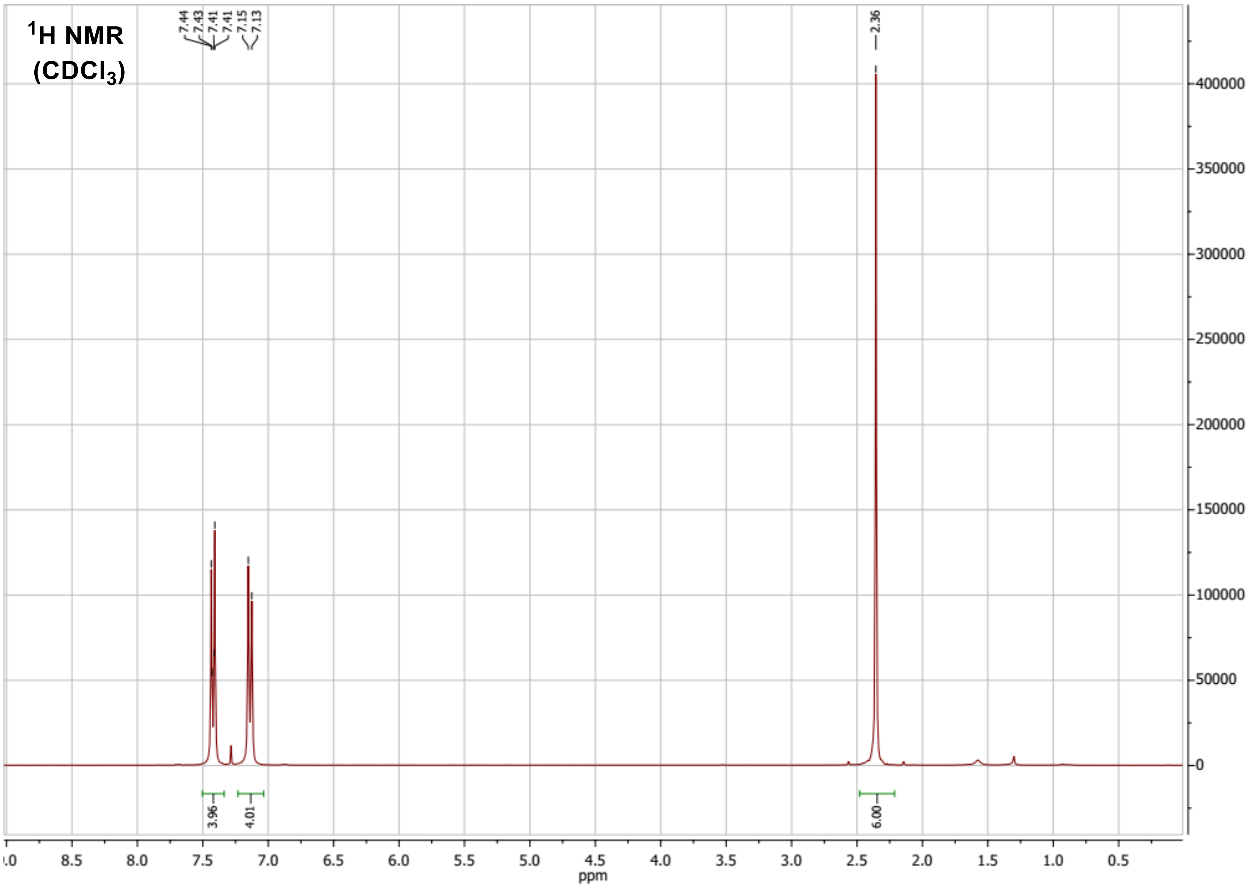

Aerobic oxidation catalyzed by polymer supported complex 3c

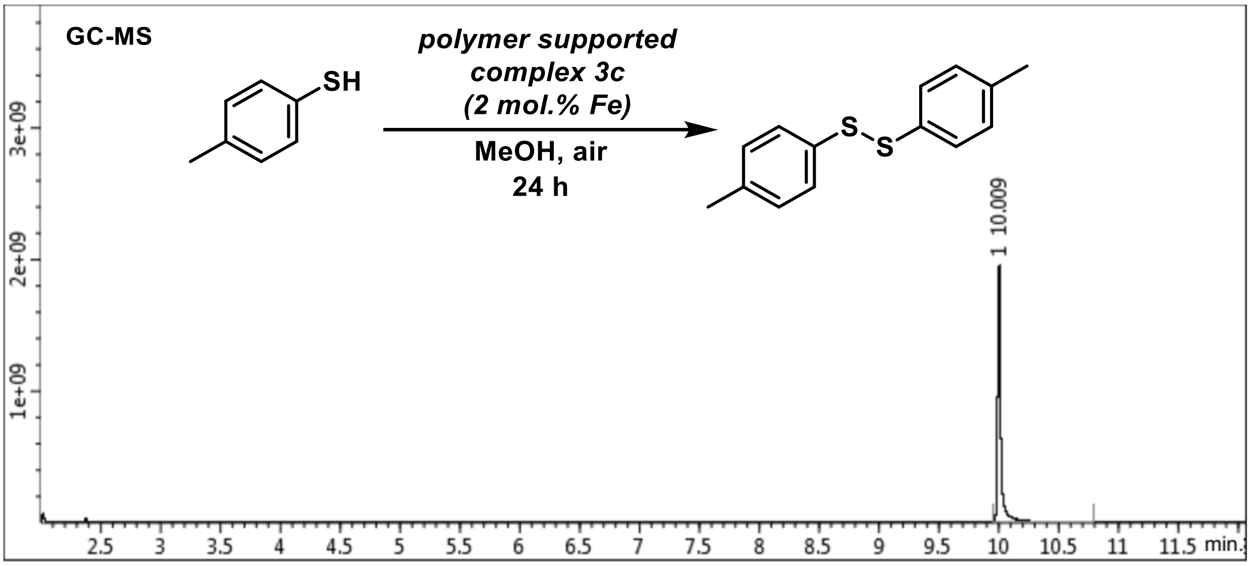

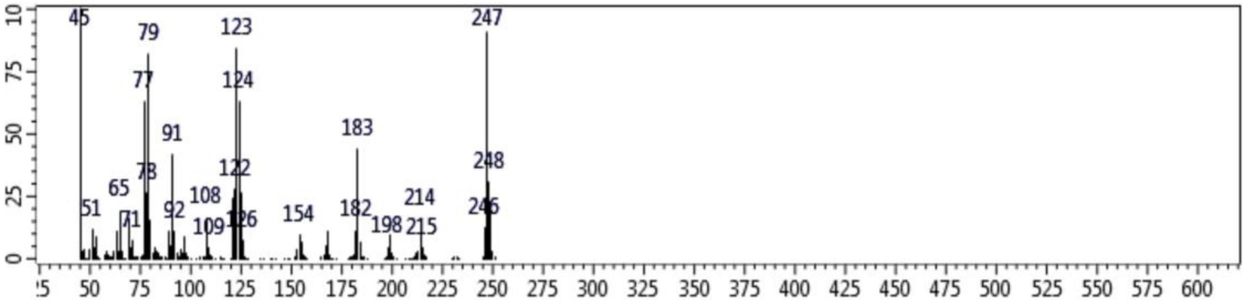

Oxidation of n-heptanethiol by air in the presence of base (blank experiment in the absence of complex 1). A solution of *n*-heptanethiol (21 mg, 0.16 mmol, 1 equiv.) and Et_3N (16 mg, 0.16 mmol, 1 equiv.) in methanol (1 mL) was stirred in a closed vessel equipped with a magnetic stirrer and an air-filled balloon for 24 hours. The resulting solution was evaporated with air flow at room temperature. Diethyl ether (1 mL) and water (1 mL) were added to the residue and the mixture was intensively shaken. The organic phase was collected and the aqueous layer was washed with diethyl ether (2 × 1 mL). The combined organic phase was dried over sodium sulfate. The solvent was evaporated with air flow at room temperature until constant weight. The product was analyzed by GC-MS, which showed no conversion of *n*-heptanethiol.

***n*-Heptanethiol**. GC-MS: retention time 4.50 min; m/z = 132 ($[M]^{+\bullet}$).

Aerobic oxidation of *n*-heptanethiol catalyzed by complex 1. *n*-Heptanethiol (21 mg, 0.16 mmol, 25 μL, 20 equiv.) and Et_3N (16 mg, 0.16 mmol, 20 equiv.) were added to a 4 mM solution of **1** in methanol (2 mL, 0.008 mmol, 1 equiv.). The mixture was stirred in a closed vessel equipped with a magnetic stirrer and an air-filled balloon for 24 hours. The resulting solution was evaporated with airflow at room temperature. Diethyl ether (1 mL) and water (1 mL) were added to the residue and the mixture was intensively shaken. The organic phase was collected and the aqueous layer was washed with diethyl ether (2 × 1 mL). The combined organic phase was dried over sodium sulfate. The solvent was evaporated with airflow at room temperature until constant weight to give 15 mg (72 %) of *n*-heptyl disulfide as a yellow oil.

***n*-Heptyl disulfide.** Yellow oil. GC-MS: retention time 9.38 min; m/z = 262 ($[M]^{+\bullet}$). ^1H NMR (300 MHz, $CDCl_3$, δ, ppm): 0.86 – 0.91 (t, J = 6.8 Hz, 6H), 1.28 – 1.40 (br m, 16H), 1.67 (m, 4H), 2.66 – 2.71 (t, J = 7.3 Hz, 4H). ^1H NMR spectrum is in agreement with literature data.[18]

GC-MS and ^{1}H NMR analyses of aerobic oxidation reactions of *n*-heptanethiol

n-Heptanethiol (authentic sample)

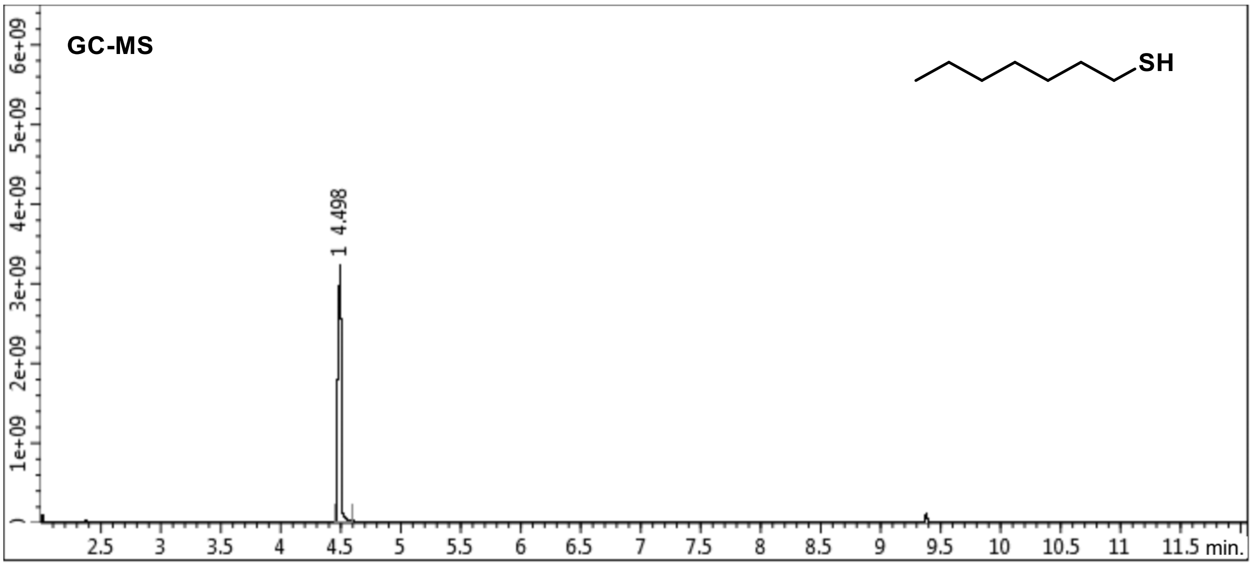

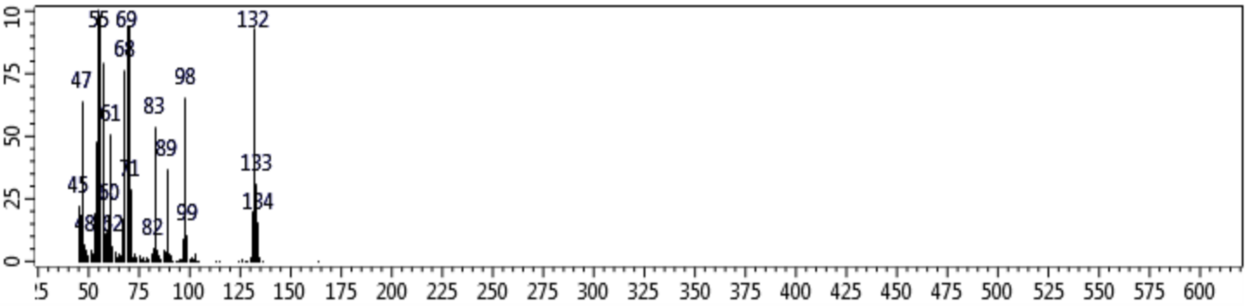

Aerobic oxidation of *n*-heptanethiol catalyzed by complex 1

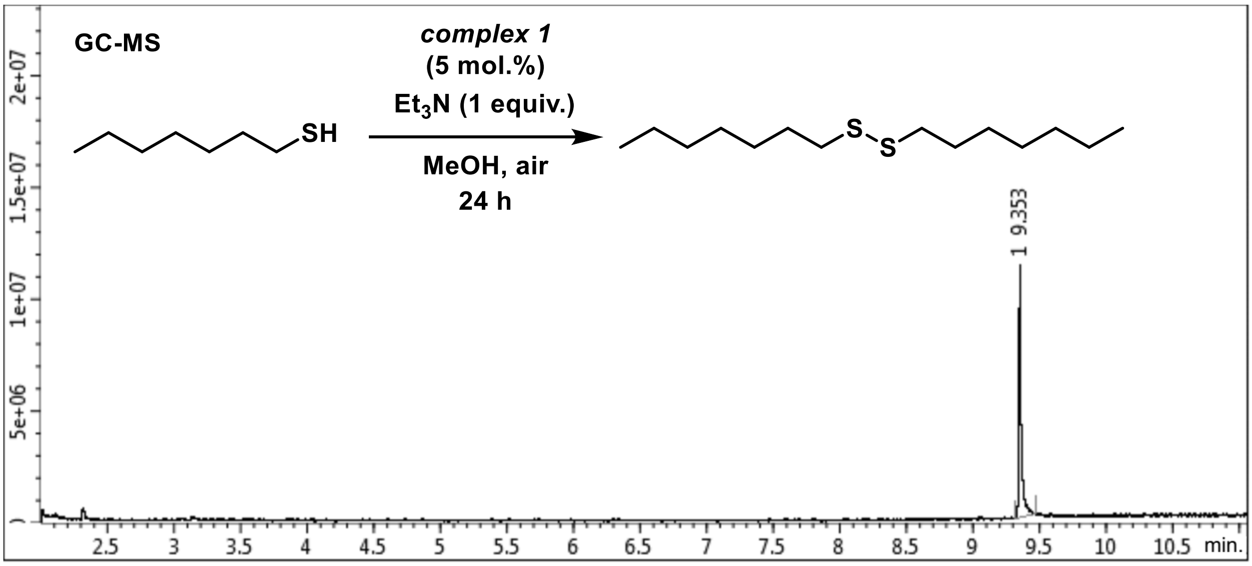

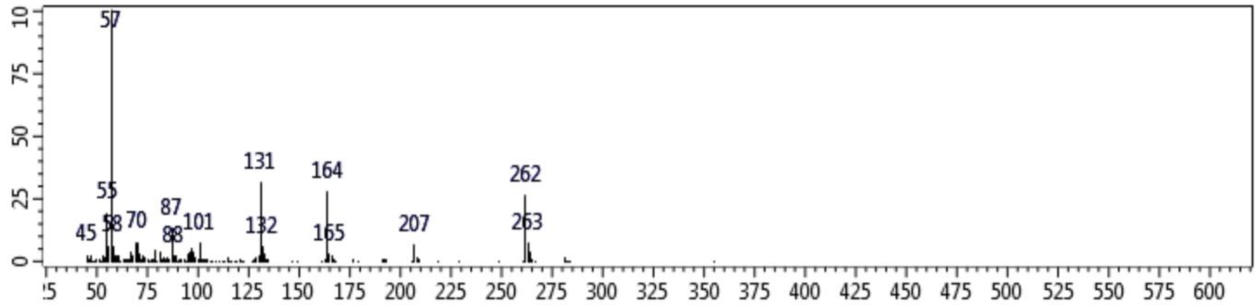

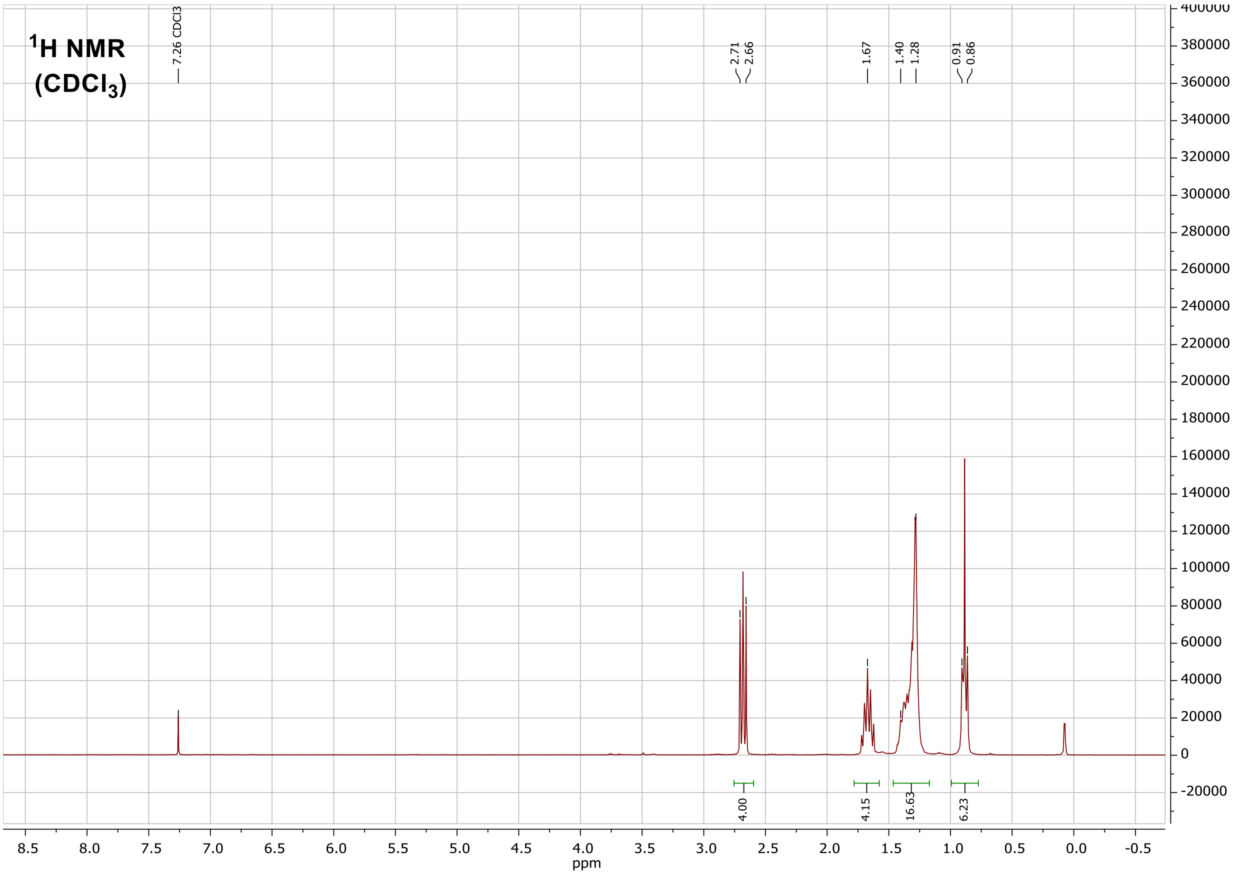

Aerobic oxidation of benzylthiol catalyzed by complex 1. Benzylthiol (25 mg, 0.20 mmol, 20 equiv.) and Et_3N (20 mg, 0.20 mmol, 20 equiv.) were added to a 4 mM solution of complex **1** in methanol (2.5 mL, 0.01 mmol, 1 equiv.). The mixture was stirred in a closed vessel equipped with a magnetic stirrer and an air-filled balloon for 24 hours. The resulting solution was evaporated with airflow at room temperature. Hexane (2 mL) was added to the residue and the mixture was intensively shaken. The organic phase was collected and the residue was washed with hexane (2 × 2 mL). The combined organic phase was dried over sodium sulfate, evaporated with air flow at room temperature until constant weight to give 23 mg (94 %) of benzyl disulfide as a white solid.

Benzyl disulfide. White solid. Mp. 67-69 °C (69-72 °C, Sigma Aldrich). GC-MS: retention time - 10.01 min; m/z = 246 ($[M]^{+\bullet}$). ^1H NMR (300 MHz, $CDCl_3$, δ, ppm): 3.58 (s, 4H), 7.20-7.33 (m, 10H). ^1H NMR spectrum is in agreement with literature data.[19]

GC-MS and ^{1}H NMR analyses of aerobic oxidation reactions of benzylthiol

Aerobic oxidation of benzylthiol catalyzed by complex 1

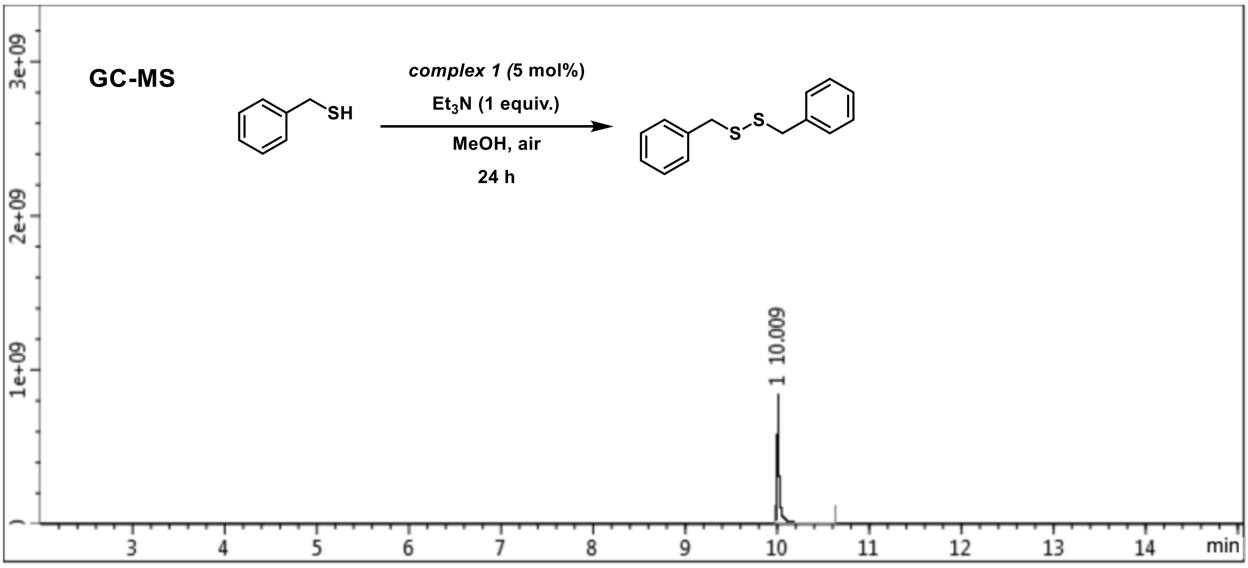

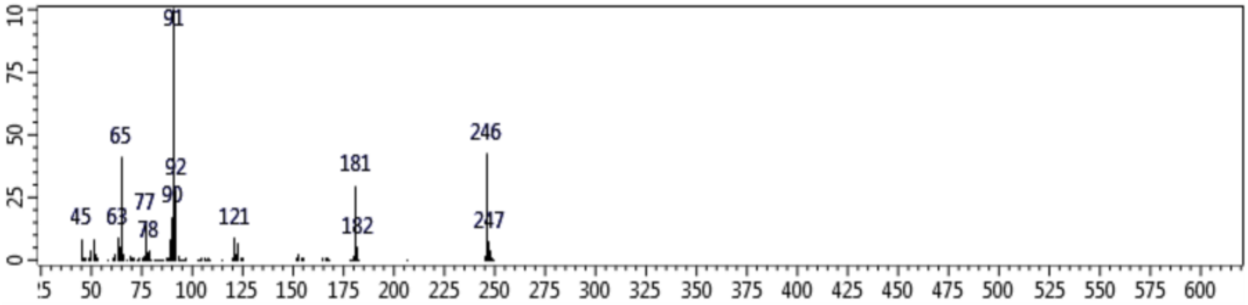

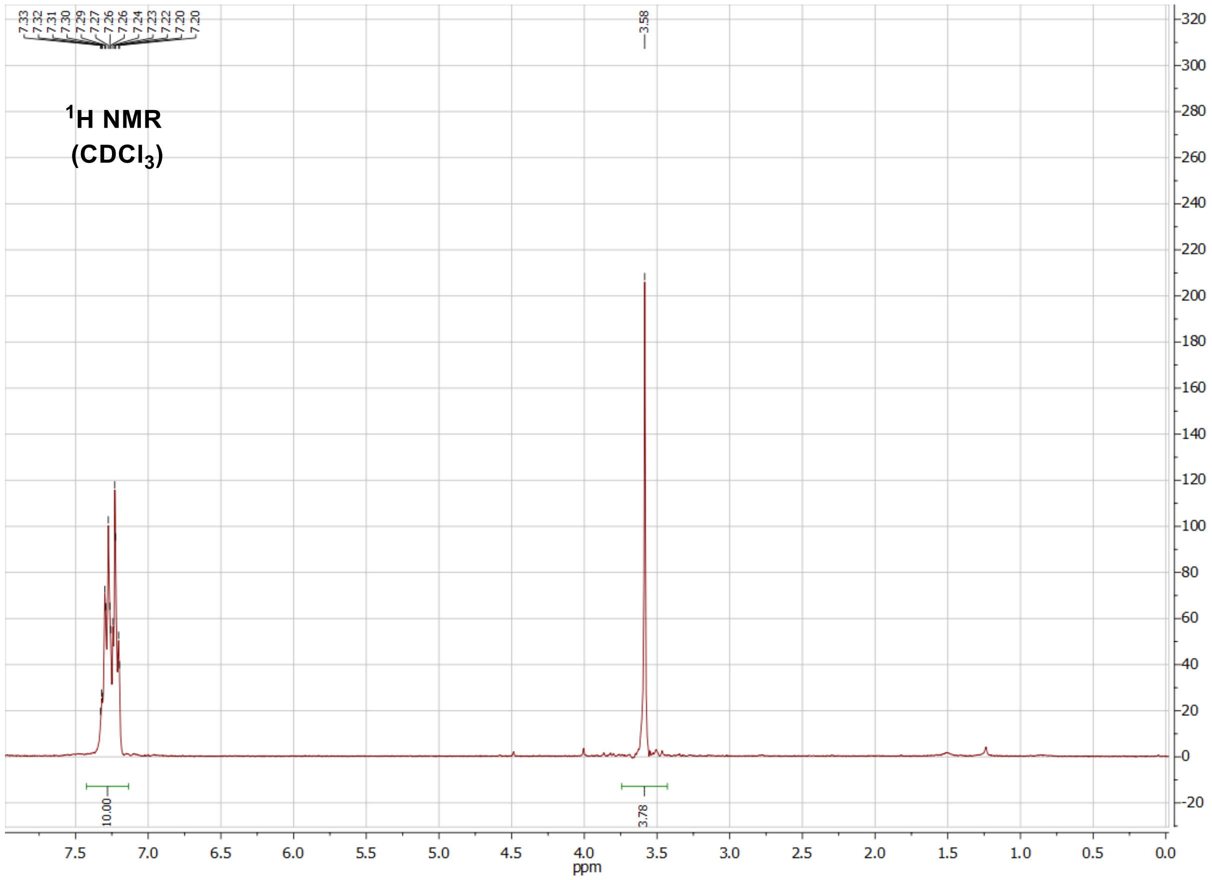

Aerobic oxidation of 2-mercaptoethanol catalyzed by complex 1. 2-Mercaptoethanol (50 mg, 0.64 mmol, 20 equiv.) and Et_3N (65 mg, 0.64 mmol, 20 equiv.) were added to a 4 mM solution of complex **1** in methanol (8 mL, 0.032 mmol, 1 equiv.). The mixture was stirred in a closed vessel equipped with a magnetic stirrer and an air-filled balloon for 24 hours. The resulting solution was evaporated with airflow at rt. Ethyl acetate (5 mL) and water (2 ml) was added to the residue and the mixture was intensively shaken. The organic phase was collected and the aqueous layer was washed with ethyl acetate (3 × 5 mL). The combined organic phase was dried over sodium sulfate, evaporated with air flow at room temperature until constant weight to give 39 mg (80 %) of 2-hydroxyethyl disulfide as a pale yellow liquid.

2-Hydroxyethyl disulfide. Pale yellow liquid**.** GC-MS: retention time 6.93 min; m/z = 154 ($[M]^{+\bullet}$). ^1H NMR (300 MHz, DMSO-d_6, δ, ppm): 2.79 (t, J = 6.5 Hz, 4H), 3.61 (t, J = 6.5 Hz, 4H), 4.82 (m, < 2H, O*H*). ^1H NMR spectrum is in agreement with literature data.[20]

GC-MS and ^{1}H NMR analyses of aerobic oxidation reactions of 2-mercaptoethanol

Aerobic oxidation of 2-mercaptoethanol catalyzed by complex 1

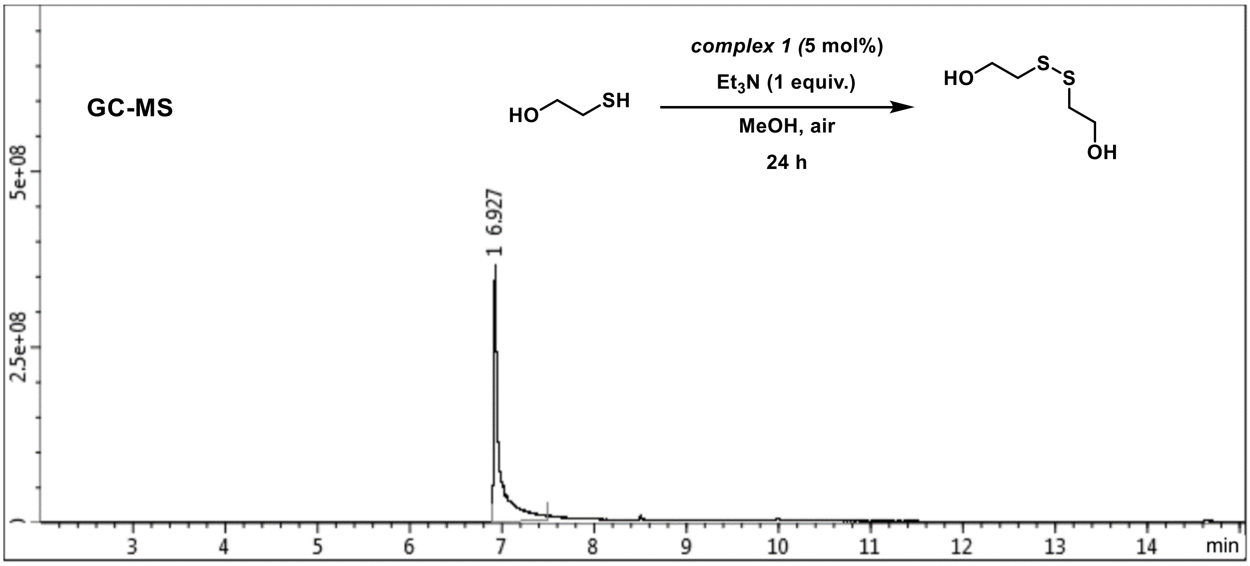

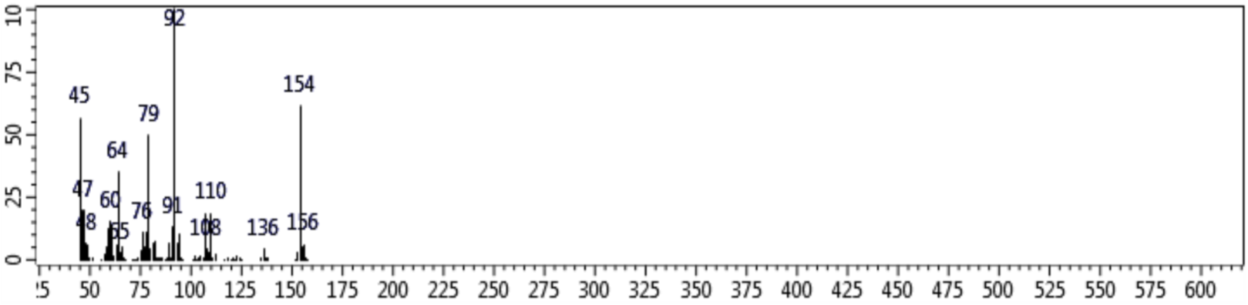

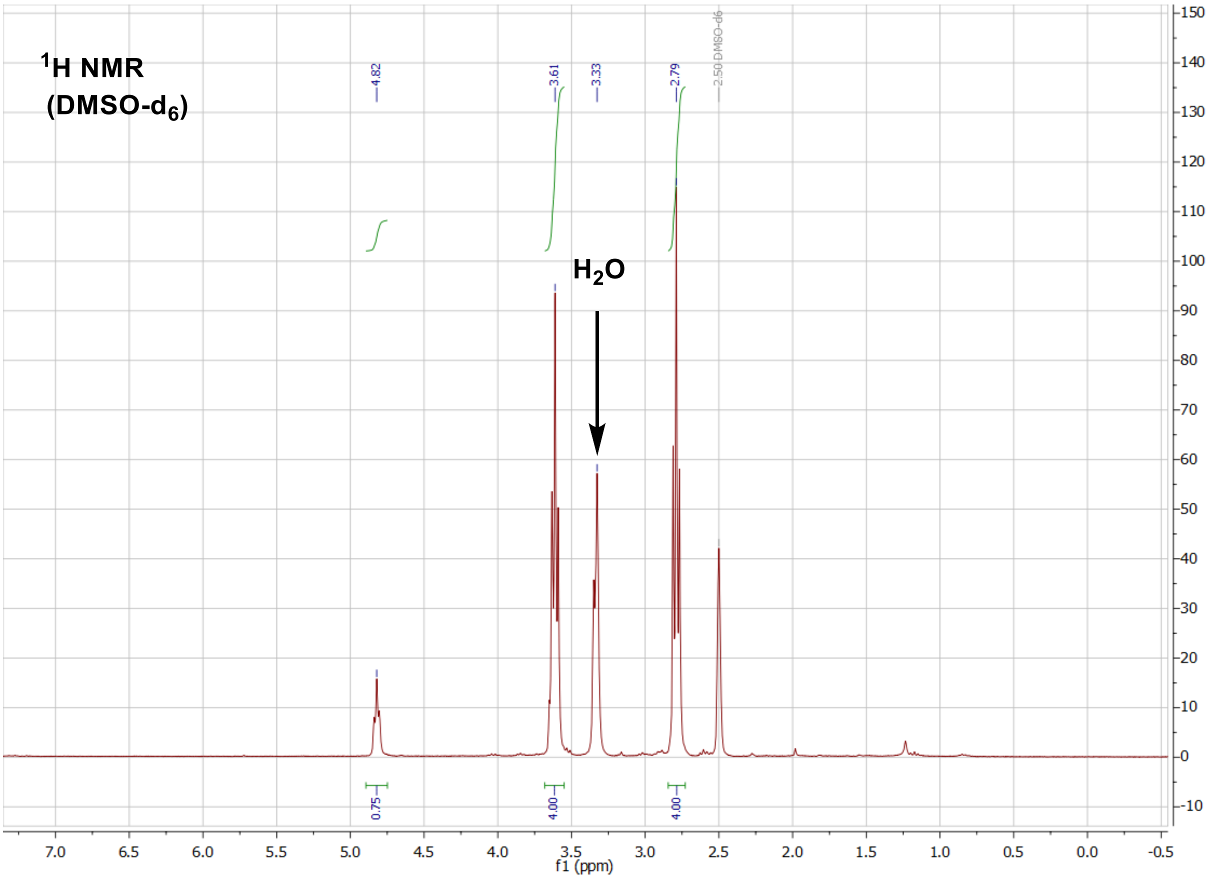

Aerobic oxidation of glutathione by air in the presence of base (blank experiment in the absence of complex 1). Glutathione GSH (9 mg, 0.029 mmol, 1 equiv.) and $NaHCO_3$ (7 mg, 0.087 mmol, 3 equiv.) were dissolved in water (1 ml). The solution was stirred in a closed vessel equipped with a magnetic stirrer and an air-filled balloon for 24 hours. The resulting solution was evaporated under reduced pressure. MeOH was added to the residue and the resulting precipitate was collected, dried under reduced pressure until constant weight and analyzed by NMR. Conversion to disulfide: 29% based on ^1H NMR.

Glutathione (GSH). ^1H NMR (300 MHz, D_2O, δ, ppm): 2.09-2.16 (m, 2H), 2.52 (t, J = 7.6 Hz, 2H), 2.83-2.98 (m, 2H), 3.71 (t, J = 6.2 Hz, 1H), 3.76 (s, 2H), 4.47 (t, J = 6.2 Hz, 1H).

Aerobic oxidation of glutathione catalyzed by complex 1. Glutathione GSH (27 mg, 0.087 mmol, 20 equiv.) and $NaHCO_3$ (21 mg, 0.26 mmol, 60 equiv.) were added to a 1 mM solution of **1** in water (4.35 mL, 4.35 μmol, 1 equiv.). The reaction mixture was stirred in a closed vessel equipped with a magnetic stirrer and an air-filled balloon for 24 hours. The resulting solution was concentrated under reduced pressure and MeOH was added to the residue. The resulting precipitate was separated from the solution and washed with MeOH until the solution became colorless. The residual solid was dried under reduced pressure to give 25 mg (83%) of GSSG sodium salt as a white solid.

Glutathione disulfide (GSSG) sodium salt. White solid. ^1H NMR (300 MHz, D_2O, δ, ppm): 1.95 (m, 4H), 2.25–2.52 (m, 4H), 2.87 (dd, J = 14.3, 9.7 Hz, 2H), 3.21 (dd, J = 14.3, 4.5 Hz, 2H), 3.45 (t, J = 6.3 Hz, 2H), 3.65 (d, J = 20.9 Hz, 2H), 3.72 (d, J = 20.9 Hz, 2H), 4.67 (m, 2H). ^1H NMR spectrum of glutathione disulfide is in agreement with literature data.[21]

^{1}H NMR analysis of aerobic oxidation reactions of glutathione

Glutathione (authentic sample)

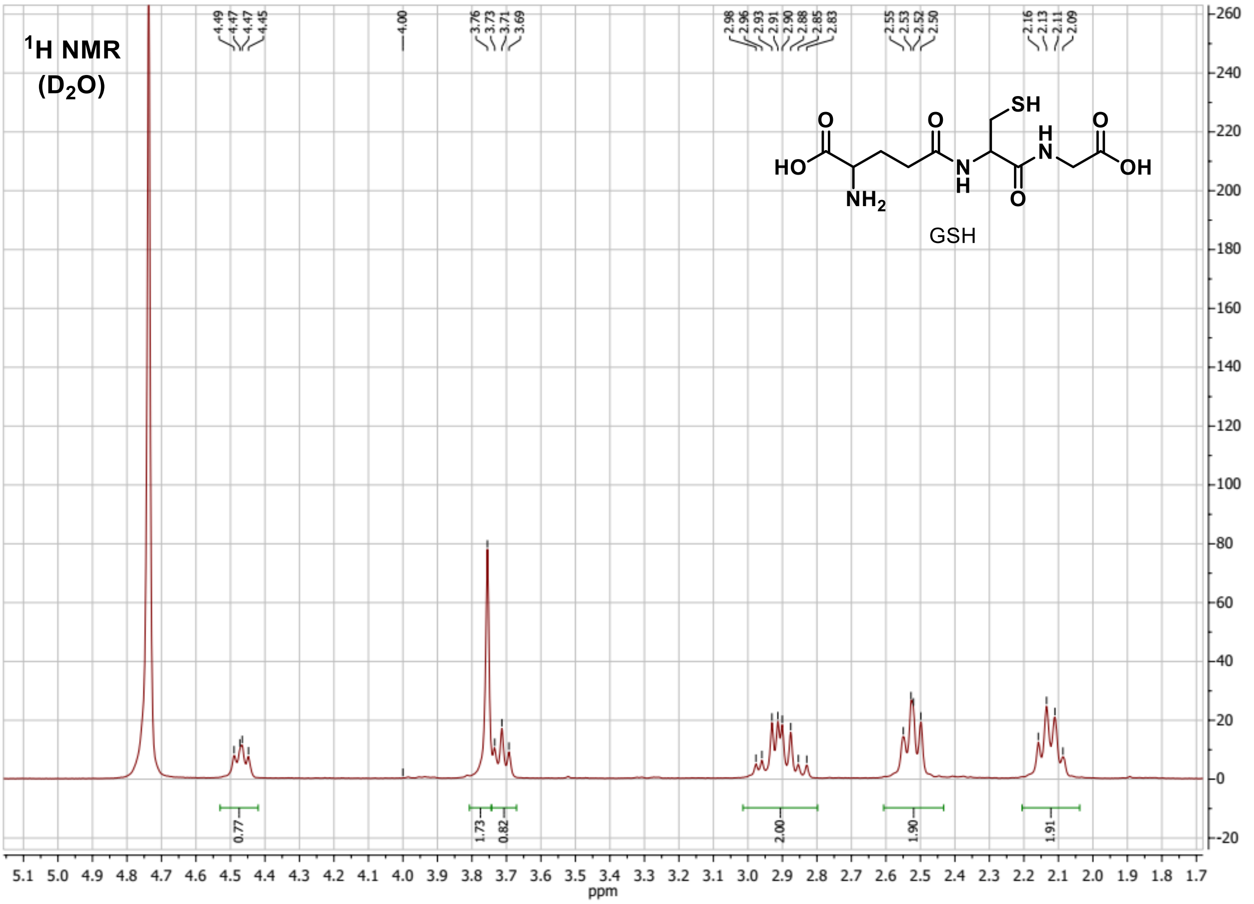

Aerobic oxidation of GSH by air in the presence of base (without catalyst)

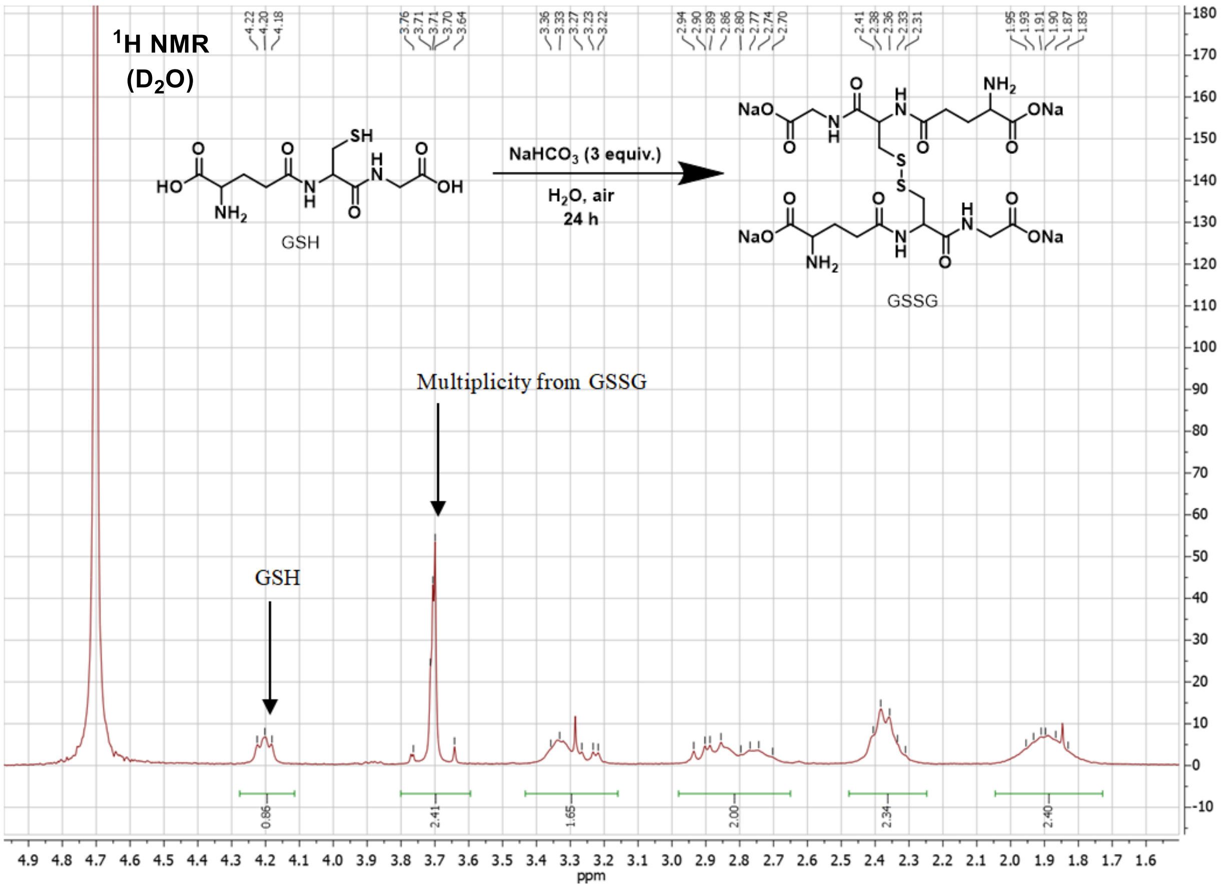

Aerobic oxidation catalyzed by complex 1

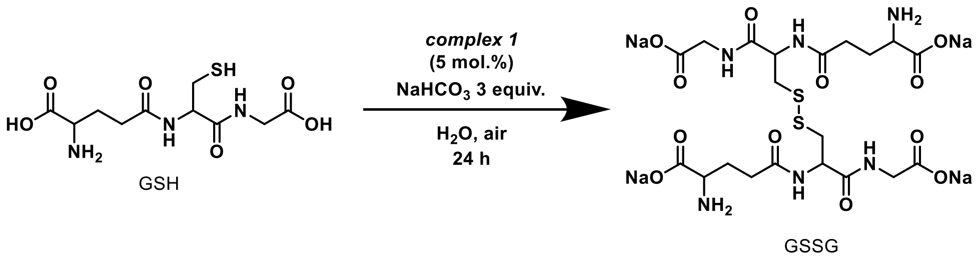

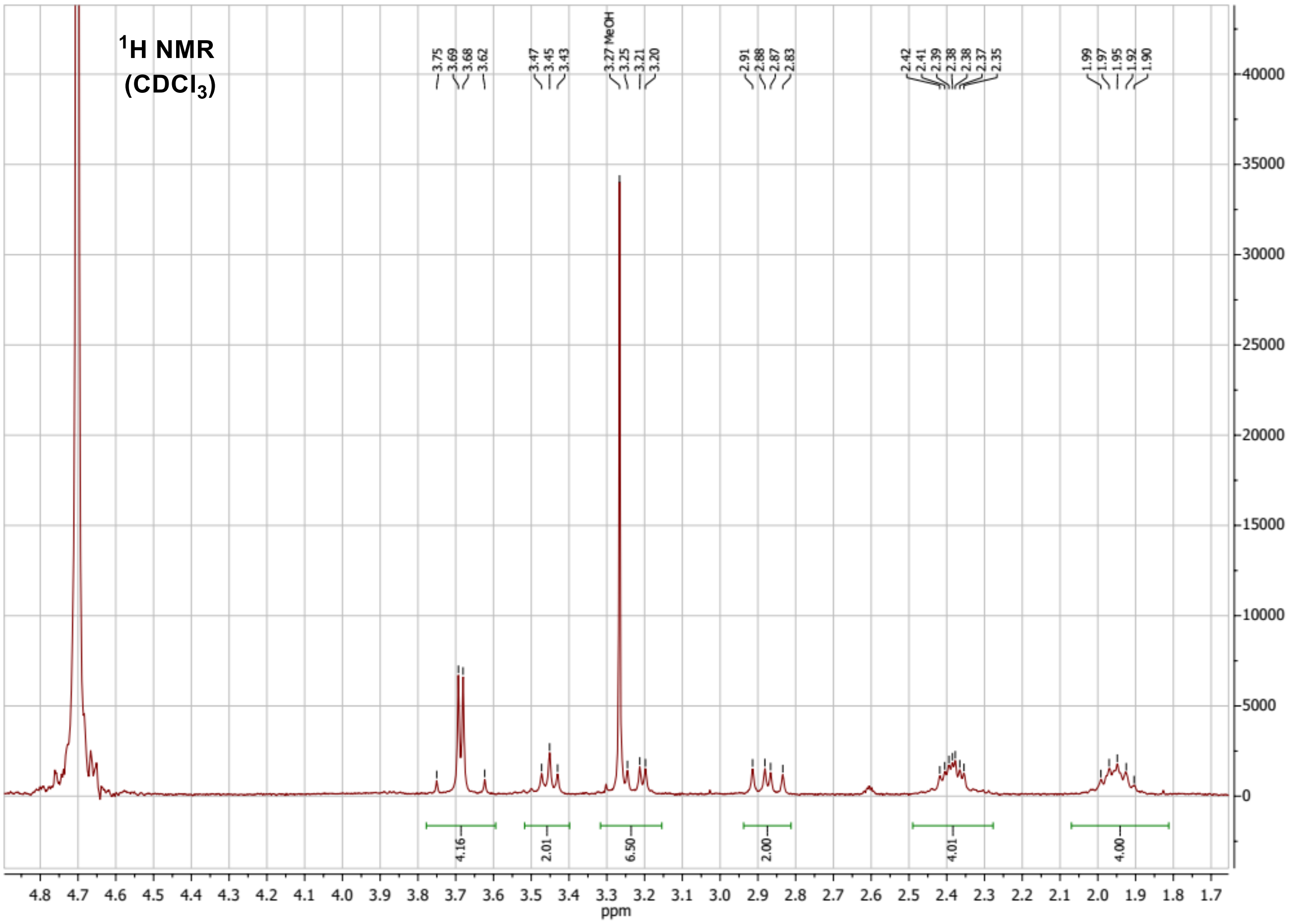

Table S3. Comparison of various iron-based catalytic systems for aerobic oxidation of thiols to disulfides.

Catalytic system for aerobic oxidation of thiols	Mol% catalyst	Oxidant	Reaction temperature	Scope of thiols (yields)	Comment	Ref
$Fe(NO_3)_3•9H_2O$, THF	10	dioxygen	rt	only benzylthiol (26 %)	- poor catalytic activity	22
$Fe(NO_3)_3•9H_2O$, MeCN	18	dioxygen	70 ^oC	only thiophenol (57 %)	- poor catalytic activity	23
$FeCl_3$, THF	10	dioxygen	rt	only benzylthiol (89 %)	- high catalyst loading - substrate scope not studied	22
Fe_2O_3, MeOH	6	dioxygen	rt	only thiophenol (conversion 85 %)	- high catalyst loading - substrate scope not studied	24
$[Cp^*Fe(MeCN)_3][PF_6]$, THF	1	dioxygen	rt	only thiophenol (9 %)	- poor catalytic activity	25
Tris-benzimidazole iron(II) complexes, MeCN	5	dioxygen	rt	only *p*-thiocresol (18-29 %)	- non-chemoselective due to over-oxidation	26
FeBTC (MOF based iron 1,3,5-benzenetricarboxylate), MeCN	20	dioxygen	70 ^oC	- aromatic (80-91 %), - heteroaromatic (72-81 %), - aliphatic (61-72 %), - thiocarboxylic acids (0-55 %), - functionalized thiols (n.i.), - biothiols (n.i.)	- high catalyst loading - elevated reaction temperature	23
Iron phthalocyanine (FePc), THF	3	air	rt	- aromatic (97-99 %), - heteroaromatic (n.i.), - aliphatic (97-99 %), - thiocarboxylic acids (n.i.), - functionalized thiols (n.i.), - biothiols (n.i.)	- investigated substrate scope is narrow	22
Graphene-immobilized FePc, H_2O, *hν* (visible light)	1	dioxygen	rt	- aromatic (75-84 %), - heteroaromatic (n.i.),	- investigated substrate scope is	27

				- aliphatic (91-98 %), - thiocarboxylic acids (n.i.), - functionalized thiols (n.i.), - biothiols (n.i.)	narrow - dioxygen atmosphere - conversion ca. 80 % - irradiation	
Thiolate-bridged iron–ruthenium complex, H_2O	1	dioxygen	rt	- aromatic (89-90 %), - heteroaromatic (n.i.), - aliphatic (only benzylthiol, 82 %), - thiocarboxylic acids (n.i.), - functionalized thiols (n.i.), - biothiols (94-97 %)	- use of precious metal (ruthenium) - investigated substrate scope is narrow	25
Fe(IV)-TAAD complex, MeOH (H_2O), base	1-5	air	rt	- aromatic (84 %), - heteroaromatic (n.i.), - aliphatic (72 - 93 %), - thiocarboxylic acids (n.i.), - functionalized thiols (79 %), - biothiols (83 %)		This work

5. X-ray and powder XRD data for 1

Crystallographic data: Crystals of **1** ($C_{16}H_{34}ClFeN_7O_4$, M = 479.80) are orthorhombic, space group Pbca, at 120 K: a = 18.597(13), b = 13.184(9), c = 19.167(13) Å, V = 4700(6) Å^3, Z = 8 (Z' = 1), d_{calc} = 1.356 g*cm^{-3}, μ(MoKα) = 7.90 cm^{-1}, F(000) = 2032. Intensities of 43471 reflections were measured with a Bruker APEX2 DUO CCD diffractometer [λ(MoKα) = 0.71073 Å, ω-scans, 2<θ52°] and 4610 independent reflections were used in the further refinement. Using Olex2,[28] the structure was solved with the ShelXT[29] structure solution program using Intrinsic Phasing and refined with the XL[30] refinement package using Least-Squares minimisation. Hydrogen atoms of NH and OH groups were located from difference Fourier synthesis while positions of others were calculated, and they all were refined in the isotropic approximation within the riding model. The refinement converged to wR2 = 0.1653 and GOF = 0.915 for all the independent reflections (R1 = 0.0678 was calculated against F for 1872 observed reflections with I>2σ(I))**.** CCDC 2110176 contains the supplementary crystallographic information for this paper.

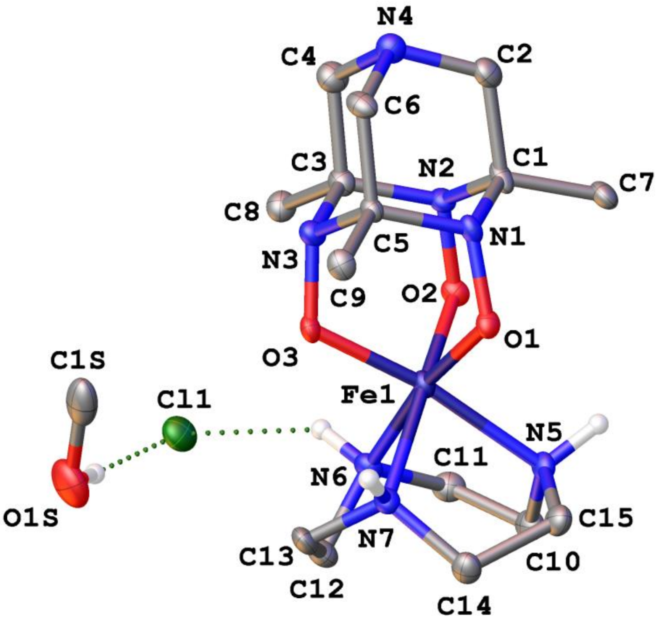

Figure S1. General view of the complex **1** in representation of non-hydrogen atoms as thermal ellipsoids at 30% probability level. Hydrogen atoms except those of the NH and OH groups are omitted for clarity.

To quantify the coordination environment of the iron (IV) ion, continuous symmetry measures were used[31] that measure how close is the shape of the coordination polyhedron to a reference shape, such as an ideal octahedron (OC) or an ideal trigonal prism (TPR). The lower the value of an appropriate symmetry measure, the better is the fit; for example, S(OC) would be zero for an ideal octahedron. For the complex **1**, the symmetry measures S(OC) and S(TPR) evaluated from the X-ray diffraction data are 0.309 and 14.007, respectively, thus confirming a very small deviation of the shape of the coordination polyhedron from an ideal octahedron.

Powder XRD analysis recorded 90 days after isolation of the complex **1** has shown that composition of sample can be described as complex **1** with unidentified impurities. The results of Pawley fit (Figure S2) started from experimental parameters at 100K converged to following values: a = 18.557(3), b = 13.4540(7), c = 19.161(3) Å, Rwp = 4.27%. Residual curve demonstrated the presence of several maxima related to unidentified crystal phase d = 8.36, 5.78, 4.88, 3.87, 3.66 and 3.10 Å. The volume ratio between complex **1** and unidentified crystalline phase is approximately 10:1. The latter value was evaluated from integral intensity related to diffraction maxima of crystalline phases in **1**. The values of volume-weighted mean crystallite sizes for complex **1** and unidentified phases (78.5(9) and 67(4) nm) calculated using fundamental parameters scheme and integral breadth has shown that all crystalline phases can be described as nano-scale.

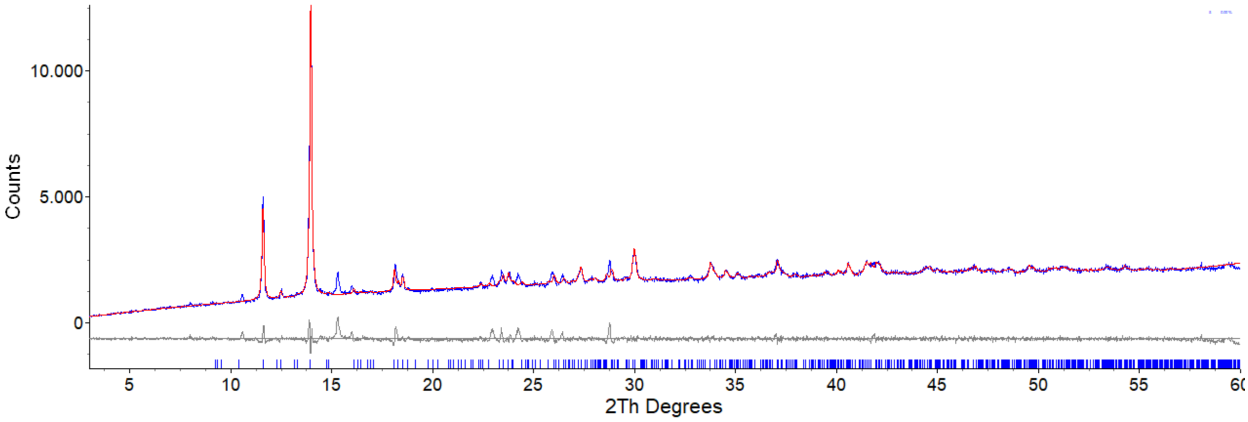

Figure S2. XRD pattern of sample **1**. The experimental, calculated using Pawley fit and residual curves are shown by blue, red and grey color, respectively.

6. Study of stability of complex 1 in MeOH

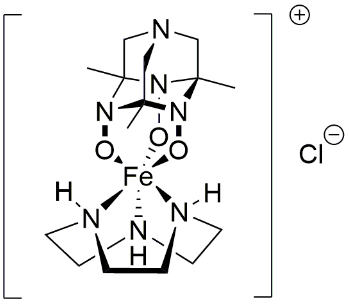

1

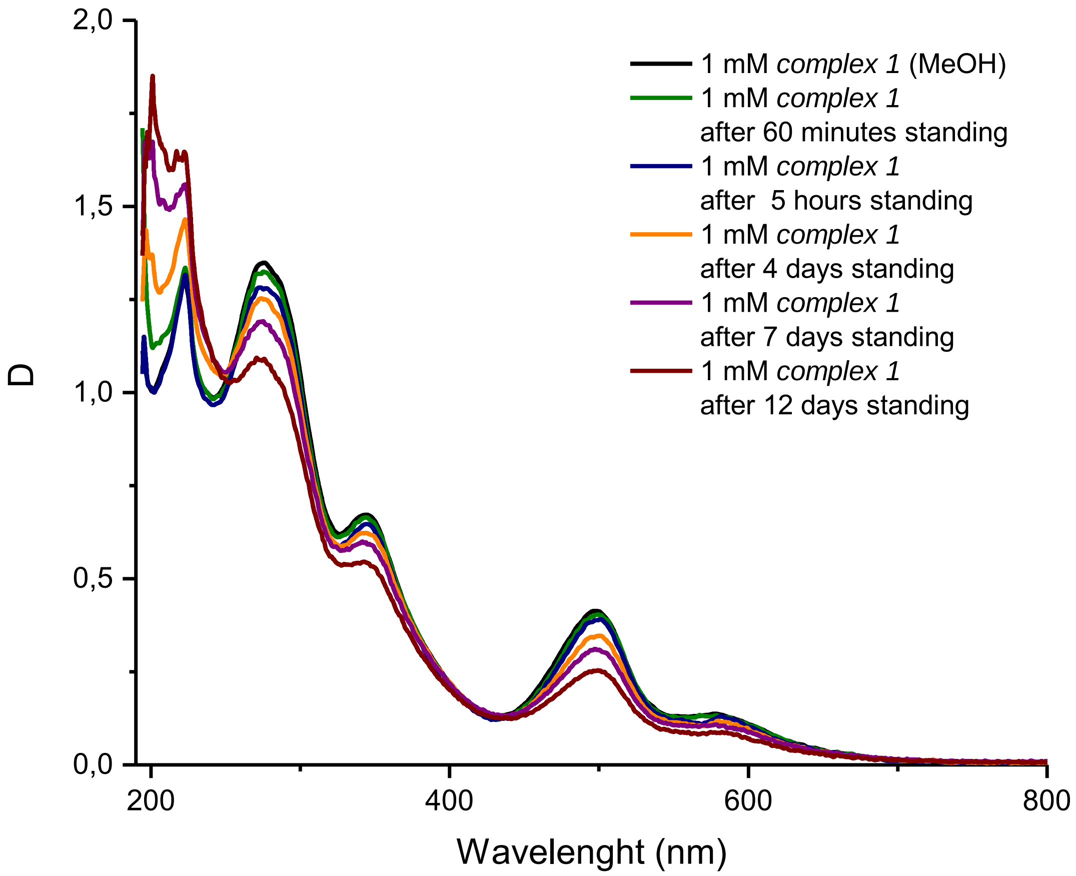

Figure S3. UV-Vis monitoring of complex **1** in MeOH. UV-Vis **s**pectra were recorded for 1mM solutions of complex **1** in methanol at room temperature (methanol was used as background).

7. NMR spectroscopy and Evans method for complex 1

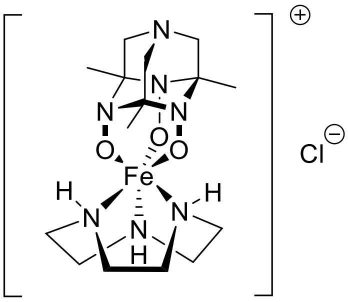

1

Table S4. Results of the Evans method for the [Fe(IV)(TAAD)(TACN)]Cl (**1**) complex at 305 K (400 MHz, CD_3OD).

Compound	**Δδ, ppm**	**C (mg/ml)**	**χT, cm^3*mol^{-1}*K**	**μ_{eff}, μ_B**
[Fe(IV)(*TAAD*)(*TACN*)]Cl (**1**)	0.13	2.8	1.58	3.55

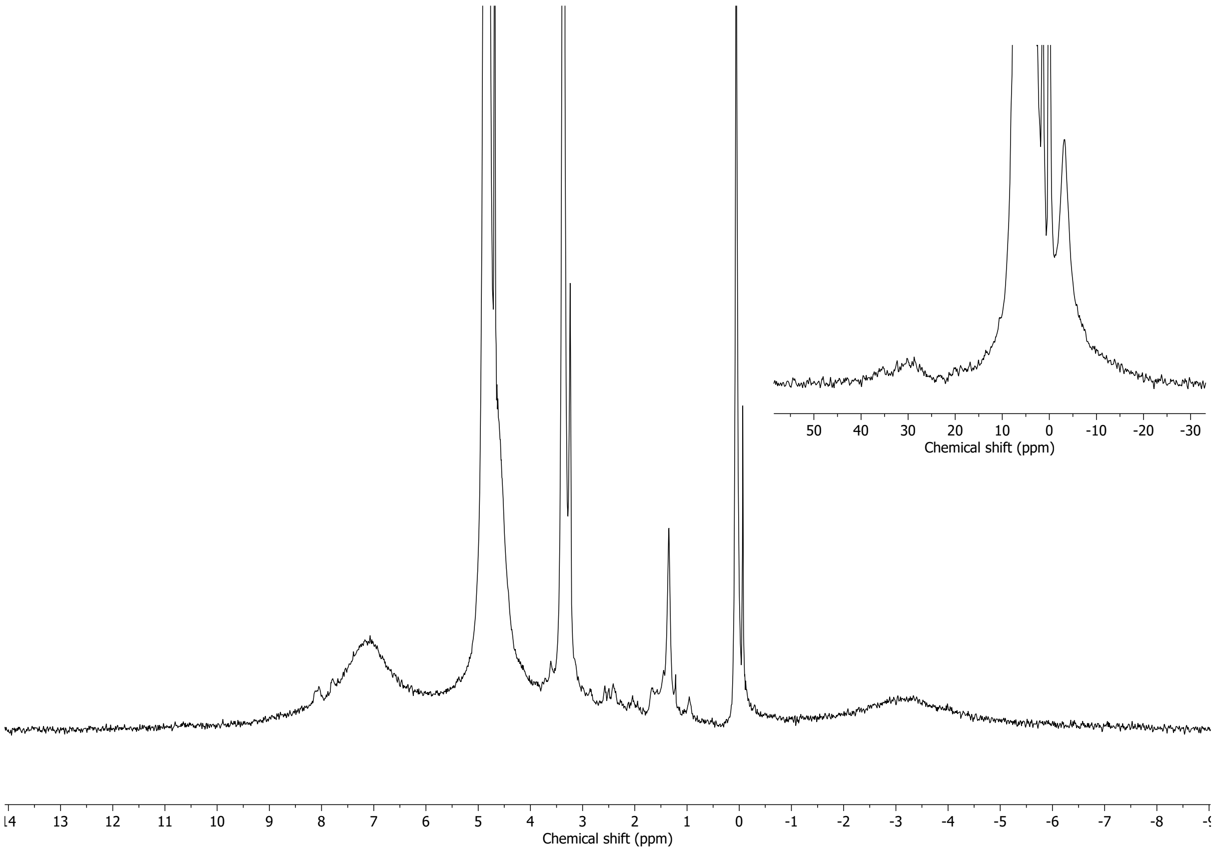

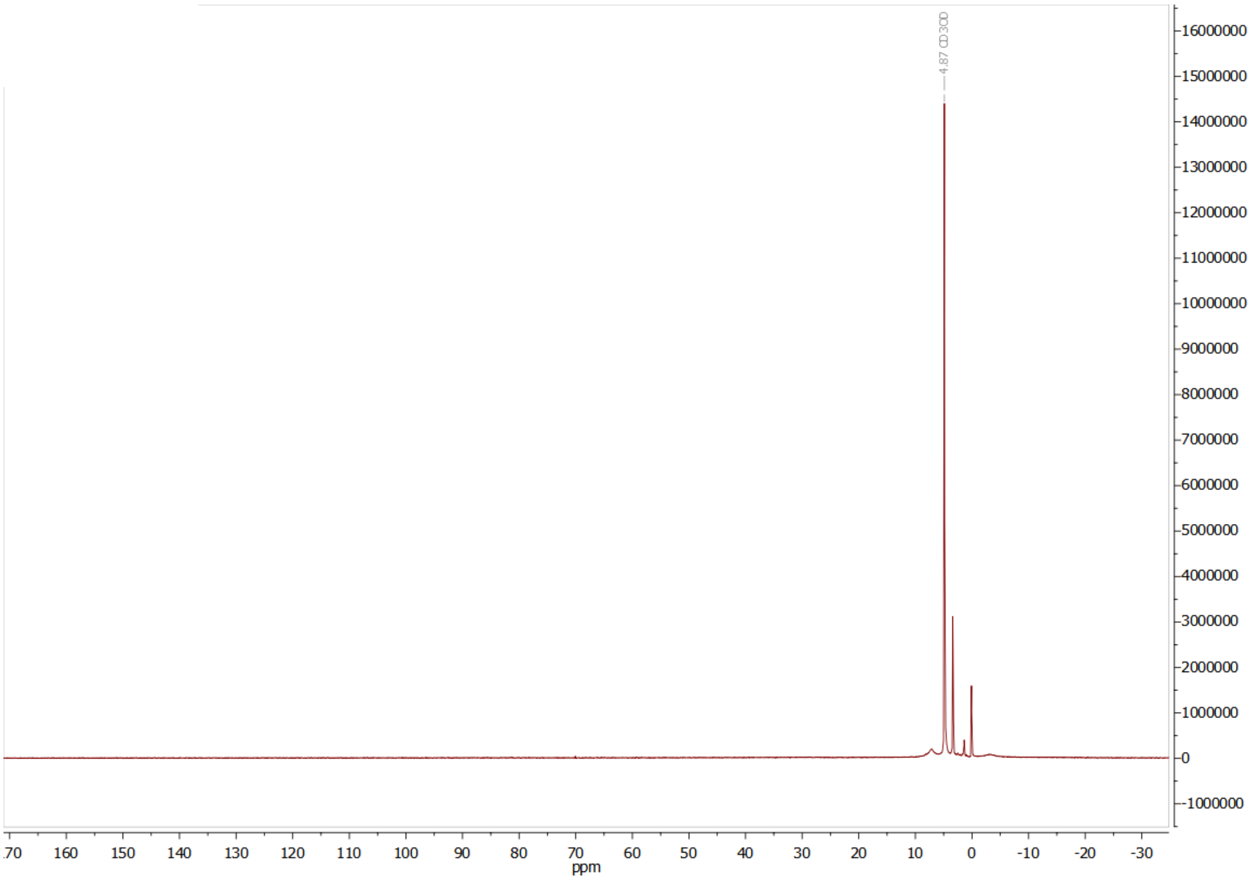
4.87 CD3OD
16000000
15000000
14000000
13000000
12000000
11000000
10000000
9000000
8000000
7000000
6000000
5000000
4000000
3000000
2000000
1000000
0
-1000000
70
160
150
140
130
120
110
100
90
80
70
60
50
40
30
20
10
0
-10
-20
-30
ppm

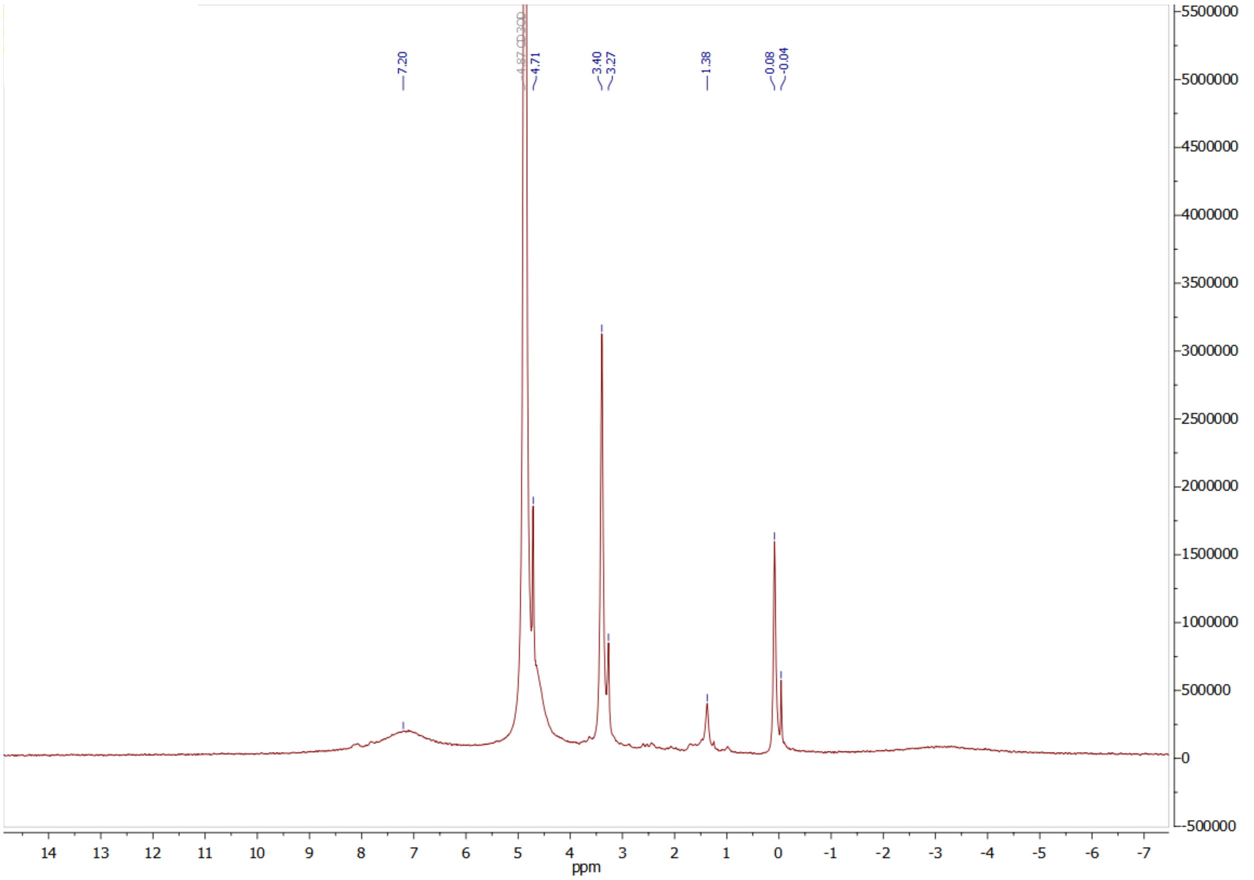
7.20
4.87 CD3OD
4.71
3.40
3.27
1.38
0.08
-0.04
5500000
5000000
4500000
4000000
3500000
3000000
2500000
2000000
1500000
1000000
500000
0
-500000
14
13
12
11
10
9
8
7
6
5
4
3
2
1
0
-1
-2
-3
-4
-5
-6
-7
ppm

8. Electrochemical properties of complex 1

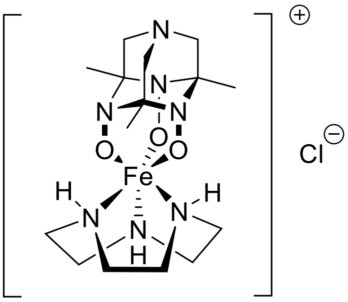

1

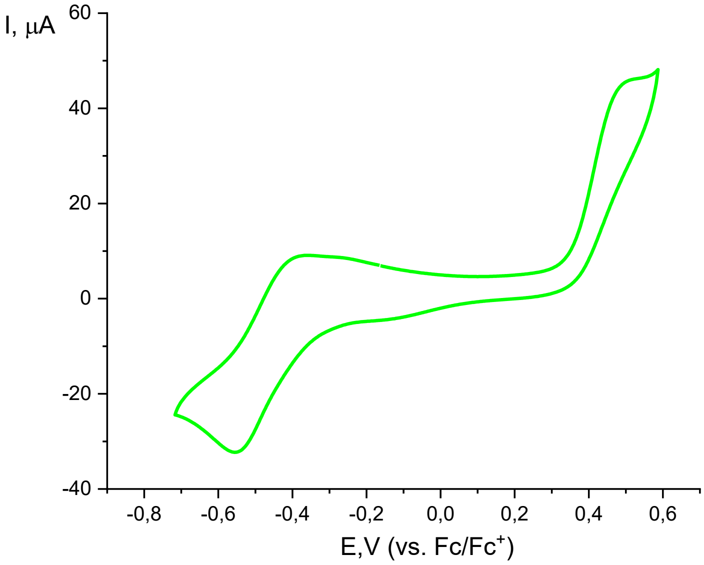

Figure S4. CV for 1 mM dimethylformamide solution of [Fe(IV)(TAAD)(TACN)]Cl **1** with 0.1 M (n-$(C_4H_9)_4N)PF_6$ as a supporting electrolyte. Conditions: scan rate 100 mV*s^{-1}, 298 K, platinum working and counter electrodes, Ag/AgCl reference electrode, the potentials are referenced to Fc/Fc$^+$ couple. A minor feature observed at -0.2 V corresponds to a small admixture of unclear origin in a supporting electrolyte.

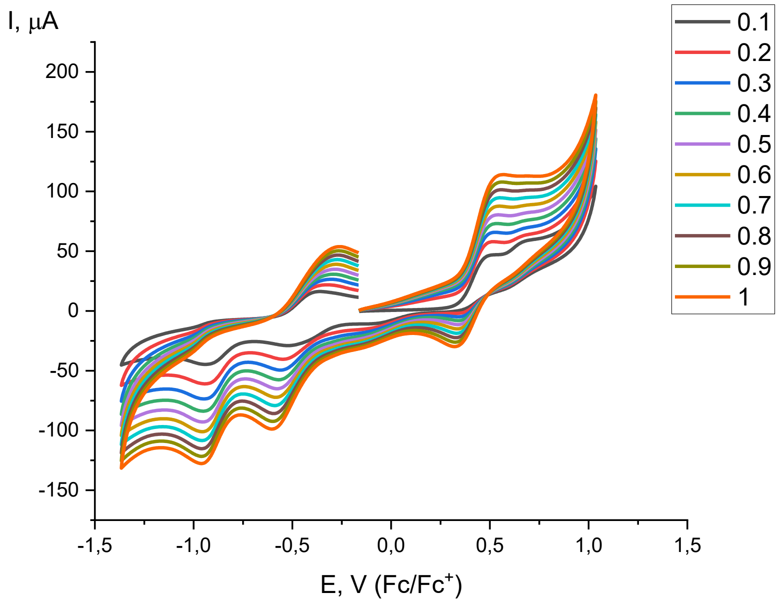

Figure S5. CV for 1 mM dimethylformamide solution of the iron complex **1** with 0.1 M (n-$(C_4H_9)_4N)PF_6$ as a supporting electrolyte at various scan rates between 0.1 and 1 V*s^{-1}. Conditions: 298 K, platinum working and counter electrodes, Ag/AgCl reference electrode, the potentials are referenced to Fc/Fc$^+$ couple.

9. Mössbauer spectra of complex 1 at different temperatures and DFT calculations of δ and ΔE_Q for 1

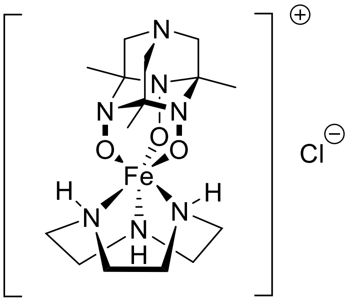

1

Mössbauer spectra within temperature range from 10 K to 293 K (Table S5, Figures S6-S9) have characteristic paramagnetic view and are well approximated by doublet. Given an octahedral coordination geometry of **1**, the observed hyperfine parameters of Mössbauer spectra are consistent with the values expected for Fe^{4+} ions with two unpaired electrons (S = 1).[32, 33] Large quadrupole splitting values $|\Delta E_Q| \approx 3$ mm/s point to relatively high value of electric field gradient. Such values are presumably arising from stretching along the axis of gradient. Mossbauer spectrum of complex **1** after 100 days reveals 30% of decomposition (Figure S6).

Table S5. Hyperfine parameters of Mössbauer spectra of **1** at different temperatures after 100 days.

Compound	T, (K)	δ, (mm/s)	$|\Delta E_Q|$, (mm/s)	Γ, (mm/s)
Complex **1** doublet Fe^{4+}	293	0.28	3.20	0.25
	180	0.34	3.20	0.27
	80	0.35	3.19	0.27
	10	0.36	3.18	0.26

T – temperature, δ – isomer shift, ΔE_Q – quadrupole splitting, Γ – full width at half-maximum of the signal.

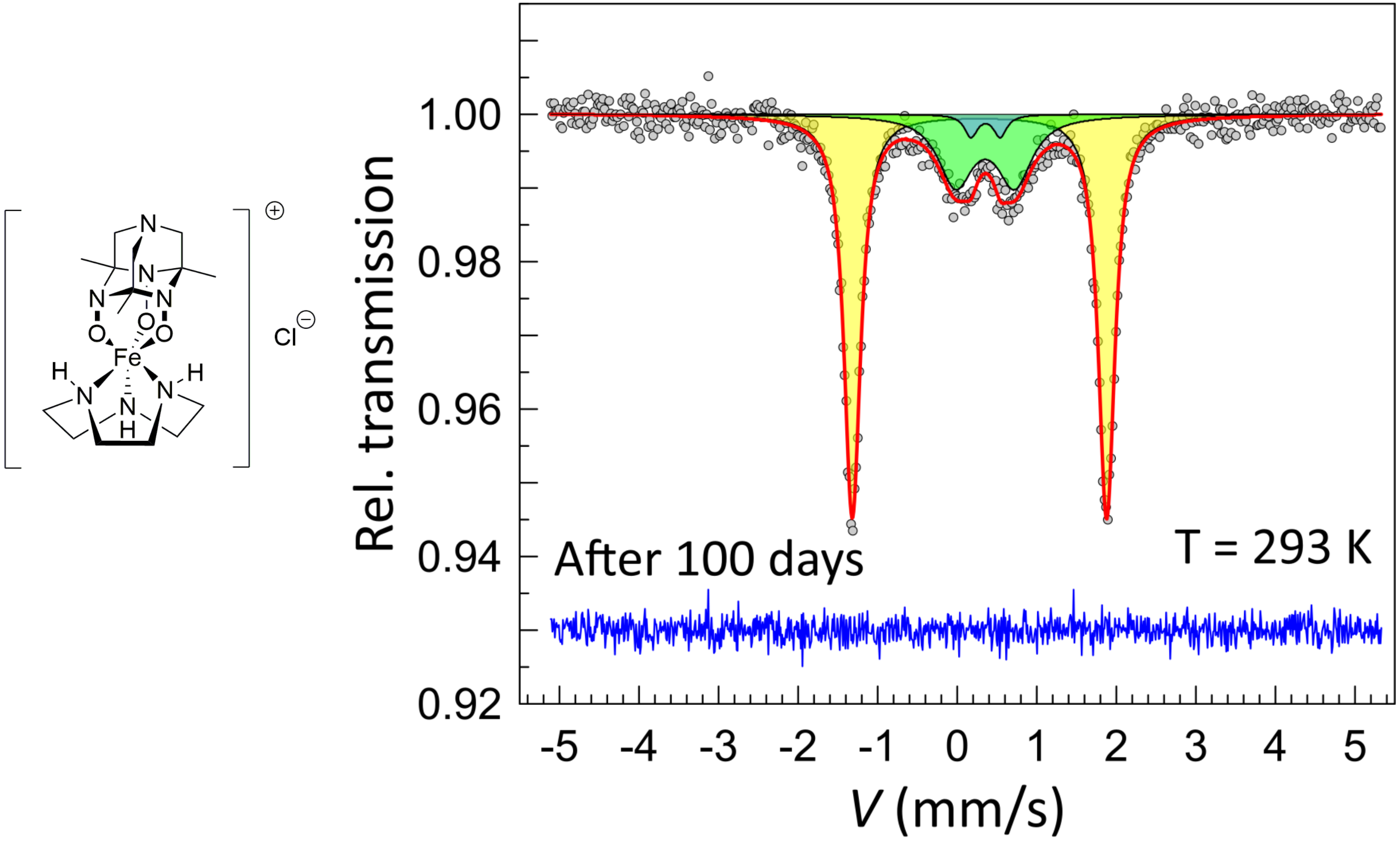

Component	δ, (mm/s)	$\lvert\Delta E_Q\rvert$, (mm/s)	S rel, %	Γ, (mm/s)
Doublet 1	0.2796	3.1971	71.24	0.2497
Doublet 2	0.3511	0.7400	25.64	0.5274
Doublet 3	0.3567	0.3671	3.12	0.1985

Figure S6. Mössbauer spectra of complex **1** at T = 293 K after 100 days.

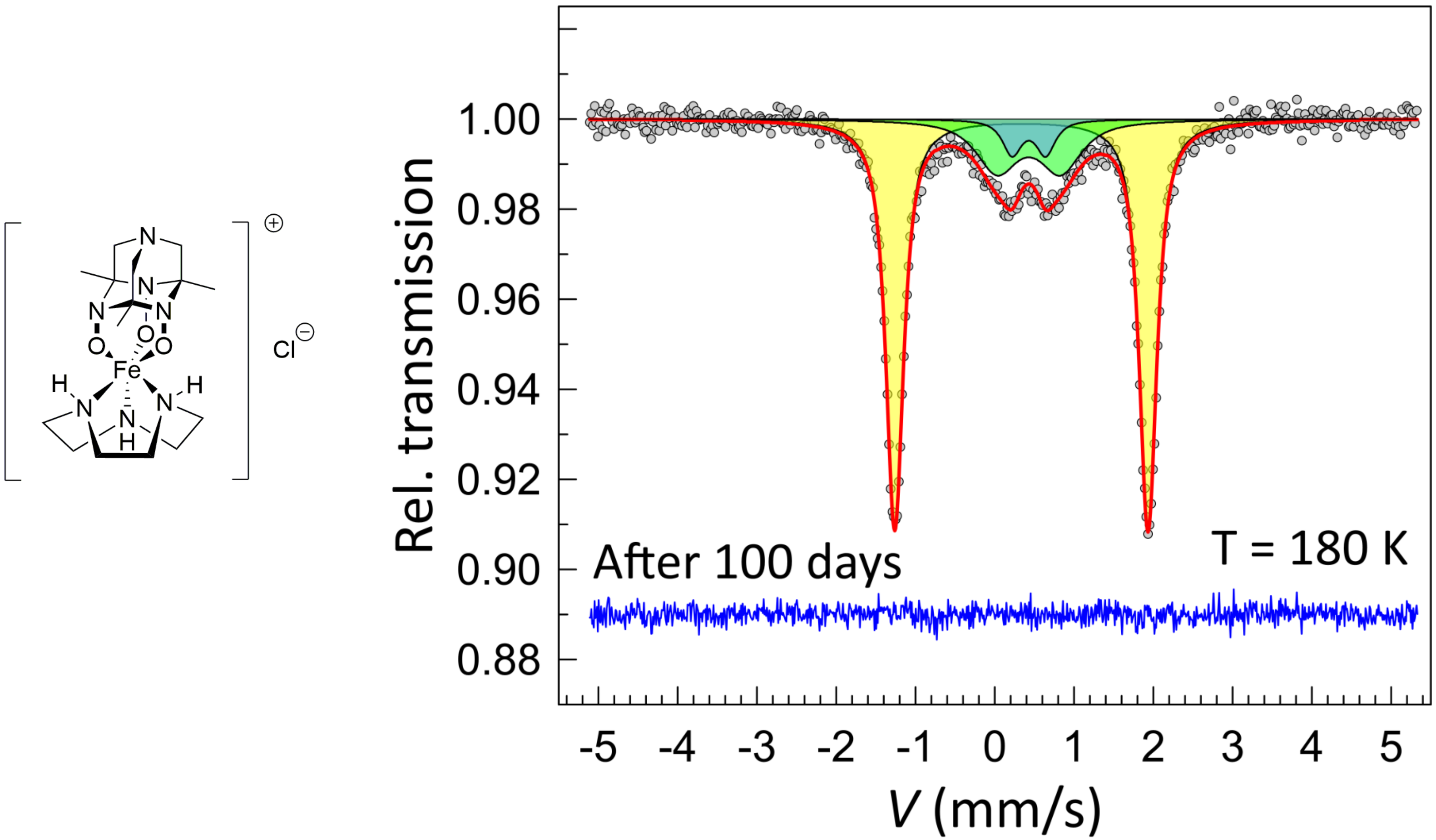

Component	δ, (mm/s)	$|\Delta E_Q|$, (mm/s)	S rel, %	Γ, (mm/s)
Doublet 1	0.3355	3.1953	72.13	0.2669
Doublet 2	0.4297	0.8007	21.15	0.6358
Doublet 3	0.4303	0.4218	6.72	0.2929

Figure S7. Mössbauer spectra of complex **1** at T = 180 K after 100 days.

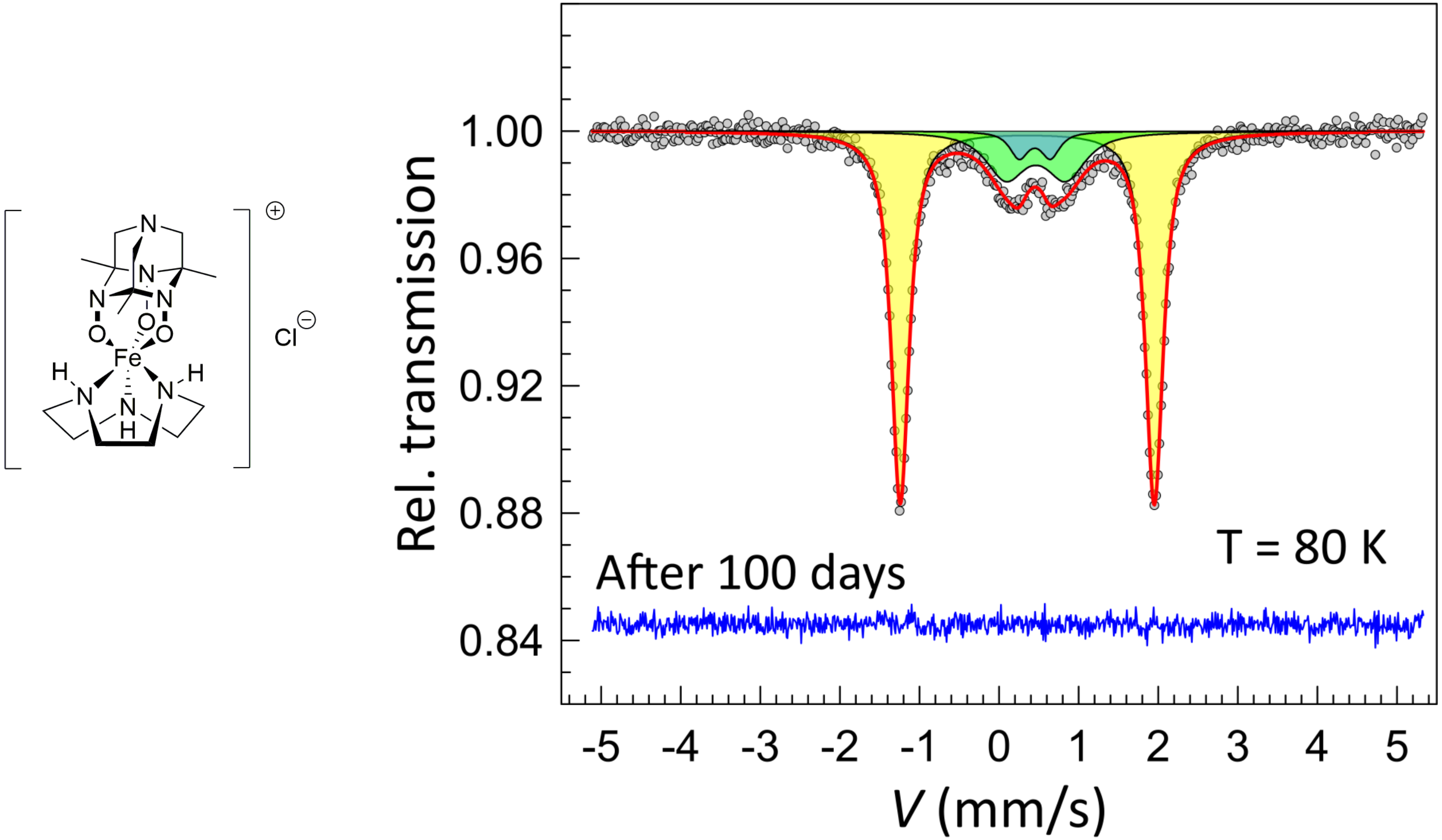

Component	δ, (mm/s)	$\lvert\Delta E_Q\rvert$, (mm/s)	S rel, %	Γ, (mm/s)
Doublet 1	0.3542	3.1933	74.37	0.2686
Doublet 2	0.4622	0.7526	20.14	0.5965
Doublet 3	0.4485	0.3922	5.49	0.2849

Figure S8. Mössbauer spectra of complex **1** at T = 80 K after 100 days.

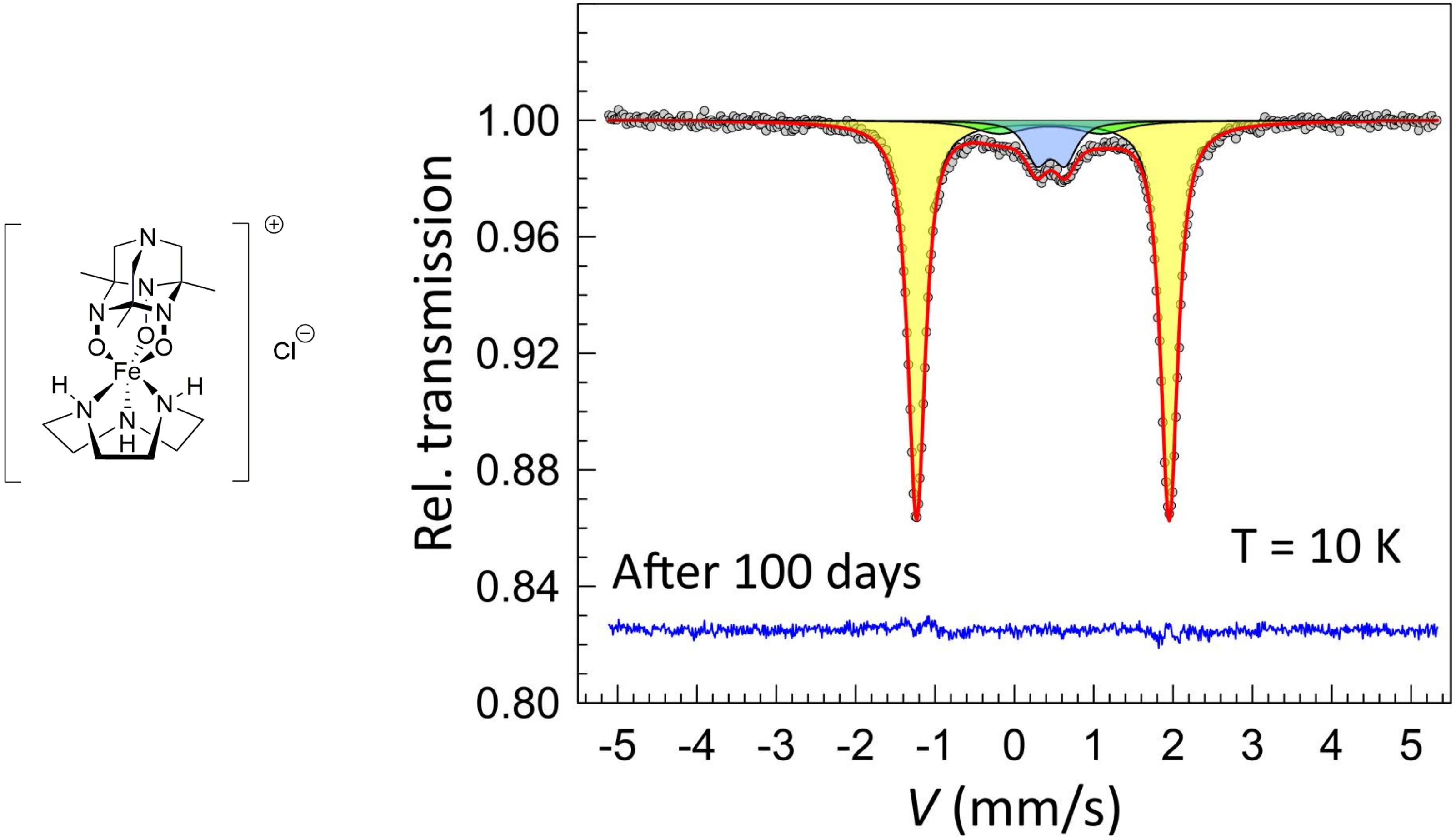

Component	δ, (mm/s)	$\lvert\Delta E_Q\rvert$, (mm/s)	S rel, %	Γ, (mm/s)
Doublet 1	0.3599	3.1837	81.61	0.2633
Doublet 2	0.4523	1.2957	7.56	0.7760
Doublet 3	0.4614	0.3528	10.83	0.3524

Figure S9. Mössbauer spectra of complex **1** at T = 10 K after 100 days.

DFT calculations of Mössbauer isomer shift (δ) and quadrupole splitting (ΔE_Q) were performed for several structures:

1) DFT optimized geometry of cation **1.1**. Charge +1; multiplicity 1.
2) DFT optimized geometry of cation **1.2**. Charge +1; multiplicity 3.
3) DFT optimized geometry of cation **1.3**. Charge +1; multiplicity 5.

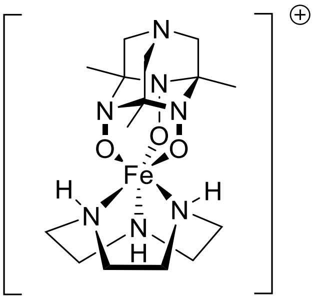

Table S6. Calculated parameters of Mössbauer spectra.

#	Structure	δ	ΔE_Q
1	DFT optimized geometry of cation **1.1**	0.21 mm/s	-1.48 mm/s
	RHO = 23615.546		
	V_{zz} = -0.9142 V_{yy} = 0.5176 V_{xx} = 0.3966		
2	DFT optimized geometry of cation **1.2**	0.24 mm/s	-2.21 mm/s
	RHO = 23615.404		
	V_{zz} = -1.3670 V_{yy} = 0.6906 V_{xx} = 0.6765		
3	DFT optimized geometry of cation **1.3**	0.47 mm/s	-1.00 mm/s
	RHO = 23613.985		
	V_{zz} = -0.6152 V_{yy} =0.3758 V_{xx} = 0.2394		

RHO – calculated contact electron density on Fe nucleus, a.u.$^{-3}$ V_{xx}, V_{yy}, V_{zz} - eigenvalues of the electric field gradient.

Table S7. Comparison of experimental and calculated Mössbauer parameters for **1**.

Parameter	**Complex 1**
$\delta_{\text{exp,}}$ (mm/s)	0.27
$\lvert\Delta E_Q\rvert_{\text{exp,}}$ (mm/s)	3.21
$\delta_{\text{calc,}}$ (mm/s)	0.24
$\Delta E_{Q\,\text{calc,}}$ (mm/s)	-2.21

10. DFT calculations

10.1. Calculation of relative energies of cations derived from complex 1.

Calculations were performed with the Gaussian 16 Rev C.01 program.[15] BP86 DFT functional with GD3BJ empirical dispersion correction and jorgetzp basis set[34, 35] was used for geometry optimization and calculations of thermodynamics. Cartesian coordinates are given in angstroms; absolute energies for all substances are given in hartrees. Analysis of vibrational frequencies was performed for all optimized structures. All compounds were characterized by only real vibrational frequencies. Wavefunction stability, using *stable* keyword, was also checked for each molecule.

Calculations were performed in methanol (SMD model). The approach of Martin and co-workers was followed.[36] Data from X-ray diffraction experiment for complex **1** (without chlorine anion and solvent) were used as starting points for geometry optimizations.

Initial charge of Fe atom was set to +4, the charge of TAAD ligand was set to -3. For better results, ***initial wavefunction*** was generated using division of the molecule into fragments.[37] Interpretation of metal spin and oxidation states in DFT optimized structures was performed on the basis of Mulliken atom spin density.

First step of calculation job:

Keywords:[38]

 # BP86/Gen guess(only,fragment=3) pop=none SCF=XQC

A structure complex 1 mult 3 jorge-tzp

```
1 3 4 3 -3 1 0 1
 Fe(Fragment=1)   15.53670000   7.46950000   14.85080000
 O(Fragment=2)    14.44800000   8.99150000   14.89660000
 O(Fragment=2)    14.60240000   6.62360000   16.23060000
 ….
```

Second step of calculation job:

 # opt freq UBP86/Gen nosymm guess=read geom=checkpoint EmpiricalDispersion=GD3BJ pressure=605 temperature=298.15 scf=xqc scrf=(smd,solvent=Methanol)

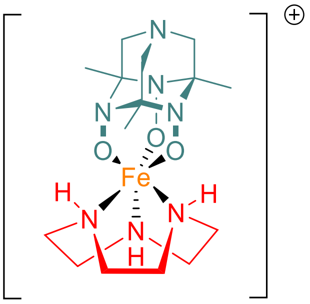

Figure S10. Fragmentation of **cation 1**.

Complex 1

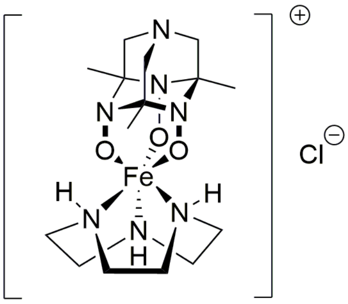

1

Table S8. Calculated relative energies of cations **1.1 – 1.3**.

cation	$\Delta G°_{298,15\ K}$ Kcal/mol	ΔE_0 Kcal/mol
1.1	+9.1	+9.2
1.2	0.0	0.0
1.3	+14.4	+18.5

Table S9. Selected X-Ray structural parameters of **complex 1**.

Fe-O bond distances in **complex 1**, Å
1.86, 1.87, 1.87
Fe-N bond distances in **complex 1**, Å
2.09, 2.10, 2.11

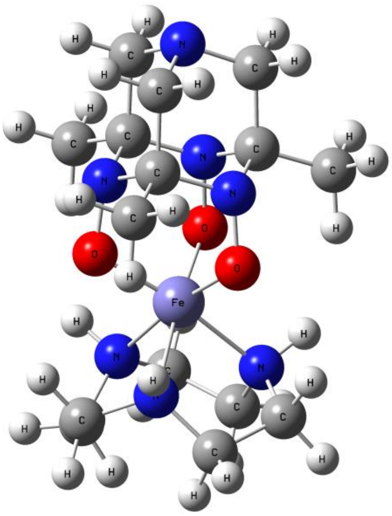

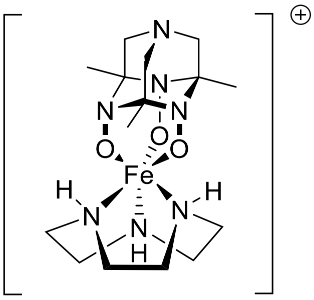

Cation 1.1

Cation **1.1** was calculated with unrestricted formalism (BS-DFT) and *stable* = *opt* additional step prior *opt freq* job due to RHF-UHF wavefunction instability.

Charge 1; multiplicity 1

Fe	0.88478300	0.00244800	0.00800800
O	-0.10740700	-1.55396500	0.24208900
O	-0.11195600	0.97453600	1.24132000
O	-0.09772100	0.57535900	-1.45519300
N	-1.48934900	-1.39884200	0.21460500
N	-1.49387800	0.88374400	1.10392600
N	-1.48129000	0.51257100	-1.32140400
N	-4.01448600	-0.00004700	-0.02005500
N	2.23799000	-0.50591600	1.49273700
H	1.71019000	-0.61724900	2.36325800
N	2.23184400	1.54489600	-0.30204300
H	1.69410100	2.35093300	-0.63463500
N	2.22679200	-1.03426500	-1.18052700
H	1.68413800	-1.72430500	-1.70894300
C	-1.96824400	-0.51751100	1.31908900
C	-3.50902200	-0.49872900	1.26012600
H	-3.87323300	-1.52332000	1.42364200
H	-3.87767000	0.14171500	2.07458100
C	-1.95513400	1.40292300	-0.21678800
C	-3.49667200	1.35454900	-0.22113000
H	-3.86572900	2.01028200	0.58071400
H	-3.85120300	1.74360800	-1.18663900
C	-1.95049900	-0.88933400	-1.11249900
C	-3.49170100	-0.85745100	-1.08571400
H	-3.84708400	-0.49043700	-2.05942600
H	-3.85611400	-1.88487100	-0.94107400
C	-1.50903300	-1.04325000	2.66570300
H	-1.91797900	-2.05182100	2.82013400
H	-1.88303600	-0.38387100	3.46153800

H	-0.41854000	-1.09550600	2.73761800
C	-1.47818400	2.82703400	-0.43105500
H	-0.38647000	2.90357700	-0.40803100
H	-1.88933000	3.47107600	0.35914000
H	-1.83537100	3.18947400	-1.40521800
C	-1.46601100	-1.78983200	-2.23299900
H	-0.37327600	-1.81809200	-2.29378900
H	-1.85983100	-1.42246700	-3.19118400
H	-1.83537300	-2.81144600	-2.06626400
C	3.26904000	0.56042500	1.68110400
H	4.20592700	0.21917400	1.22091400
H	3.46843500	0.71293900	2.75087200
C	2.79330900	1.85537700	1.03766700
H	1.98269100	2.30564800	1.62673000
H	3.61986700	2.58183000	0.97002000
C	3.25641600	1.17925800	-1.32813100
H	4.19961800	0.95811000	-0.81130500
H	3.44444600	2.02978900	-1.99787200
C	2.78289100	-0.02983200	-2.12312800
H	1.96981500	0.25008400	-2.80655700
H	3.60953200	-0.45062600	-2.71884900
C	3.25416600	-1.74269500	-0.35703500
H	4.19865000	-1.18748100	-0.43016500
H	3.43659500	-2.74870700	-0.75956900
C	2.78820800	-1.82567400	1.08999300
H	1.97342700	-2.55523000	1.19330900
H	3.61782300	-2.13411400	1.74727500

DFT-D3 UBP86/ jorgeTZP, solvent methanol, SMD model	
Total electronic energy=	-2462.957733 E_0
Sum of electronic and zero-point Energies=	-2462.487687 $E_0 + E_{ZPE}$
Sum of electronic and thermal Energies=	-2462.464171 $E_0 + E_{tot}$
Sum of electronic and thermal Enthalpies=	-2462.463227 $E_0 + H_{corr}$
Sum of electronic and thermal Free Energies=	-2462.529318 $E_0 + G_{corr}$
Zero-point correction *(unscaled)* =	0.470046

Table S10. Selected structural parameters of **cation 1.1**.

Fe-O bond distances in **cation 1.1**, Å
1.86, 1.86, 1.85
Fe-N bond distances in **cation 1.1**, Å
2.07, 2.07, 2.07

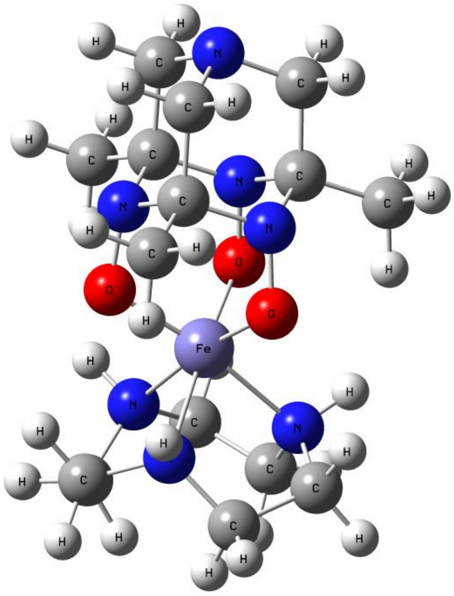

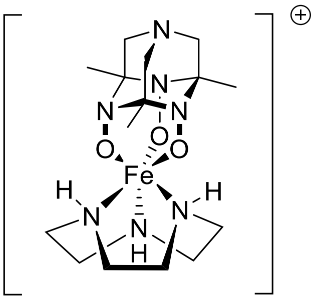

Cation 1.2

Charge 1; multiplicity 3

Fe	0.87966300	-0.00061200	0.00802000
O	-0.11598600	-1.55104200	0.26169200
O	-0.11917800	0.99393200	1.22285700
O	-0.10693300	0.55393500	-1.46699300
N	-1.49494700	-1.39520900	0.23005500
N	-1.49811800	0.89732900	1.09138000
N	-1.48582800	0.49676600	-1.32608500
N	-4.02037600	0.00199800	-0.01866200
N	2.24792300	-0.53756400	1.49365100
H	1.72658200	-0.66882700	2.36501900
N	2.23952900	1.55710700	-0.27573300
H	1.70738900	2.37330800	-0.59188300
N	2.23866900	-1.02253400	-1.20426200
H	1.70509200	-1.70596300	-1.74974500
C	-1.97356600	-0.50025000	1.32535400
C	-3.51409000	-0.48066000	1.26724300
H	-3.87908700	-1.50283500	1.44398800
H	-3.88183200	0.17019100	2.07382900
C	-1.96142600	1.40203800	-0.23584800
C	-3.50245100	1.35376200	-0.23816600
H	-3.87075600	2.02015400	0.55526200
H	-3.85827200	1.72996500	-1.20833100
C	-1.95829200	-0.90189300	-1.10292900
C	-3.49912200	-0.86908400	-1.07379100
H	-3.85578700	-0.51443800	-2.05167000
H	-3.86385800	-1.89442600	-0.91567100
C	-1.51389600	-1.00947400	2.67810200
H	-1.91784500	-2.01848900	2.84221500
H	-1.89352600	-0.34381800	3.46602800
H	-0.42332600	-1.05477700	2.75357800
C	-1.48349600	2.82278700	-0.46815600
H	-0.39134200	2.89664200	-0.45754400
H	-1.88540900	3.47546600	0.31961200

H	-1.84973800	3.17631600	-1.44227700
C	-1.47730400	-1.81621600	-2.21355600
H	-0.38494300	-1.84560300	-2.27864100
H	-1.87471300	-1.46078500	-3.17477200
H	-1.84657300	-2.83545300	-2.03272300
C	3.27478100	0.52955200	1.69359300
H	4.21272800	0.19842200	1.22823700
H	3.47568900	0.66884200	2.76499100
C	2.79797600	1.83582200	1.07155600
H	1.98601500	2.27417700	1.66807200
H	3.62470900	2.56379100	1.02321300
C	3.26142900	1.20316500	-1.30718400
H	4.20577200	0.97548600	-0.79529900
H	3.44951300	2.06191100	-1.96650800
C	2.79037100	0.00534600	-2.12290700
H	1.97621300	0.29561200	-2.80102600
H	3.61894900	-0.39755400	-2.72847900
C	3.26453300	-1.73791600	-0.38648800
H	4.20791800	-1.17947300	-0.44837400
H	3.45219600	-2.73789600	-0.80169700
C	2.79750600	-1.84680700	1.05951700
H	1.98297600	-2.57882500	1.14861300
H	3.62776300	-2.17092800	1.70861900

DFT-D3 UBP86/ jorgeTZP, solvent methanol, SMD model		
Total electronic energy=	-2462.972396	E_0
Sum of electronic and zero-point Energies=	-2462.501379	$E_0 + E_{ZPE}$
Sum of electronic and thermal Energies=	-2462.478150	$E_0 + E_{tot}$
Sum of electronic and thermal Enthalpies=	-2462.477206	$E_0 + H_{corr}$
Sum of electronic and thermal Free Energies=	-2462.543820	$E_0 + G_{corr}$
Zero-point correction *(unscaled)* =	0.471017	

Table S11. Selected structural parameters of **cation 1.2**.

Fe-O bond distances in **cation 1.2**, Å
1.86, 1.86, 1.86
Fe-N bond distances in **cation 1.2**, Å
2.09, 2.09, 2.09
Mulliken atom spin density
Fe: 1.83

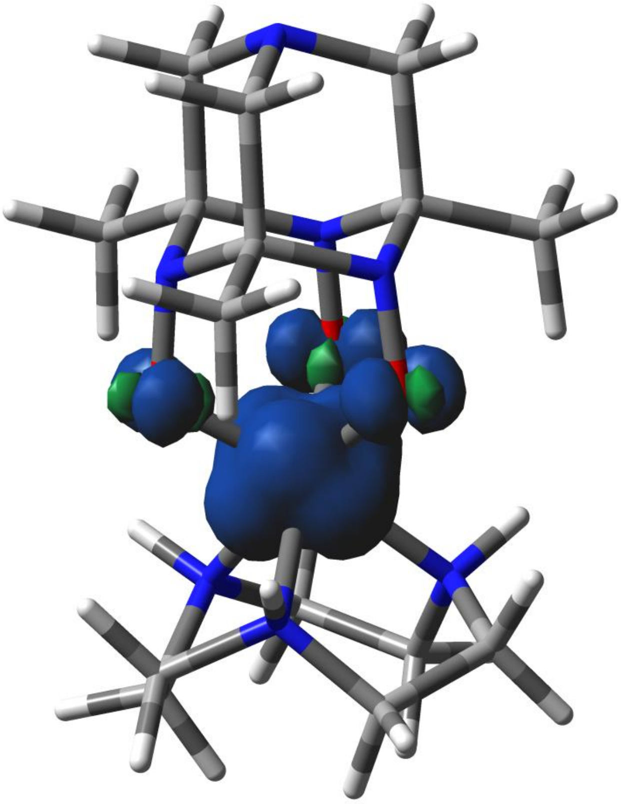

Figure S11. Spin density of **cation 1.2**.

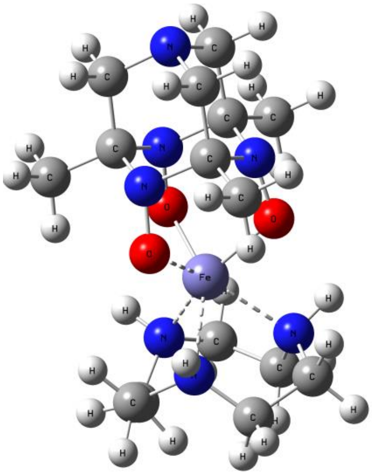

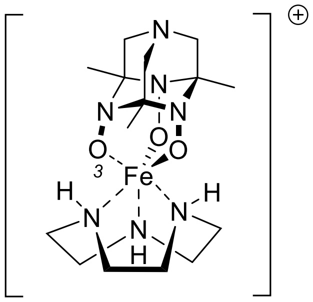

Cation 1.3

Charge 1; multiplicity 5

Fe	0.86491400	-0.05561200	0.01184300
O	-0.27054900	-1.44733900	0.72289400
O	-0.23741500	1.38380600	0.89950700
O	-0.24047800	0.07873500	-1.56957200
N	-1.60963100	-1.24331400	0.60651600
N	-1.62470700	1.21529300	0.80477200
N	-1.58440900	0.09218400	-1.37826300
N	-4.13300800	0.01461300	-0.01825800
N	2.38535400	-1.10340500	1.16732100
H	1.85634500	-1.57610800	1.90607000
N	2.40080700	1.54454600	0.36549600
H	1.84387400	2.40222900	0.39358100
N	2.41837600	-0.46553700	-1.53957800
H	1.88899600	-0.86857900	-2.31700000
C	-2.08622100	-0.06660200	1.41275600
C	-3.62822600	-0.07663300	1.35380600
H	-3.99105600	-1.00661100	1.81508800
H	-4.00058100	0.77631800	1.93881500
C	-2.07102900	1.29060600	-0.61877900
C	-3.61269000	1.24165000	-0.62539200
H	-3.98369800	2.11322000	-0.06735100
H	-3.96432300	1.31212500	-1.66479200
C	-2.08866400	-1.18727800	-0.80177000
C	-3.62711700	-1.12854500	-0.77831300
H	-3.98320700	-1.06613400	-1.81692100
H	-3.99979100	-2.06201300	-0.33244000
C	-1.60534200	-0.18678900	2.84574700
H	-1.97603600	-1.12491400	3.28227900
H	-2.00047800	0.65611700	3.42986200
H	-0.51194700	-0.17502600	2.90721700
C	-1.57569800	2.56474300	-1.27509000
H	-0.48178500	2.60750400	-1.30253800
H	-1.94762600	3.42978300	-0.70822300
H	-1.96065100	2.62310000	-2.30296500
C	-1.60046200	-2.37915800	-1.59930700
H	-0.50716200	-2.43851400	-1.61703100
H	-1.96830300	-2.29811900	-2.63173400

H	-1.99915600	-3.30063600	-1.15264300
C	3.39968600	-0.19958600	1.77241300
H	4.34188600	-0.31272400	1.21943500
H	3.59933000	-0.49079400	2.81362100
C	2.91950000	1.24665600	1.71625800
H	2.08810500	1.39920200	2.41945500
H	3.74090500	1.92583600	2.00555800
C	3.42148600	1.61824500	-0.70488300
H	4.36008100	1.19073700	-0.32534100
H	3.63110600	2.66395000	-0.97444800
C	2.95540900	0.85012300	-1.94045900
H	2.13628900	1.39020400	-2.43767600
H	3.78866600	0.75750800	-2.65913500
C	3.42212600	-1.43956500	-1.04191400
H	4.36187700	-0.90523200	-0.84507200
H	3.63959500	-2.20030600	-1.80594100
C	2.92304900	-2.11851000	0.23119300
H	2.09650900	-2.80599000	-0.00089200
H	3.73704300	-2.70499100	0.69111300

DFT-D3 UBP86/ jorgeTZP, solvent methanol, SMD model		
Total electronic energy=	-2462.942889	E_0
Sum of electronic and zero-point Energies=	-2462.475654	$E_0 + E_{ZPE}$
Sum of electronic and thermal Energies=	-2462.451054	$E_0 + E_{tot}$
Sum of electronic and thermal Enthalpies=	-2462.450110	$E_0 + H_{corr}$
Sum of electronic and thermal Free Energies=	-2462.520870	$E_0 + G_{corr}$
Zero-point correction *(unscaled)* =	0.467235	

Table S12. Selected structural parameters of **cation 1.3**.

Fe-O bond distances in **cation 1.3**, Å
1.93, 1.93, 2.02 - (Fe-O*3*)
Fe-N bond distances in **cation 1.3**, Å
2.18, 2.23, 2.25
Mulliken atom spin density
Fe: 3.52; O*3*: 0.24

10.2. Procedure for DFT calculation of Mössbauer parameters

Calculation of Mössbauer isomer shift.

Calculations were performed with the ORCA 4.2.1[16] quantum chemistry program. For calculation of Mössbauer isomer shift calibration line is needed.[39] Afterwards the line is obtained then substitution of calculated contact electron density RHO (taken directly from ORCA output) as x gives a calculated isomer shift as y. Calibration set was taken from Romelt et al.[40] Procedure for geometry optimization and calculation of contact electron density on Fe nucleus was taken from Bjornsson et al.[41] Calibration line for ^{57}Fe Mössbauer isomer shift was taken from Golovanov et al.[42]

RHO was calculated with B3LYP DFT functional using CP(PPP) basis set on Fe and def2-TZVP basis set on other atoms. Relativistic effects were taken into account by requesting a Douglas-Kroll-Hess 2nd order scalar relativistic calculation.

Keywords:

```
! SP UKS B3LYP NORI DKH2 DKH-def2-TZVP TightSCF Grid5 FinalGrid6 SlowConv CPCMC(water)
%basis
newgto Fe "CP(PPP)" end
end
%method SpecialGridAtoms 26
SpecialGridIntAcc 7
end
%scf MaxIter 2000 end
*xyz 1 5
Fe        0.86491400   -0.05561200    0.01184300
 O       -0.27054900   -1.44733900    0.72289400
 …
H         3.73704300   -2.70499100    0.69111300
*
%eprnmr nuclei = all 26 {rho, fgrad}
End
```

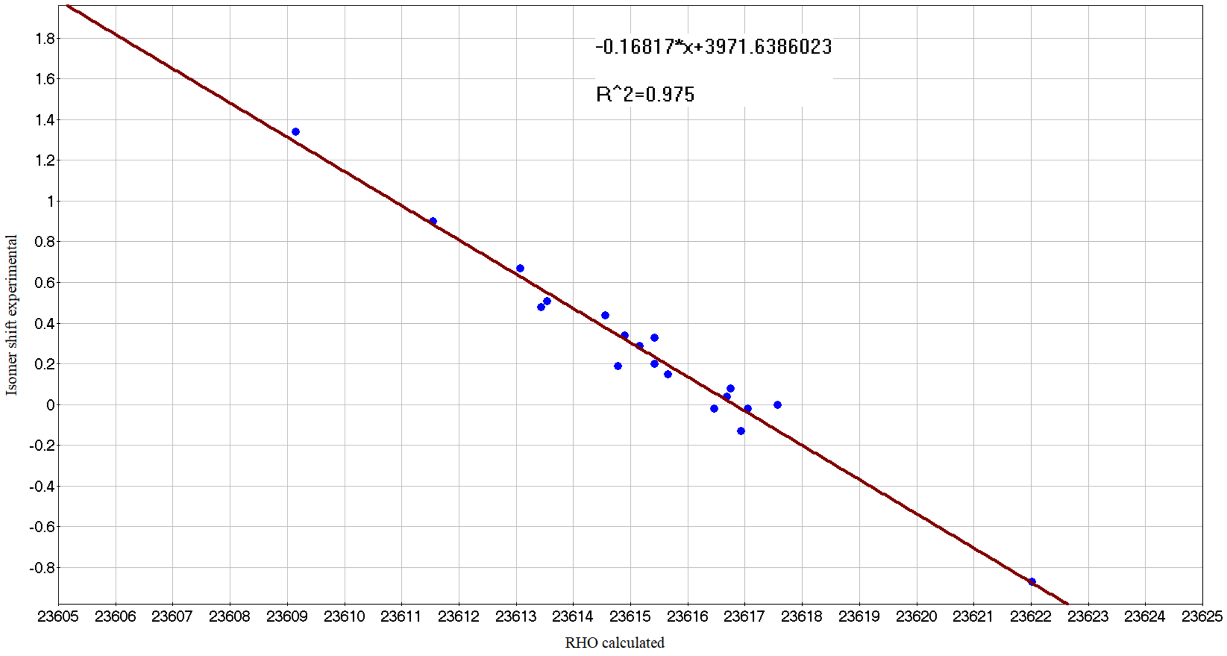

Figure S12. Calibration line[42] for ^{57}Fe Mössbauer isomer shift.

Table S13. Cartesian coordinates for the calibration line.

#	Compound	Exp. isomer shift δ, (mm/s)	Contact electron density on Fe nucleus (RHO) calculated a.u.$^{-3}$
1	$[FeCl_4]^{2-}$	0.9	23611.543
2	$[FeCl_4]^{-}$	0.19	23614.784
3	$[Fe(CN_6)]^{4-}$	-0.02	23616.463
4	$[Fe(CN_6)]^{3-}$	-0.13	23616.936
5	$[FeF_6]^{4-}$	1.34	23609.151
6	$[FeF_6]^{3-}$	0.48	23613.435
7	$[Fe(H_2O_6)]^{3+}$	0.51	23613.535
8	$[FeO_4]^{2-}$	-0.87	23622.017
9	$Fe(CO)_5$	0	23617.562
10	$[FeAz]^{+}$	0.29	23615.154
11	$[Fe(MAC)]^{2-}$	0.15	23615.655
12	$[Fe(OEPPY)]^{+}$	0.2	23615.417
13	$[Fe(Por(O_2))]^{-}$	0.67	23613.064
14	$[Fe(MAC)]^{-}$	-0.02	23617.045
15	$[Fe(Por(O))]^{+}$	0.08	23616.745
16	$[\{FeNO\}^{6}]^{+}$	0.04	23616.677
17	$[\{FeNO\}^{7}]$	0.33	23615.418
18	$[Fe(PH_3)]$	0.34	23614.893
19	[Fe(SMe)]	0.44	23614.562

Calculation of electric field gradient

Electric field gradient was calculated[43] for cations **1.1** – **1.3** as a single point job. Calculations were performed with the ORCA 4.2.1[16] quantum chemistry program. TPSS DFT functional with DKH-def2-QZVPP basis set on Fe and def2-TZVP basis set on other atoms was used. Relativistic effects were taken into account by requesting a Douglas-Kroll-Hess 2nd order scalar relativistic calculation with inclusion of picture change effects.

Sample input file:

```
! SP UKS TPSS NORI DKH2 DKH-def2-TZVP Decontract VERYTIGHTSCF Grid5
FinalGrid6 SlowConv

%basis

newgto Fe "DKH-def2-QZVPP" end

end

%method SpecialGridAtoms 26

SpecialGridIntAcc 7

end

%scf MaxIter 2000 end

*xyz 1 3

Fe      0.879663000    -0.000612000     0.008020000

…

H       3.627763000    -2.170928000     1.708619000

*

%eprnmr nuclei = all 26 {fgrad}

end

%rel PictureChange true

end
```

11. References

1. A. N. Semakin, A. Y. Sukhorukov, A. V. Lesiv, S. L. Ioffe, K. A. Lyssenko, Y. V. Nelyubina and V. A. Tartakovsky, *Org. Lett.*, 2009, **11**, 4072-4075.
2. V. V. Ozerova, I. S. Zhidkov, A. Boldyreva, N. N. Dremova, N. A. Emelianov, G. V. Shilov, L. A. Frolova, E. Z. Kurmaev, A. Y. Sukhorukov, S. M. Aldoshin and P. A. Troshin, *Energies*, 2021, **14**, 669.
3. A. S. Komendantova, A. M. Scherbakov, A. V. Komkov, V. V. Chertkova, A. O. Gudovanniy, E. I. Chernoburova, D. V. Sorokin, Y. U. Dzichenka, V. Z. Shirinian, Y. A. Volkova and I. V. Zavarzin, *Bioorg Chem.*, 2019, **91**, 103142.
4. A. N. Semakin, I. S. Golovanov, A. Y. Sukhorukov, S. L. Ioffe and V. A. Tartakovsky, *Russ. Chem. Bull*, 2016, **65**, 2270-2277.
5. P. Jiao, P. Jin, C. Li, L. Cui, L. Dong, B. Pan, W. Song, L. Ma, J. Dong, L. Song, X. Jin, F. Li, M. Wan, Z. Lv, Q. Geng, *Bioorg. Med. Chem. Lett.*, 2016, **26**, 4679-4683.
6. I. S. Golovanov, G. S. Mazeina, Y. V. Nelyubina, R. A. Novikov, A. S. Mazur, S. N. Britvin, V. A. Tartakovsky, S. L. Ioffe and A. Y. Sukhorukov, *J. Org. Chem.*, 2018, **83**, 9756-9773.
7. G. R. Fulmer, A. J. M. Miller, N. H. Sherden, H. E. Gottlieb, A. Nudelman, B. M. Stoltz, J. E. Bercaw and K. I. Goldberg, *Organometallics*, 2010, **29**, 2176-2179.
8. D. F. Evans, *Journal of the Chemical Society (Resumed)*, 1959, **0**, 2003-2005.
9. C. Piguet, *J. Chem. Educ.*, 1997, **74**, 815.
10. G. A. Bain and J. F. Berry, *J. Chem. Educ.*, 2008, **85**, 532.
11. P. G. Naumov, I. S. Lyubutin, K. V. Frolov and E. I. Demikhov, *Instrum. Exp. Tech*, 2010, **53**, 770-776.
12. https://ritverc.com/en/products/sources/mossbauer-sources/57co.
13. https://ritverc.com/en/products/sources/mossbauer-sources/reference-absorbers.
14. A. Coelho, TOPAS 4.2, Bruker AXS GmbH, Karlsruhe, Germany, 2009.
15. M. J. Frisch, G. W. Trucks, H. B. Schlegel, G. E. Scuseria, M. A. Robb, J. R. Cheeseman, G. Scalmani, V. Barone, G. A. Petersson, H. Nakatsuji, X. Li, M. Caricato, A. V. Marenich, J. Bloino, B. G. Janesko, R. Gomperts, B. Mennucci, H. P. Hratchian, J. V. Ortiz, A. F. Izmaylov, J. L. Sonnenberg, Williams, F. Ding, F. Lipparini, F. Egidi, J. Goings, B. Peng, A. Petrone, T. Henderson, D. Ranasinghe, V. G. Zakrzewski, J. Gao, N. Rega, G. Zheng, W. Liang, M. Hada, M. Ehara, K. Toyota, R. Fukuda, J. Hasegawa, M. Ishida, T. Nakajima, Y. Honda, O. Kitao, H. Nakai, T. Vreven, K. Throssell, J. A. Montgomery Jr., J. E. Peralta, F. Ogliaro, M. J. Bearpark, J. J. Heyd, E. N. Brothers, K. N. Kudin, V. N. Staroverov, T. A. Keith, R. Kobayashi, J. Normand, K. Raghavachari, A. P. Rendell, J. C. Burant, S. S. Iyengar, J. Tomasi, M. Cossi, J. M. Millam,

M. Klene, C. Adamo, R. Cammi, J. W. Ochterski, R. L. Martin, K. Morokuma, O. Farkas, J. B. Foresman and D. J. Fox, *Gaussian 16, Revision C.01*, Gaussian, Inc., Wallingford CT, 2016.

16. F. Neese, *Wiley Interdiscip. Rev. Comput. Mol. Sci.*, 2018, **8**, e1327.
17. N. Iranpoor, H. Firouzabadi and A. Jamalian, *Synlett*, 2005**, 2005**, 1447-1449.
18. I. Steinfatt, G. G. Hoffmann, L. Brouwer, F. Menzel and W. Brockner, *Phosphorus, Sulfur, Silicon Relat. Elem.*, 1998, **134**, 31-55.
19. N. Spiliopoulou and C. G. Kokotos, *Green Chem.*, 2021, **23**, 546-551.
20. H. R. Shaterian and H. Hadadzadeh, *Phosphorus Sulfur Silicon Relat. Elem.*, 2006, **181**, 1059-1071.
21. S.-Y. Cui, H. Jin, S.-J. Kim, A. P. Kumar and Y.-I. Lee, *J. Biochem.*, 2008, **143**, 685-693.
22. H. Huang, J. Ash and J. Y. Kang, *Org. Biomol. Chem.*, 2018, **16**, 4236-4242.
23. A. Dhakshinamoorthy, M. Alvaro and H. Garcia, *Chem. Commun.*, 2010, **46**, 6476-6478.
24. S. Paul and S. M. Islam, *RSC Advances*, 2016, **6**, 95753-95759.
25. Y. Zhang, D. Yang, Y. Li, X. Zhao, B. Wang and J. Qu, *Catal. Sci. Technol.*, 2019, **9**, 6492-6502.
26. P. S. Gunasekera, P. C. Abhyankar, S. N. MacMillan and D. C. Lacy, *ChemRxiv*, 2020, 10.26434/chemrxiv.13011617.v1
27. P. Kumar, G. Singh, D. Tripathi and S. L. Jain, *RSC Advances*, 2014, **4**, 50331-50337.
28. O. V. Dolomanov, L. J. Bourhis, R. J. Gildea, J. A. K. Howard and H. Puschmann, *J. Appl. Crystallogr.*, 2009, **42**, 339-341.
29. G. Sheldrick, *Acta Crystallogr. A*, 2015, **71**, 3-8.
30. G. Sheldrick, *Acta Crystallogr. A*, 2008, **64**, 112-122.
31. S. Alvarez, *J. Am. Chem. Soc.*, 2003, **125**, 6795-6802.
32. J. Hohenberger, K. Ray and K. Meyer, *Nat. Commun.*, 2012, **3**, 720.
33. S. Tomyn, S. I. Shylin, D. Bykov, V. Ksenofontov, E. Gumienna-Kontecka, V. Bon and I. O. Fritsky, *Nat. Commun.*, 2017, **8**, 14099.
34. P. L. Barbieri, P. A. Fantin and F. E. Jorge, *Mol. Phys.*, 2006, **104**, 2945-2954.
35. S. F. Machado, G. G. Camiletti, A. C. Neto, F. E. Jorge and R. S. Jorge, *Mol. Phys.*, 2009, **107**, 1713-1727.
36. R. L. Martin, P. J. Hay and L. R. Pratt, *J. Phys. Chem. A*, 1998, **102**, 3565-3573.
37. J. B. Foresman and Æ Frisch, Exploring Chemistry with Electronic Structure Methods, 3rd ed., Gaussian, Inc.: Wallingford, CT, 2015.
38. For detailed description of all keywords, basis sets and functionals please refer to Gaussian 16 manual or http://www.gaussian.com/keywords and references therein.
39. M. Pápai and G. Vankó, *J. Chem. Theory Comput.*, 2013, **9**, 5004-5020.

40. M. Römelt, S. Ye and F. Neese, *Inorg. Chem.*, 2009, **48**, 784-785.

41. R. Bjornsson, F. Neese and S. DeBeer, *Inorg. Chem.*, 2017, **56**, 1470-1477.

42. I. S. Golovanov, R. S. Malykhin, V. K. Lesnikov, Y. V. Nelyubina, V. V. Novikov, K. V. Frolov, A. I. Stadnichenko, E. V. Tretyakov, S. L. Ioffe and A. Y. Sukhorukov, *Inorg. Chem.*, 2021, **60**, 5523-5537.

43. R. Bjornsson and M. Bühl, *Chem. Phys. Lett.*, 2013, **559**, 112-116.